# Gas Therapy: generating, delivery, and biomedical applications

Pejman Ghaffari-Bohlouli[1,4], Hafez Jafari[1], Oseweuba Valentine Okoro[1], Houman Alimoradi[1], Lei Nie[1,2], Guohua Jiang[3], Ashok Kakkar[4], Amin Shavandi[1*]

[1] BioMatter Unit—BTL, École Polytechnique de Bruxelles, Université Libre de Bruxelles, Avenue F.D. Roosevelt, 50-CP 165/61, Brussels 1050, Belgium

[2] *College of Life Sciences, Xinyang Normal University, Xinyang 464000, China*

[3] *School of Materials Science and Engineering, Zhejiang Sci-Tech University, Hangzhou, 310018, China*

[4] *Department of Chemistry, McGill University, 801 Sherbrooke Street West, Montréal, Québec H3A 0B8, Canada*

Corresponding author:

Amin Shavandi, amin.shavandi@ulb.be

**Abstract**

Oxygen ($O_2$), nitric oxide (NO), carbon monoxide (CO), hydrogen sulfide ($H_2S$), and hydrogen ($H_2$) with direct effects, and carbon dioxide ($CO_2$) with complementary effects on the condition of various diseases are known as therapeutic gases. The targeted delivery and in situ generation of these therapeutic gases with controllable release at the site of disease has attracted attention to avoid the risk of gas poisoning and improve their performance in treating various diseases such as cancer therapy, cardiovascular therapy, bone tissue engineering, and wound healing. Stimuli-responsive gas-generating sources and delivery systems based on biomaterials that enable on-demand and controllable release are promising approaches for precise gas therapy. This review highlights current advances in the design and development of new approaches and systems to generate and deliver therapeutic gases at the site of disease with on-demand release behavior. The performance of the delivered gases in various biomedical applications is then discussed.

**Keywords:** Gas generating; Gas delivery; Gas therapy; Therapeutic gases; Biomedical applications

**Graphical abstract**

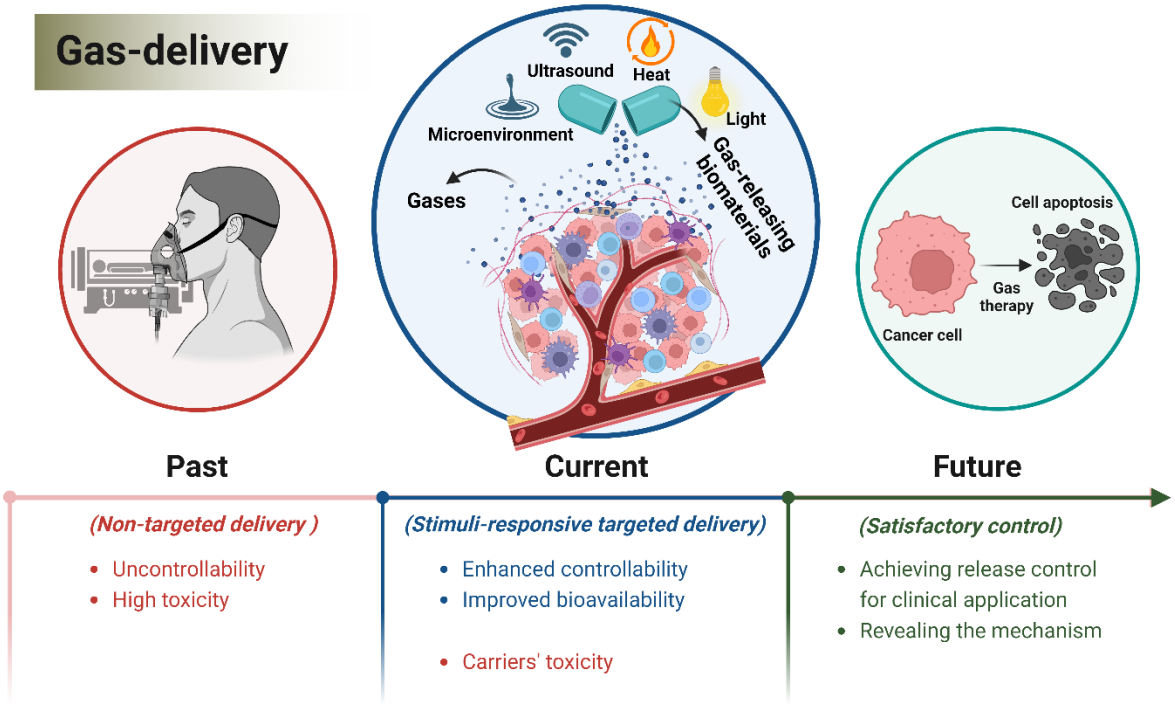

Table of Content

# 1 Introduction

Oxygen ($O_2$), nitric oxide (NO), carbon monoxide (CO), carbon dioxide ($CO_2$), hydrogen sulfide ($H_2S$), and hydrogen ($H_2$) are gaseous molecules with a therapeutic performance that have been used for gas therapy for the treatment of versatile biomedical applications [1]. NO, CO, and $H_2S$ were previously considered toxic gases to humans. The recent discovery of their critical physiological properties makes them suitable candidates as molecules of choice for biomedical applications [1b, 2]. $O_2$, NO, CO, $H_2S$, and $H_2$ are categorized as therapeutic gases with a direct influence on disease status. Conversely, $CO_2$ has supplementary assistance in disease treatment [1b].

Nevertheless, handling these gases which have high kinetic energy and a narrow therapeutic window remains the major challenge limiting their biomedical applications [2]. For example, while high levels of NO (>1 μM) within the circulatory system can be life-threatening, by triggering hypovolemic shock and cardiac arrest, lower concentrations of NO (< $10^{-9}$ M) in specific pathological conditions, such as ulcers can stimulate cell proliferation and accelerate the healing process [3]. Therefore, the control of therapeutic gas release constitutes a significant interest for further clinical translation, with gas-releasing biomaterials emerging as a promising approach.

Gas-releasing biomaterials possess the ability to effectively store therapeutic gases and release them effectively in the target tissues to achieve a desired concentration without inducing critical toxicities [1b, 4]. This can be achieved through either the enhanced retention effect and permeability or active targeting mechanisms [1b, 2, 5]. Furthermore, the gases can show a sustained release by modulating the composition, structure, and functionality of the gas-releasing biomaterials [2, 6]. The use of gas-releasing biomaterials for gas therapy provides opportunities for developing new therapeutic modalities or enhancing the efficacy of existing first-line therapies [1b].

In this review, the gas generating and delivery approaches, methods to control the gases, gas-releasing biomaterials functionality, and their unique theranostic performance are discussed. In contrast to existing reviews on gas therapy, which predominantly focus on specific aspects such as gas delivery strategies [2], gas-generating nanoplatforms [1b, 6-7], or the applications of delivered gases in cancer therapy [1b, 7], our review offers a distinctive and comprehensive perspective. This review highlights the use of various therapeutic gases, including $O_2$, NO, CO, $H_2$, $H_2S$, and $CO_2$ (Figure 1), with an emphasis on the intricate interplay between these therapeutic gases and biomaterials. We explore the multifaced ways in which the therapeutic gases can produced, whether through direct release or triggered by exogenous factors, such as the lesion microenvironment, heat, and light.

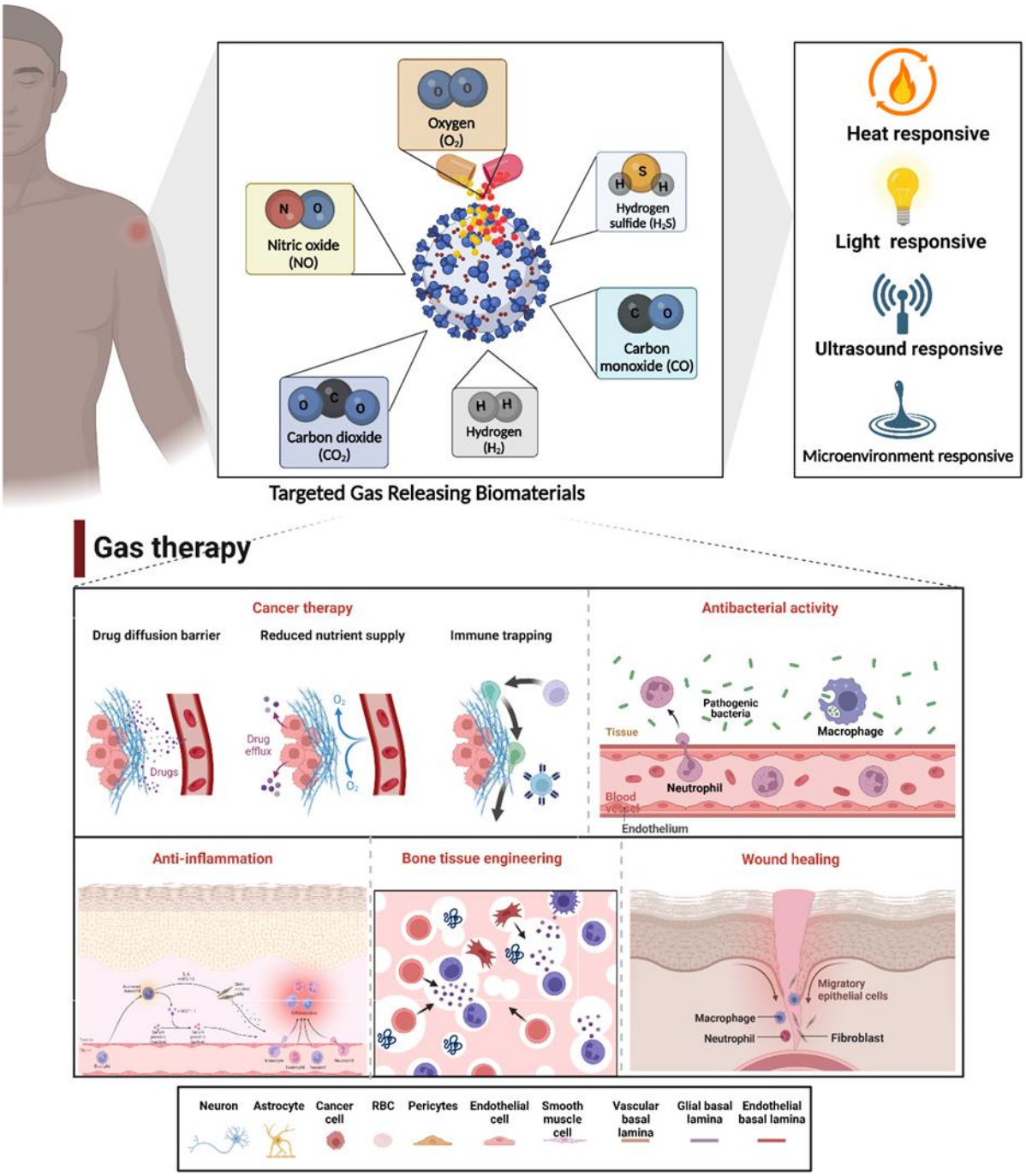


171

172 Figure 1. Schematic representation of therapeutic gases, such as oxygen ($O_2$), nitric oxide (NO), carbon
173 monoxide (CO), hydrogen sulfide ($H_2S$), hydrogen ($H_2$), and carbon dioxide ($CO_2$), illustrating the
174 multifaceted ways in which these therapeutic gases can be generated. The schematic also depicts
175 various biomedical applications of these therapeutic gases, including cancer therapy, wound healing,
176 bone tissue engineering, and antibacterial, and anti-inflammatory activities.

177 Furthermore, the recent gas-releasing biomaterials, which have been successfully designed for
178 various biomedical applications, such as cancer therapy, enhanced radio-sensitization, photodynamic
179 therapy (PDT), chemotherapy, sonodynamic therapy (SDT), synergistic high-intensity focused

ultrasound (HIFU), anti-inflammation, antibacterial treatments, and diagnostic imaging, are discussed (Figure 1). The future developments and upcoming challenges of gas-releasing biomaterials for promoting their clinical translation to benefit patients are considered.

## 2 Oxygen ($O_2$)

Oxygen ($O_2$) has a pivotal role in the metabolic activity of cells in the human body via the process of oxidation of nutrients and subsequent production of energy [8]. This energy is generated by the metabolization of glucose molecules and transferred using adenosine triphosphate (ATPs) molecules. The process of oxidative phosphorylation, occurring in the presence of sufficient $O_2$, involves the acceptance of electrons by $O_2$, which acts as an electron acceptor in aerobic respiration [8a].

When the cells have access to adequate levels of $O_2$, they can generate approximately 30 ATP molecules from each glucose molecule through a process known as physioxia. However, in the absence of $O_2$, the number of ATP molecules generated drops to two molecules, leading to the formation of ROS and triggering a cascade of metabolic stress responses within cells. This stress response can ultimately lead to cell death through processes such as autophagy, apoptosis, and necrosis [8]. Figure 2 illustrates the causes of hypoxia and the consequences of hypoxia on cell behavior [8a].

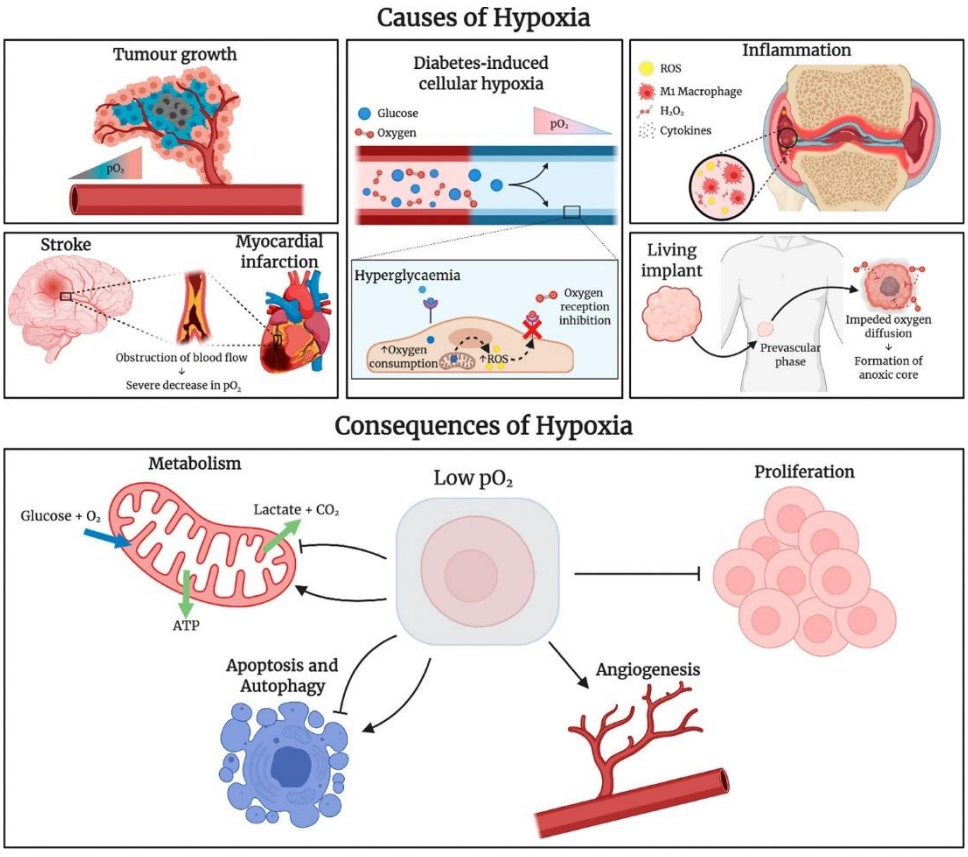

Figure 2. Schematic representing pathological conditions, including altered blood flow, inflammation, or an increase in tissue mass, which are observed in cases of tissue trauma, cancer, diabetes, stroke, coronary heart disease, and can cause hypoxia. In the short term, hypoxia can be associated with regenerative responses, such as neovasculogenesis, stem cell differentiation, and tissue regeneration. (Copyright © 2021, Elsevier) [8a].

Depending on the $O_2$ consumption rate and the supply to the tissues, the partial pressure of $O_2$ ($pO_2$) may vary, from low $pO_2$ (20 mmHg) in cartilage to high $pO_2$ (100 mmHg) in arterial blood [9]. Cells are categorized based on their sensitivity toward hypoxia, which has been published by Huaifa Zhang et al. [10]. Although the degree to which cells are able to adapt to $O_2$ concentrations varies from cell to cell [10-11], the range of this adaptation is relatively limited and to maintain homeostasis, keeping $pO_2$ within a certain range is critical [10]. When the adaptive mechanisms to hypoxia are saturated, prolonged exposure to hypoxia and depletion of energy resources lead to apoptotic and necrotic cell death and permanent tissue injury (Figure 2) [12]. Inflammation and disrupted blood flow resulting in tissue hypoxia can arise from a range of causes including diabetes, cancer, tissue trauma, coronary heart disease, stroke, and implantation [13].

Cells attempt to adapt to hypoxia through the activation of several signaling pathways predominantly governed by hypoxia-inducible factor (HIF) stabilization. HIF is responsible for regulating metabolism in many tissues and is composed of $O_2$-sensitive (HIFα) and independent (HIFβ) subunits [11]. Activation of HIFα results in the transcription of several genes that are important for tissue protection and adaptation, such as lactate dehydrogenase A (*LDHA*), phosphoglycerate kinase (*PGK*), erythropoietin (*EPO*) and vascular endothelial growth factor (*VEGF*) [11]. Figure 3 illustrates the activity of HIF in hypoxia and normoxia.

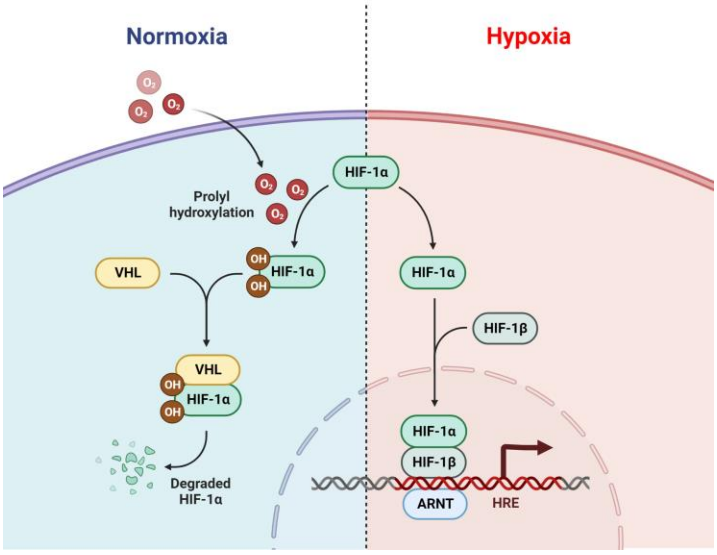

Figure 3. Schematic of mechanism of HIF in hypoxia and normoxia. In normoxia, prolyl hydroxylases enzyme and HIF-1α utilize $O_2$ and cofactors to hydroxylate HIF-1α. The hydroxylated HIF-1α binds with the von Hippel-Lindau (VHL). This interaction results in Lys48-linked polyubiquitination and dissociation via the proteasome. In hypoxia, the activity of prolyl hydroxylases enzyme reduces and leads to HIF-1α stabilization and dimerization with HIF-1β, which results in consensus hypoxia-responsive elements (HRE) [14]. Engineered tissues rely on the $O_2$ and nutrient supply [15]. For a growing tissue, the lack of a proper microvascular system that can supply $O_2$ and nutrients is a major challenge [16]. $O_2$-releasing scaffolds would be one feasible strategy to address this issue. This section explores different approaches that have been explored for $O_2$ delivery.

## 2.1 $O_2$ delivery

Approaches for $O_2$ delivery can be categorized into three main groups: clinical $O_2$ delivery, $O_2$ $O_2$-carriers, and $O_2$-generating materials (Figure 4) [15b, 16-17]. These different approaches have their unique advantages, disadvantages, performance, and functionalities, which are discussed in detail in this section.

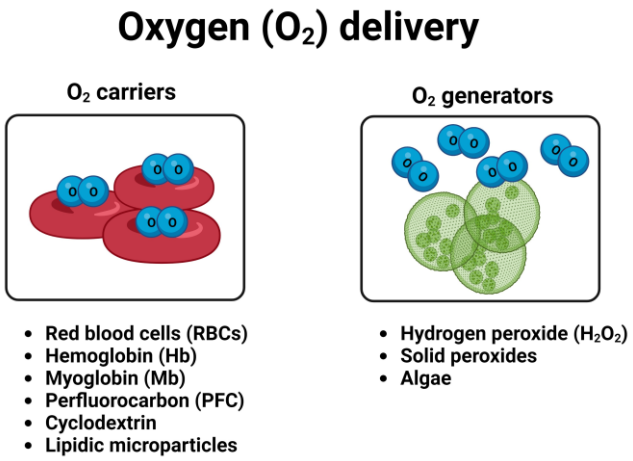


Figure 4. Schematic representation of the timeline development of oxygen ($O_2$) delivery approaches, which can be classified into two categories: $O_2$ carriers and $O_2$ generators. Oxygen carriers, such as red blood cells, hemoglobin, myoglobin, perfluorocarbons, cyclodextrin, and lipidic microparticles, can bond with $O_2$ and are used for local delivery. On the other hand, $O_2$ generators can produce in situ $O_2$ through decomposition and photosynthesis.

### 2.1.1 $O_2$ carriers

Systemic increase of $O_2$ level or random $O_2$ release wastes $O_2$, and may also lead to the formation of ROS and RNS. Hence, targeted $O_2$ delivery has attracted significant attention to gain the benefits of high $pO_2$ with minimal systemic toxicities. $O_2$-carrying materials such as red blood cells (RBCs), hemoglobin (Hb), myoglobin (Mb), perfluorocarbons (PFCs), cyclodextrin, and lipidic

microparticles (LMPs) have been applied (Figure 5). These materials can store $O_2$ and release it to targeted tissues and organs [18]. $O_2$ carriers are either synthetic or natural such as carriers derived from mammalian blood [10].

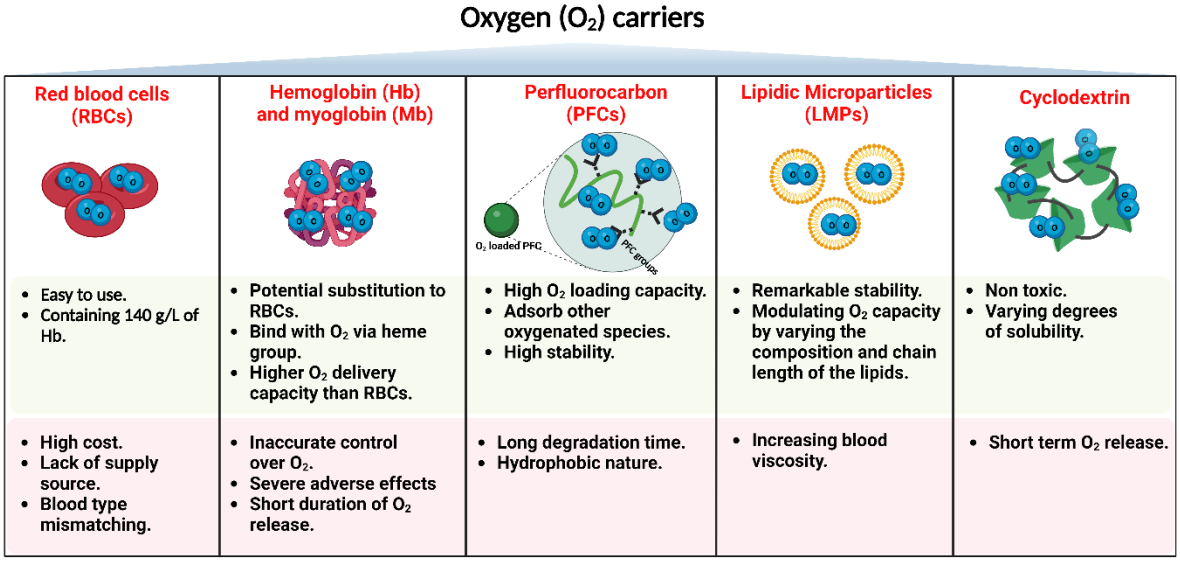


Figure 5. The schematic represents a summary of the advantages and disadvantages of $O_2$ carriers, including red blood cells (RBCs), hemoglobin (Hb), myoglobin (Mb), perfluorocarbons (PFCs), cyclodextrin, and lipidic microparticles (LMPs). All $O_2$ carriers suffer from a short-term $O_2$ release time due to their low $O_2$ payload. Synthetic $O_2$ carriers such as PFCs, cyclodextrin, and LMPs have a higher $O_2$ payload capacity compared to natural $O_2$ carriers like RBCs, Hb, and Mb.

#### *2.1.1.1 Red blood cells (RBCs)*

Red blood cell (RBC) transfusion is a commonly used method to improve $O_2$ delivery to organs and tissues [19]. RBCs with a Hb concentration of approximately 140 g/L are able to store their $O_2$ content for up to 42 days at 2 °C or up to 10 years at freezing temperatures [20]. However, studies have reported an association between transfusions and increased morbidity and mortality [21]. Medical complications such as infections, blood type mismatching, social challenges like generating biohazardous waste, high cost, and lack of supply for high-demand situations such as war, limit the effectiveness of RBCs [22].

#### *2.1.1.2 Hemoglobin (Hb) and myoglobin (Mb)*

Hb and Mb are the primary $O_2$ delivery units in blood cells, skeletal, and cardiac myocytes [23], and were thought to be a potential substitution for RBCs transfusion and their associated issues. Their heme groups can bind $O_2$ and release it at different concentrations, depending on the $pO_2$ [23]. The main difference between Hb and Mb comes from their $O_2$-binding subunits, which for Hb are four subunits, whereas Mb has one subunit [24]. Therefore, the $O_2$ saturation capacity of Hb is more than

Mb [10]. Additionally, compared to transfused RBCs, Hb can be stored for up to two years at ambient temperature, and its $O_2$ delivery capacity is 1.3 times higher than that of RBCs at the same volume. The potential of Hb to transfer $O_2$ without red corpuscle is proven [25]. Synthesized monodisperse zeolitic imidazolate framework (ZIF-8) particles containing Hb showed a lower constant rate for haptoglobin binding, which is a marker for in vivo clearance, compared to cell-free hemoglobin's rate. The hemolysis of the particles was investigated with incubation with RBCs for 30 min at 37 °C, which was less than 5% [26]. However, free Hb and Mb are toxic and induce Hb-driven diseases [27]. Having good gas (e.g. $O_2$) binding properties is involved in the toxic effects of Hb and Mb as well. For example, they can adsorb NO in the blood circulation system and induce vasoconstriction aberrant hemodynamics, and chronic manifestations of endothelial dysfunction.

Besides, the heme group in cell-free Hb and Mb has several oxidation states and this can interfere with several redox reactions in the body. In blood, most of the free Hb and Mb remain in the reduced $Fe(II)O_2$ state, capable of reactions with NO. However, in conditions with enhanced oxidative stress (including hypoxic conditions), they can go through autoxidation and obtain higher iron oxidation states (Fe(III), Fe(IV), Fe(IV)) which leads to the generation of ROS, degradation of Hb and Mb and generating crosslinking products with cytotoxic and inflammatory activities.

To address these issues, several approaches have been proposed, such as stabilization via polymer surface conjugation [28], intramolecular cross-linking [29], intermolecular polymerization [30], and encapsulation into drug delivery carriers such as liposomes [31]. However, the effectiveness of each approach depends on factors such as molecular mass, Hb concentration, temperature, and the characteristics of the media used for loading and release, as well as the type of stabilization method [32]. Among all these approaches, Hb vesicles with a moderate size of around 250 nm have shown the most promising results due to their high biocompatibility, loading capacity, stability, and efficacy. Additionally, their size is larger than the diameter of hepatic sinusoidal capillaries' fenestration, which helps to minimize their clearance by the reticuloendothelial system [22].

#### *2.1.1.3 Stem Cell-based $O_2$ carriers*

Stem cell-based $O_2$ carriers, such as human embryonic stem cells (hESCs), natural hematopoietic stem and progenitor cells (hSPCs), or induced pluripotent stem cells (iPSCs), have great potential for $O_2$ delivery and transfusion, similar to RBCs, and are particularly useful for patients with rare blood types, as they can be induced to differentiate hematopoietic cells [33]. However, despite their efficacy, cell-based $O_2$ carriers have limited shelf-life, storage, and shipping capabilities. Even with conjugation, cross-linking, and other modifications, the half-life of $O_2$ carriers derived from human or mammalian blood is shorter than that of natural RBCs, making them suitable only for short-

term tissue oxygenation and a limitation of RBC donors or transfusions. To address this issue, PFCs have been introduced as $O_2$ carriers with improved stability and performance.

#### *2.1.1.4 Perfluorocarbons (PFCs)*

Perfluorocarbons (PFCs) have emerged as a promising class of artificial $O_2$ carriers due to their high $O_2$ loading capacity. At standard pressure and room temperature, PFCs exhibit an $O_2$ dissolving capacity of 44 nM, which is 20 times greater than that of water [34]. Unlike Hb and Mb, the $O_2$ delivery capacity of PFCs exhibits a positive linear relationship with $pO_2$ [9]. Moreover, PFCs can adsorb other oxygenated species such as NO, CO, $CO_2$, ROS, and RNS via Fick's law, thereby acting as a scavenger and mitigating ROS and RNS [35]. PFCs exhibit relatively high stability and can extract up to 90% of the dissolved $O_2$ in blood [36]. The degradation time of PFCs is around 2 to 8 years due to the strongest bond between fluorine and carbon [37]. Such unique properties of PFCs have prompted researchers to explore their potential biomedical applications such as blood substitution, wound healing, liquid ventilation, organ preservation, and blood oxygenation [38]. However, the hydrophobic nature of PFCs necessitates their emulsification, suspension, or conjugation with hydrophilic polymers to enhance their efficiency in aqueous media [34].

The $O_2$ loading capacity and $O_2$ releasing rate of PFC-based materials can be modulated by a range of internal and external factors. Internal factors, such as the number of fluorine groups, the structure of PFCs, and the substitution degree, alongside external factors such as irradiation and loading and releasing media properties, play crucial roles in the controlled $O_2$-delivery properties of PFCs [39]. For instance, a critical substitution degree of 39-42% has been identified for pentadecafluorocarbons on methacrylate chitosan, with samples having higher substitution degrees exhibiting reduced cell viability [34]. In another study, PFCs conjugated with tetrafluorophenyl bacteriochlorin were shown to enhance the efficacy of photodynamic antibacterial agents by generating ROS *in vitro* and *in vivo* assays [40]. These findings highlight the versatility and potential of PFC-based materials as tunable platforms for biomedical applications.

#### *2.1.1.5 Cyclodextrin*

Cyclodextrin represents a class of non-toxic $O_2$ carriers with varying degrees of solubility, comprising multiple cross-linked cyclodextrins [41]. Although cross-linking reduces the solubility of cyclodextrins, it enables the formation of a 3-dimensional porous structure with lipophilic cavities and hydrophilic channels, allowing for the incorporation of a wide range of compounds [41]. The capacity and hydrophilicity of cyclodextrin sponges can be tailored by adjusting the cross-linker type and ratio to cyclodextrin [42]. The $O_2$ uptake capacity and release rate of different types of cyclodextrin (α, β, and γ) have been characterized, revealing variations in $O_2$ uptake and release kinetics ranging from 1 hour

to more than 2 days [43]. These findings underscore the potential of cyclodextrin sponges as versatile platforms for $O_2$ delivery and related applications, which can be further tuned by manipulating their structural and physicochemical properties.

#### *2.1.1.6 Lipidic microparticles (LMPs)*

Lipidic microparticles (LMPs) represent another $O_2$ carrier with remarkable stability, lasting for up to 2 weeks and potentially extended to several months by incorporating oligosaccharides and cholesterol [44]. The $O_2$ capacity of LMPs is primarily determined by the composition and chain length of the lipids, while the stability of lipids can be modulated by the molecular weight of the selected surfactant [45]. Due to their excellent stability, LMPs have potential applications in a wide range of $O_2$-consuming conditions, including refractory hypoxemia and acute respiratory distress syndrome [45]. However, the large size of LMPs can increase blood viscosity, and their accumulation in tissues can induce toxicity [46]. Surface modification is an approach to minimize the immunogenicity and toxicity of LMPs [46b]. By reducing the lipidic particle size from micro to nano, $O_2$ loading capacity increases, and the blood viscosity does not change significantly [47]. In recent years, $O_2$ carriers have garnered attention for their potential to release $O_2$ in targeted tissues or organs, thereby minimizing the risk of damaging other organs. Nevertheless, their practical application has been hindered by their low $O_2$-loading and short-term $O_2$ supply in an uncontrolled manner, harmful burst release, and $O_2$ loading dependency.

### 2.1.2 In situ $O_2$ generators

To overcome the limitations of utilizing $O_2$ carriers and clinical $O_2$ delivery, researchers have focused on the development of $O_2$-generating sources that can produce in situ $O_2$, thus enabling the production of independent $O_2$-loaded biomaterials. Figure 6 represents a summary of $O_2$ generators, which have been used up to now, with their advantages and drawbacks.

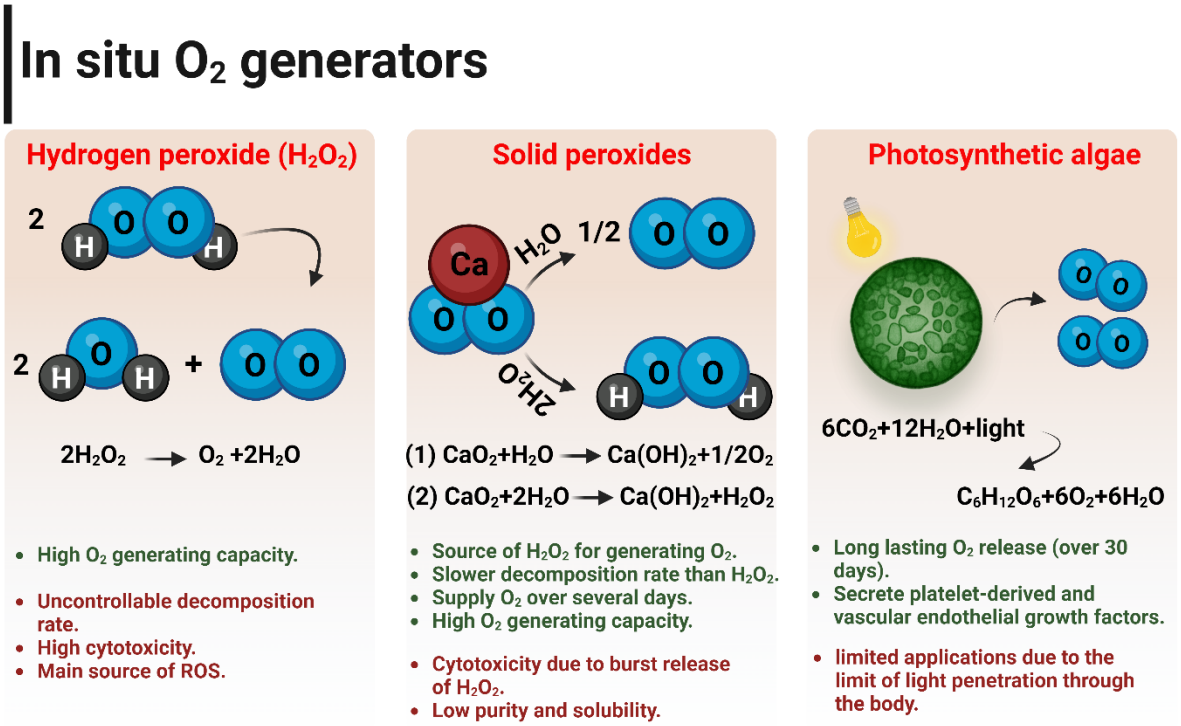


Figure 6. Current in situ oxygen ($O_2$) generators can be classified into hydrogen peroxide ($H_2O_2$, liquid), solid peroxides such as calcium peroxide (CPO), sodium percarbonate (SPO), and magnesium peroxide (MPO) (solids), and algae (living organisms). Hydrogen peroxide and solid peroxides have cytotoxicity due to fast decomposition. Solid peroxides can decompose into $O_2$ and $H_2O_2$, providing a source of $O_2$. Algae possess long-lasting $O_2$ release via light irradiation.

#### *2.1.2.1 Hydrogen peroxide ($H_2O_2$)*

Hydrogen peroxide ($H_2O_2$), a widely used liquid peroxide, has a high rate of decomposition into water and $O_2$. In the absence of a decomposition agent, one gram of $H_2O_2$ can generate 12 mL of $O_2$ [48]. This process is facilitated by factors such as light, temperature, and pH, as well as by the presence of certain catalysts such as silver, manganese, potassium dichromate, iron oxide, and catalases [48].

#### *2.1.2.2 Solid peroxides*

Solid peroxides, including calcium peroxide (CPO), sodium percarbonate (SPO), and magnesium peroxide (MPO), have been investigated as a source of $H_2O_2$ for generating $O_2$ over an extended period [8a]. The solubility, purity, and rate of decomposition of the solid peroxides, and the temperature and pH of the surrounding medium, are critical factors that control the rate of $O_2$ generation [16]. Although the solubility of SPO in water at 20 °C is considerably higher than that of MPO (120 g/L vs. 0.086 g/L), the amount of $O_2$ released through SPO decomposition is approximately 13 mg/L lower than that of MPO [15b]. Nonetheless, the use of solid peroxides has limitations in biomedical

applications due to the cytotoxic effects caused by $H_2O_2$ burst release and the generation of ROS during rapid dissociation [15b, 49]. Despite their drawbacks, solid peroxides can release $O_2$ over several days, making them a promising approach for $O_2$ generation.

Table 1. The mechanism, $O_2$ release capacity, solubility in water, and purity of different peroxides (Liquid and solid peroxides).

| Compound | Mechanism | $O_2$ release capacity | Solubility in water | Purity | Refs |
|---|---|---|---|---|---|
| **$H_2O_2$** | $H_2O_2$ decomposition | 12 mL per 1 g of $H_2O_2$ (in the presence of catalase) | Soluble | 30% v/v in water | [50] |
| **CPO** | $H_2O_2$ generation and decomposition | 22+/−3.3 mg/L | 1.65 g/L at 20 °C | ~ 60-80% | [50b, 51] |
| **SPO** | $H_2O_2$ generation and decomposition | 31+/−2.0 mg/L | 120 g/L at 20 °C | ~ 20-30% | [50b, 51a, 52] |
| **MPO** | $H_2O_2$ generation and decomposition | 44.38 mg/L | 1.65 g/L at 20 °C | ~15-25% | [50b, 51a, 53] |

To tackle the difficulties linked with burst release and the generation of ROS during rapid dissociation, two approaches have been employed. The first approach involves the use of hydrophobic materials to trap generator sources, thereby limiting water accessibility and degradation rate, and reducing burst release [8a]. The second approach employs catalysts such as silver, manganese compounds, iron oxide, and catalase to accelerate $H_2O_2$ decomposition and prevent ROS generation [48]. These approaches have proven successful for concentrations lower than 1% of hydrophobic $O_2$ generations in living tissue, although significant toxicity has been observed for higher concentrations [8a]. At concentrations exceeding 30 µM of the $H_2O_2$ produced by the dissociation of any peroxide, cytotoxicity has been reported due to the production of free radicals [10, 48]. However, the cytotoxicity can be avoided by the addition of catalase at a concentration of 50 U/mL or higher [10].

In addition to the use of catalase, another approach to mitigate the toxicity associated with the production of free radicals during rapid peroxides decomposition is the use of antioxidant materials to scavenge these radicals and reduce oxidative stress [54]. Solid peroxides offer several benefits, including low cost, easy storage, controllable $O_2$ release, in-situ $O_2$ release, and metabolizable byproducts [16]. It has been demonstrated that burst $O_2$ release is the primary cause of adverse effects on cells. Therefore, the development of a safe and sustained $O_2$-generating platform is crucial.

#### *2.1.2.3 Photosynthetic algae*

Photosynthetic algae have emerged as a potential alternative for sustained $O_2$ generation and delivery to hypoxic tissues (Figure 1). They have been reported to generate a constant amount of $O_2$ for over 30 days [55]. Additionally, photosynthetic algae secrete platelet-derived and vascular

endothelial growth factors, which promote an environment conducive to enhancing regeneration in the wound healing process [56]. Microalgae encapsulated in carboxymethyl chitosan gels have been found to produce $O_2$ and ROS at higher UV irradiation levels, thereby promoting the recovery process of wounds by reducing hypoxia and killing bacteria [57]. However, since the algae's $O_2$ generation depends on light, their applications in tissue engineering are limited to the depth of light penetration through the body [58].

### 2.1.3 Comparison between $O_2$ generating and carrier

Comparing the theoretical and practical ultimate $O_2$ release rate of $O_2$-generating and $O_2$ carriers, biomaterials with higher theoretical $O_2$ generation or carrying capacity exhibit prolonged $O_2$ delivery (Figure 7 and Table 2). While $O_2$ carriers such as lipidic micro and NPs have a high capacity, they cannot release $O_2$ in a sustained manner for more than a few days. Conversely, $O_2$-generating materials with a high $O_2$ payload and extended-release time are limited by toxic burst release and decomposition byproducts. For instance, CPO decomposition generates $Ca^{2+}$ ions that, at a concentration lower than 320 ppm, increase the proliferation of adipose-derived stem cells and accelerate their differentiation to the bone, without any adverse effects on viability. However, utilizing more CPO showed cytotoxicity due to the generated $H_2O_2$ [59]. Despite progress in controlling the $O_2$ release rate from $O_2$-generating materials, the initial burst release and scavenging of decomposed components remain challenging even with encapsulation into hydrophobic polymers. Therefore, using materials with smart and controllable degradation rates with enzymes, light, and heat could help attain a smart $O_2$-generating biomaterial with a sustained release rate.

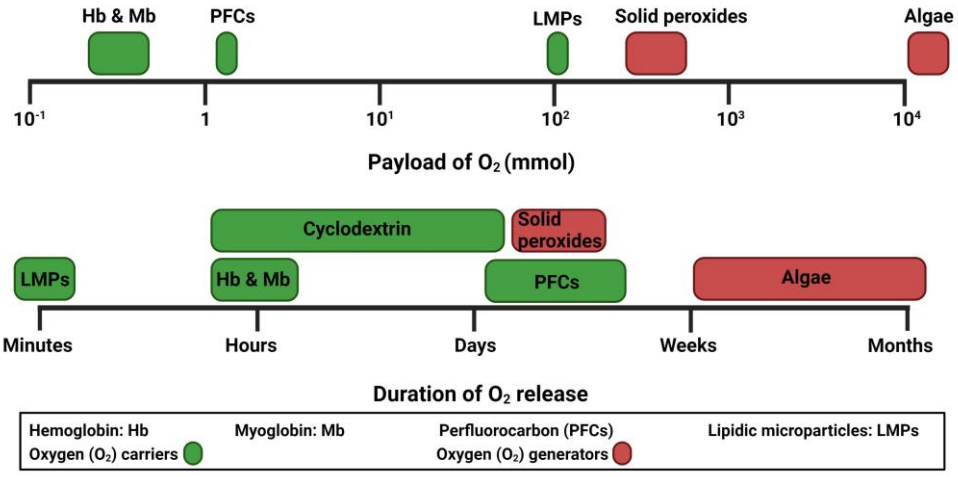


Figure 7. Diagram representing $O_2$ payload capacity and $O_2$ release duration. A higher $O_2$ payload results in a longer $O_2$ release. Therefore, $O_2$ generators with a higher $O_2$ payload capacity than $O_2$ carriers can supply $O_2$ for a longer time. Algae in a suitable condition can generate $O_2$ for months. While $O_2$ carriers can provide $O_2$ for a few days. (Adapted, 2021, Elsevier [8a]).

In the continuum of oxygen utilization, the methodologies outlined in the preceding section (2.1) lay the groundwork for understanding the intricacies of oxygen administration. This sets the stage for an exploration of therapeutic interventions involving oxygen in the next Section 2.2 which focuses on oxygen therapy.

Table 2. A summary of the comparison between $O_2$ delivery methods with their advantages and disadvantages.

| Method | Mechanism | $O_2$ payload | $O_2$ release duration | Advantages | Disadvantages | Refs |
|---|---|---|---|---|---|---|
| **Clinical $O_2$ delivery methods** | | | | | | |
| **HBOT** | supplying pure $O_2$ under high pressure | 1-3 atm | 1-3 h | Easy to use | Time-consuming, high-cost, large equipment, can be toxic under high pressures, relative efficiency | [8a, 60] |
| **NBOT** | supplying pure $O_2$ under normal pressure | 1 atm | 1-3 h | Easy to use | Time-consuming, high cost, large equipment, relative efficiency | [61] |
| **$O_2$ carriers** | | | | | | |
| **Hemoglobin and myoglobin** | Binding of haem groups with $O_2$ | <1 mmol | Minutes to hours < less than a day | Utilizing natural human protein, ability to bond and connect to polymers, long shelf life, local delivery | Ability to bond to NO and induce oxidative damage, short half-life in blood circulation | [24, 27, 31, 62] |
| **PFC** | Increasing $O_2$ solubility via Van der Waals forces | <10 mmol | From hours to days < weeks | Low cost, synthetic, long shelf life, bonding with polymers, local delivery | Hydrophobic, Low $O_2$-carrying ability at physiological $O_2$ level, can bind to NO and induce oxidative damage, should recharge | [8a, 16, 34, 63] |
| **Cyclodextrin** | Binding with $O_2$ | - | From hours to days < weeks | Non-toxic, biodegradable, binding with other polymers, local delivery | Short $O_2$ release time, low $O_2$ payload capacity | [8a, 41] |
| **Lipidic microparticles** | Encapsulation of $O_2$ | $<10^3$ mmol | < hours | Increasing the $O_2$ loading by lipidic bubbles, providing a high concentration of $O_2$ in a short time, useful for ultrasound imaging | Short release time, relatively large size (≥10 µm), toxic burst release | [8a, 46a, 54] |
| **$O_2$-generators** | | | | | | |
| **$H_2O_2$** | $H_2O_2$ decomposition | - | - | Rapid $O_2$ release, incorporating in particles, the catalyst can be used to increase the reaction rate | High toxicity without catalyst, low controllability on $O_2$ release, toxic burst release | [8a] |
| **Solid peroxides** | Generating $H_2O_2$ | $<10^3$ | <a week | Easy to use, high $O_2$ payload, biocompatible byproducts, long shelf life | low controllability on $O_2$ release, toxic burst release, change the pH of release media with by- | [8a, 54, 64] |

| | | | | | | |
|---|---|---|---|---|---|---|
| | | | | | products, High toxicity without catalyst | |
| **Algae** | Photosynthesis | ≥$10^4$ mmol | ≥ weeks | Theoretically, infinite $O_2$-generating, biocompatible, secrete growth factors | Limited application in the deep tissues, not extensively investigated for safety in vivo | [8a, 16, 58, 65] |

## 2.2 $O_2$ Therapy

All $O_2$ carriers and generating materials, according to their advantages, disadvantages, and application requirements, can be used in a variety of biomedical applications (Figure 8 and Table 3). For example, photosynthetic algae have the potential for use in skin tissue regeneration; however, it is not practical for inner organs due to a lack of light. CPO decomposition not only compensates for $O_2$ defection in bone tissue engineering but also generates $Ca^{2+}$, which improves cell differentiation. Generally, the applications of the $O_2$ generating and carrier biomaterials can be categorized into three main categories: 1) Cell and tissue survival, 2) Cancer therapy, and 3) Metabolic reprogramming (Figure 8).

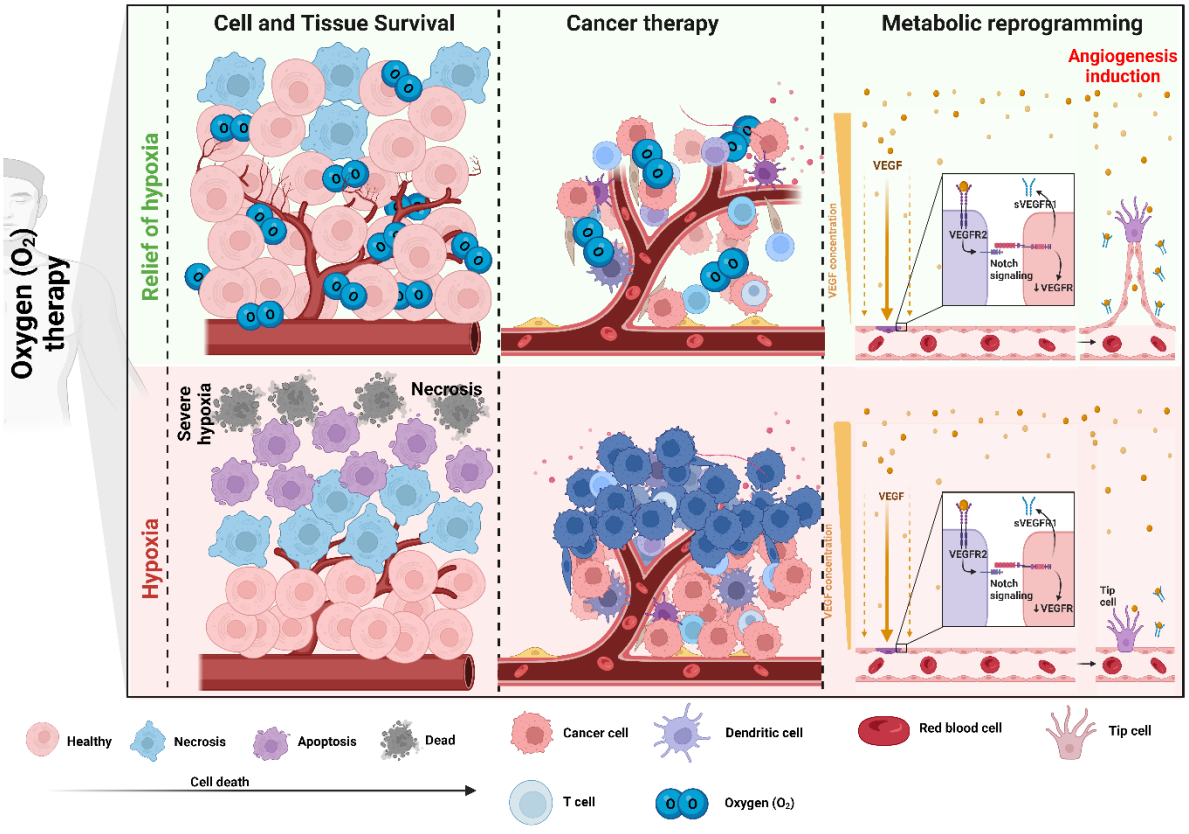


Figure 8. Schematic representation of the main applications of $O_2$ carriers and generators in biomedicine. Based on the function of the delivered $O_2$, the applications of $O_2$ carrier and generator biomaterials can be divided into 1) Cell and tissue survival, 2) Cancer therapy, and 3) Metabolic

reprogramming. Oxygen carriers and generators can alleviate hypoxia, thereby enhancing cell survival. Moreover, adequate $O_2$ improves the efficiency of cancer therapy approaches.

### 2.2.1 Cell and tissue survival

The success and viability of an implant depend on the avoidance of anoxia [8a], which can result in inactivating proteins and DNA [66], as well as cellular damage through free radicals leading to cell death *in vivo* implantations [67]. Despite efforts such as growth factor supplementation, 3D bioprinting, and modification of the 3D structure to enhance $O_2$ supply within the implanted tissue, the challenge of limited $O_2$ diffusion remains [67]. Hence, 3D scaffolds and implants based on $O_2$-carrying and generating biomaterials have been proposed [8a, 10]. However, precise adjustment of the $O_2$ release rate is crucial, varying based on the source of $O_2$, release media, targeted tissue, and materials. While $O_2$ improves implant performance, its delivery must be carefully optimized to avoid unintended consequences. For example, to enhance osteogenesis and angiogenesis while controlling osteoclastogenesis in bone tissue, PFC and catalase MPs were incorporated into a gelatin methacrylate hydrogel acting as an $O_2$ carrier and ROS scavenger (Figure 9a) [68]. In another approach, a 3D-printed hydrogel with CPO and IL-10 microspheres boosted DNA content, eNOS gene, and CD31 gene expression under dynamic microbioreactor circumstances [69]. In addition, using hydrophobic antioxidant materials extended $O_2$ release for up to 10 days, by decreasing CPO water accessibility, thus extending and scavenging free radicals of the decomposition reaction and enhancing cell viability [54].

### 2.2.2 Cancer therapy

The hypoxic microenvironment of advanced solid tumors is associated with the resistance of cancer cells to first-line therapeutics such as chemotherapy, RT, PDT, and sono-dynamic therapy (SDT) [70]. Photosensitizers can convert $O_2$ into ROS and singlet $O_2$, which can damage tumor cells' nucleic acids and proteins [71]. Thus, alleviation of tumor hypoxia by $O_2$ carrier and generating biomaterials has been offered efficiently to deliver $O_2$ via direct delivery or catalyze the decomposition of $H_2O_2$. Stabilized $O_2$ microbubbles with polydopamine shells have been shown to increase $O_2$ concentration to 6 mg/L within 25 minutes and maintain it under saturated conditions for 36 hours. Even with this short $O_2$ supply, tumor weight exposed to the MPs and PDT decreased compared to the control sample [72]. Sustainable $O_2$ release not only provides sufficient $O_2$ for photosensitizers and enhances PDT performance but also promotes the activation of dendritic cells [73]. Light-controlled $O_2$ generation and sustained release with CPO have been used to alleviate hypoxia and induce anti-tumor immunity (Figure 9b) [74]. Under laser irradiation, phase change lauric acid melts and thereby water access to CPO for generating $O_2$. The designed materials showed synergistic potential in CDT and PDT.

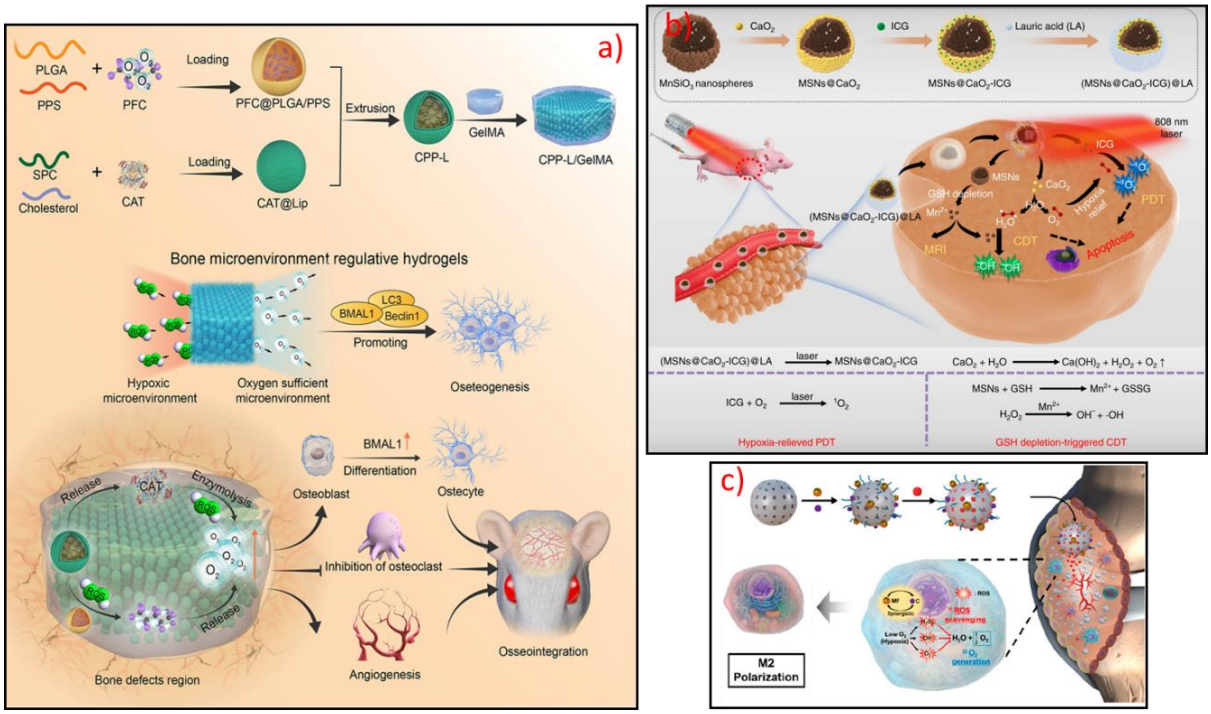


481

482 Figure 9. (a) The schematic represents the regulation of the bone microenvironment by an $O_2$-
483 generating and ROS-scavenging hydrogels based on GelMA containing PFC and CAT (Open Access,
484 2023, ScienceDirect [68]), (b) a schematic illustration of the synthesizing and therapeutic mechanism of
485 thermos-responsive $O_2$ and $H_2O_2$ generating NPs for synergistic CDT/PDT (Open Access, 2020, nature
486 [74]), and (c) therapeutic mechanism of manganese ferrite and ceria NPs-anchored MSNPs that can
487 simultaneously generate $O_2$ and scavenge ROS to decrease the level of M1 macrophage for
488 rheumatoid arthritis (copyright © 2019, American Chemical Society).

489 ### 2.2.3 Metabolic reprogramming and angiogenesis

490 Angiogenesis, the formation of new blood vessels, is primarily induced by hypoxia, but
491 prolonged hypoxia can hinder this process [8a]. The $O_2$ tension can be manipulated to modulate the
492 angiogenic process, which is hypothesized to be accelerated by ROS as a signaling molecule in the
493 presence of $O_2$, decreasing the activity of the prolyl hydroxylase protein [8a]. One practical approach
494 for improving angiogenesis is to cover $O_2$-generating sources with multi-layer shells for sustained $O_2$
495 delivery.

496 $O_2$-releasing 3D scaffolds have been developed to extend the release of $O_2$ for up to 19 days,
497 resulting in better angiogenesis in the early stage (4 weeks) after surgery [75]. Polycaprolactone-sodium
498 percarbonate (PCL-SPC) nanofiber mats formed blood vessels rapidly at CAM assay, and their HIF-1α
499 gene expression was 2.39-fold higher than the sample without an $O_2$-generating source [76]. Hydrogels
500 with CPO-loaded PCL MPs were designed for controlled $O_2$ release in bone regeneration.
501 Preosteoclasts showed increased LDH, and ALP activity with CPO concentrations up to 60 mg/ml, while

declining at higher concentrations. [64a]. $O_2$ carriers and generators have been hypothesized to induce the pro-inflammatory M2 phenotypes by downregulating HIF-1α under hypoxic conditions (Figure 9c) [77]. Therefore, controlling $O_2$ tension could impact macrophage behavior, thereby regulating the M1 and M2 phenotypes. ROS facilitated by Nox2, regulates cell function, inflammation, and pathophysiology in tissues [78].

Optimization of ROS concentration in the oxidative microenvironment of a tumor is required to maintain proper M1 and M2 function [79]. The potential cytotoxicity of ROS highlights the need for a delicate balance between ROS generation and regulation, as ROS plays a critical role in both tumor treatment and pathological diseases. In a joint environment, for instance, elevated $pO_2$ levels can prevent the degradation of the extracellular matrix, chondrocyte death, and joint inflammation caused by high levels of peroxides, NO, and hydroxylated radicals [8a, 35]. Enzymes and molecules such as catalase, superoxide dismutase, and glutathione act as natural antioxidants and play a crucial role in ROS regulation [80].

Inherent antioxidant materials or systems capable of releasing and generating antioxidant materials are the primary approaches to regulating ROS concentrations [81]. $O_2$-generating biomaterials have proven to be effective in ROS regulation [80]. For example, released $O_2$ generated from the degradation of $MnO_2$ NPs has been shown to protect against cartilage inflammation, while $MnO_2$ NPs coated with collagen have defended fibroblast cells against oxidative stress [82]. Modified $MnO_2$ with polyethylene glycol (PEG) has also been investigated for its role in ischemic stroke, with the relative expression of inflammatory factors such as IL-1β, IL-6, and TNF-α decreasing remarkably after treatment with $MnO_2$ particles, according to a study by Song-Bin Yang et al. ELISA assay [83].

Table 3. The typical paradigms of $O_2$-releasing biomaterials for versatile biomedical applications. Listed 2022 and 2023.

| Gas | Source | Mechanism | Control method | Ultimate gas release | Release duration | Application | Remarks | Refs |
|---|---|---|---|---|---|---|---|---|
| **$O_2$** | Hb ($O_2$ carrier) | Binding with $O_2$ via heme group | NPs containing Hb and Mn-phthalocyanine | ~6 mg/L | In 15 min | Tumor inhibition (cancer therapy) | The Hb showed faster release in hypoxia than in normoxia. | [84] |
| | | | Loading Hb with poly(lactide-co-glycolide) into a nanozyme shell | - | - | Biocompatible and antioxidant $O_2$ carrier | The particle showed a potential to be used as a blood surrogate. | [85] |
| | PFC ($O_2$ carrier) | Dissolving $O_2$ via Waan der Vals interaction | NPs based on PFC, PLGA, and superparamagnetic oxide | ~10-12.5 mg/L | 4 h without high-intensity focused ultrasound (HIFU), and ≤30 min with HIFU | Imaging-guided cancer therapy | HIFU shows remarkable promise in solid tumor treatment | [86] |
| | | | Incorporating periodic mesoporous organosilica-PFC particles into GelMA hydrogel | - | 12 days in normoxia and 14 days in hypoxia | Enhancing cell viability of fibroblast | Particles increased the cell viability of fibroblast under hypoxia and normoxia | [87] |
| | | | Core-shell particles based on perfluorooctyl bromide (core) and PLGA (shell) | ~30 mg/L | In 10 min | Tissue engineering and blood substitution | $O_2$ carrier had a concave shape. | [88] |
| | | | Conjugation on polydopamine | ~225mmHg | 12 h | Bone regeneration | PFC not only supplied O2 continuously but also improved the antibacterial activity of the hydrogel | [89] |
| | | | Encapsulating PFC droplet into alginate shell | ~8 mg/L with low-intensity ultrasound | In 5 min | Cancer therapy | The PFC droplets broke the alginate shell via liquid-to-gas transition with ultrasound | [90] |
| | | | Conjugating PFC on methacrylamide chitosan microparticles | - | - | Alleviating hypoxia (cancer therapy) | The fluorinated microparticles reduced the number of hypoxic cells within the core regions of the particles. | [91] |
| | Liposome ($O_2$ | Encapsulating $O_2$ | Loading Hb to a phototherapeutic liposomal | ~7-12 mg/mL | 300 min | Rheumatoid arthritis treatment | In the presence of infrared light, the liposome reduced M1 macrophage population and | [92] |

| | | | | | | | |
|---|---|---|---|---|---|---|---|
| | carrier ) | | | | | expression of hypoxia-inducible factor-1α | |
| | $H_2O_2$ (Liquid peroxide) | Decomposition of $H_2O_2$ by $MnO_2$ | Composite nanoplatforms based on peptide, chlorin, and $MnO_2$ | - | - | Improvement of the immunosuppression microenvironment and alleviating hypoxia | $MnO_2$ can react with the in situ $H_2O_2$ to generate $O_2$ and alleviate the hypoxia | [93] |
| | | | Synthesis composite hydrogels based on GelMA containing MnO2, calcium phosphate, and fibroblast activating protein inhibitor | - | - | Repair of bone osteoporotic bone defects | The hydrogels regulated macrophage, eliminate ROS, and promote the repair of bone defects | [94] |
| | | Decomposition of $H_2O_2$ | Nano catalytic particles based on hollow mesoporous Prussian blue | - | - | Alleviate tumor hypoxia (cancer therapy) | The photothermal activity of the particles elevated the catalase activity of the particle for $O_2$ | [95] |
| | | | Ultrasound-activated NPs based on manganese dioxide and chlorine e6 | - | - | Alleviate tumor hypoxia to enhance STD therapy (cancer therapy) | The expression level of factor 1α and vascular endothelial growth factors was detected by immunofluorescence | [96] |
| | | | Light-triggered $O_2$ self-supplied phototherapeutic platforms to decompose $H_2O_2$ | - | - | Alleviate tumor hypoxia (cancer therapy) | The singlet $O_2$ enhanced the mortality rate of ID8 cells. PDT increased the $O_2$-generating rate | [97] |
| | | | Co-loaded catalase and PFC NPs into GelMA hydrogels | ~5mg/mL from 10mM of H2O2 | 18 days | Enhancing bone repair | Although $O_2$ enriched microenvironment inhibited osteoclastogenesis, osteogenesis, and angiogenesis increased | [68] |
| | | | Incorporation of hollow manganese dioxide NPs into GelMA | - | - | Bone Repair | Bone formation | [98] |
| | CPO | Decomposition of CPO | Incorporating CPO into alginate hydrogel | ~25 mmHg | 20 days | Bone tissue engineering | 3% w/w of CPO represented 22% enhancement in cell viability under hypoxia | [99] |
| | | | Incorporating into PLGA microparticles | ~20-80% | 24 h | Alleviating myocardial hypoxia | The generated $O_2$ from PLGA microparticles containing CPO increased primary rat cardiomyocyte | [100] |

| | | | | | | | | |
|---|---|---|---|---|---|---|---|---|
| | | | Encapsulation into microenvironment sensitive NPs based on ZIF-67- hyperbranched-poly-l-lysine | ~2 mg/mL in pH of 7.4 and ~ 6 mg/mL in pH of 5.5 | 60 min | Alleviating hypoxia in infected wounds | The particles contusing $O_2$ generating source improved the healing process of S. aureus-infected wounds | [101] |
| | | | Immobilization of CPO and catalase into an inducible hydrogel | $pO_2$=~80% | 60 min | Accelerate wound proliferation and remodeling phases | The hydrogels facilitate cell proliferation and neovascularization | [102] |
| | | | Covering COP by liposomal nanoplatforms | ~60% | 24 h | For cooperative in chemo dynamic/starvation cancer therapy | CPO provided the efficient $H_2O_2$ for effective chemo dynamic therapy | [103] |
| | | | Developing a composite nanogenerator based on a cobalt metal-organic framework with CPO | ~6 mg/L | 60 min | Hypoxia improvement, chemodynamic therapy, and wound healing | The generated $H_2O_2$ not only generated $O_2$ to alleviate hypoxia but also showed a synergistic anti-biofilm capacity | [101] |
| | | | Embedding CPO into nanohybrid NPs | ~5 to 30 % in different pH | 30 min | PDT and $Ca^{2+}$ overloaded therapy | The generated singlet $O_2$ via $H_2O_2$ decomposition in the presence of Ce6 showed promising performance in PDT | [104] |
| | | | Loading into polyoxometalate NPs | - | - | Electrically enhanced chemodynamic therapy | Simultaneous endogenous and exogenous stimulation improved the Fenton-like response | [105] |
| | | | Loading in PCL particles | ~50% | 14 days | Regenerate critical bone defects | In vivo, bone remodeling and vascularization results revealed that the PCL particles containing CPO embedded into GelMA hydrogels can provide sufficient $O_2$ for a bone defect with the size of 70 $mm^3$ | [64a] |
| | Micro algae | Photosynthesis | Loading Chlamydomonas reinhardtii into alginate hydrogel | 11.2 ±2.5 nmol/$cm^2$.min for $5.10^7$ microalgae/mL | - | Wound healing | The optimal $O_2$ generation was at $5.10^7$ microalgae/mL. The hydrogels did not show any skin irritation on the skin of 20 healthy human volunteers. | [106] |
| | | | In situ printed alginate and GelMA containing Chlorella pyrenoidosa | From 0.9 to 9.9 mg/L with microalgae content of $10^5$ to $10^7$ cells/mL | Equilibrium at 60 min | Wound healing | The hydrogel containing microalgae was printable. Generated $O_2$-facilitated cell proliferation, migration, and differentiation under hypoxia. | [107] |

| | | | | | | |
|---|---|---|---|---|---|---|
| | Chlorophyceae was functionalized with phosphorus nanosheets through polyprotic acid | ~4 mg/L | 20 min | Cancer therapy | The microalgae relieved tumor hypoxia, promoted infiltration of T cells, and provided sufficient substrates for improving photodynamic therapy. | [108] |
| | Chlorella was covered with macrophage membrane | ~8 mg/L | In 40 min | Hypoxia alleviation | The microalgae were efficient $O_2$ generators and immune adjuvants. | [109] |

525

# 3 Nitric oxide (NO)

Nitric oxide (NO) is a crucial component of life since NO is known as a utilizable nitrogen source by organisms [110]. Plants and bacteria synthesize NO via the reduction of nitrite ($NO_2^-$) and nitrate ($NO_3^-$). In Mammalian physiology, it is generated through enzymatic oxidation of L-arginine to NO and L-citrulline. At least 3 isoforms of NOS have been discovered so far: neuronal (nNOS), inducible (iNOS), and endothelial NOS (eNOS). NO is an odorless and colorless gas with intense active free radical activity [63]. NO is also an important signaling molecule that directly and indirectly affects various cellular and physiological functions, such as vasorelaxation, gene regulation, bronchodilation platelet aggregation, vascular permeability, angiogenesis, hormone secretion, neuronal communication, inflammation and immune system, wound healing, and gastrointestinal mobility [63, 111]. NO, regulating the immune system exerts anti-inflammatory effects, and intercede endothelial function as a vasodilator at low concentration around pM-nM [112]. However, at abnormally high concentrations (~μM), can lead to cell death and contribute to chronic inflammation via the creation of strong nitrosative stress [113]. Therefore, the biological application of NO has been defined by the kinetic behavior and the exposure time of NO. However, uncontrolled diffusion to other parts, challenging accumulation in the targeted tissue, and short half-life (<10s) are current limitations that reduce the efficiency of NO therapy [63]. In order to overcome the NO delivery limitations, NO donors with the ability to control and targeted delivery have been developed by researchers, which will be explained in detail in the next section.

## 3.1 NO delivery

Due to the multimodal behavior of NO and the dependency on the concentration and duration of action, controllable NO delivery systems have been emerging for several biomedical applications [63, 113-114]. Controllable NO delivery systems involve the delivery of gaseous NO, the delivery of NOS substrates as the precursor of NO, using low molecular weight NO donors, and the controlled delivery of NO using sophisticated biomaterials. Figure 10 shows the main NO delivery systems with their NO-releasing mechanisms.

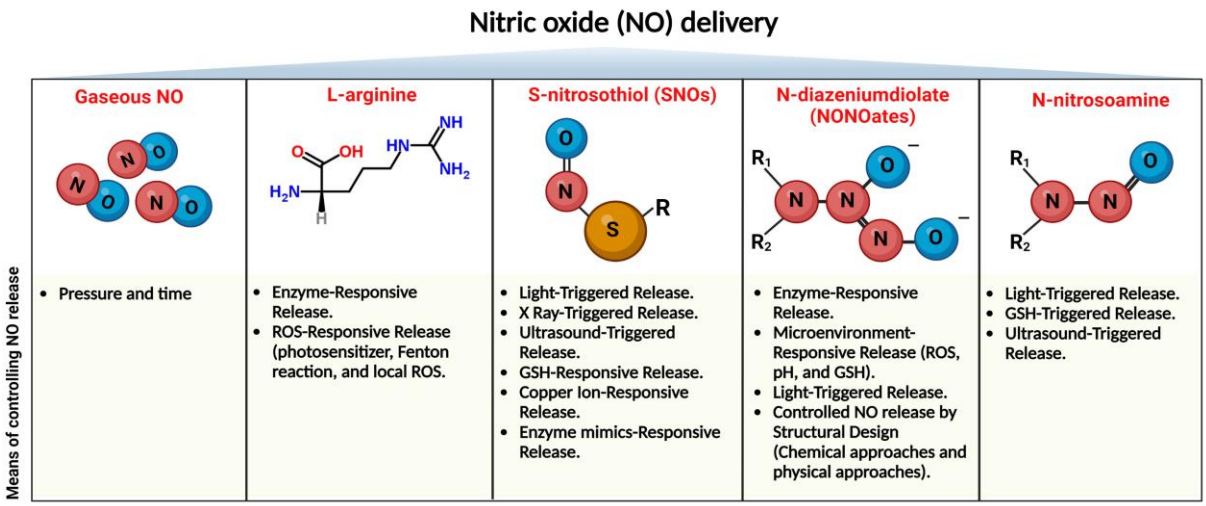


Figure 10. The schematic represents a summary of the main categories of NO delivery and their corresponding NO-releasing mechanisms. Depending on the chemical structure of the NO donors, they can have different releasing mechanisms, such as enzymes, ROS, light, ultrasound, and temperature-responsive release. Therefore, the rate of NO release can be controlled through structural design, employing either physical or chemical approaches.

### 3.1.1 Gaseous NO

The most straightforward way to deliver NO is by utilizing the gaseous form of NO. Similar to HBOT, NO can also be applied in hyperbaric therapy. However, the NO pressure and exposure time should be tolerated to avoid the toxic effect of high pressure. The safe dose and exposure time of gaseous NO for wound healing has been reported by Rezakhanlou et al using a mouse lymphocyte model, which is 5, 25, 75, and 200 ppm for 8 hours [115]. A pressure higher than 200 ppm decreased immune cell proliferation and cell viability. Although the gaseous NO delivery for wound healing has been accompanied by promising achievements, has not shown remarkable outcomes in other therapeutic applications due to a lack of targeted delivery, increasing the NO concentration all over the body, and generating RNS via reaction with $O_2$. Continuous oversight of pressurized NO cylinders, time-consuming, high reactivity of NO with the $O_2$ in the air, and requiring an anoxic environment are some factors that limit the hospital setting [116].

### 3.1.2 L-arginine

L-arginine, an amino acid found in typical diets, plays a crucial role in generating citrulline and NO in the presence of NO synthases. This process occurs immediately via the terminal guanidine residue of L-arginine. Additionally, $H_2O_2$ oxidation in the presence of catalyze produces citrulline and NO. Almost 60% of absorbed L-arginine provided by a typical diet (5 g) can survive degradation in the intestine and enter the circulation system, resulting in a circulating L-arginine concentration of 75 ×

$10^{-6}$ to 100 × $10^{-6}$ M [116]. It is important to note that only free L-arginine can react with NO synthases because protein-conjugated L-arginine cannot be oxidized by these enzymes [117]. However, dietary supplementation with L-arginine can increase the overall NO concentration in the body.

In terms of targeted and controlled L-arginine release, the enzyme-response release is one approach. For example, incorporating L-arginine and glucose oxidase (GOx) into a CU-metal-organic framework (CU-MOF) with Fenton-like catalytic activity can develop a NO-generating antibacterial biomimetic multienzyme system [118]. The $H_2O_2$ generated from the oxidation of glucose catalyzes L-arginine to release NO in a sustained manner. Another approach involves using a photosensitizer to generate reactive ROS, which can then catalyze L-arginine to produce NO. By loading L-arginine and a photosensitizer onto a scaffold based on bovine serum protein, ~30 μM of NO could be generated for 30 minutes with laser irradiation [119]. Local ROS in the body can catalyze L-arginine and produce NO in the body's circulation before reaching the targeted tissue [120].

### 3.1.3 S-nitrosothiols (SNOs)

S-nitrosothiols (SNOs) are another NO donor, also known as thionitrite, that include S-nitrosoalbumin (AlbSNO), S-nitrosoglutathione (GSNO), S-nitrosocysteine (cySNO), and S-nitrosohemoglobin (HbSNO). SNOs have a weak energy bond (~150 kJ/mol) and can easily decompose to NO through various environmental factors such as light, pH, heavy metals, heat, and sodium ascorbate [5]. SNOs can be produced through redox reactions or disproportionation between nitrosating agents like $NO_2$, $N_2O_4$, NOCl, $HNO_2$, and $N_2O_3$ with thiols in an inert solvent [121]. Since SNOs are sensitive to light, near-infrared (NIR), UV-vis, and X-ray have been utilized to trigger NO release from SNOs [122]. Using X-ray radiation with higher energy than UV-vis and NIR can overcome the limitations in penetration and obstacles of endogenous differences. Moreover, X-ray radiation has exhibited an improvement in the killing effect of radio-therapy to inhibit tumor cell growth [123]. A hypoxic microenvironment of tumor cells decreases the X-ray efficiency in generating NO by reducing X-ray absorption, which can be compensated for with higher doses of radiation. However, higher X-ray radiation may damage normal tissues near the targeted tumor [5].

To improve X-ray absorption and convert the absorbed photons into heat for photothermal therapy (PTT), materials with high photoelectric absorption coefficients, along with SNOs, can be used [124]. To oxidation of heavy metals such as $Cu^{2+}$ and $Cu^{+}$ with SNOs can promulgate the generation of NO from SNO decomposition. However, the concentration of heavy metals should be considered to avoid undesired toxicity [5]. Controlling of NO production by tuning the percentage of Cu doped into zeolitic imidazolate framework (ZIF-8) has been reported [125].

Organoselenium compounds, such as natural glutathione peroxides (GPx) and diselenide selenocystamine (SeCA), are enzyme-mimicking catalysts that can catalyze long-term NO release from SNO decomposition due to the leakage of catalytic sites [5]. To increase the stability and activity of the selenium catalyst, it was suggested to introduce catalytic sites into the backbone of a polymer [126]. Selenium-containing polyurethane films provided a sustained release of NO ($5.05\times10^{-10}$ mol/cm$^{-2}$ min$^{-1}$ for 30 days) [123]. Catalyzing SNOs to generate NO by utilizing glutathione (GSH) is another effective way to deliver NO. Li et al. reported that GSH could break the disulfide bonds of keratin to thiol such that the produced thiol catalyzed the GSNO and generated NO, attaining a concentration of ~10 uM after 36 hours [126].

SNOs can decompose to NO via an autocatalytic reaction [127]. The S-N bonds of SNOs cleavage to form NO$^{\bullet}$, which then reacts with $O_2$ to generate $N_2O_3$, leading to further decomposition of SNOs [5]. The autocatalytic process of SNOs can be promoted by ultrasound. Ultrasound increased the concentration of the generated NO from the decomposition of GSNO from ~1 μM to ~10μM in the first 5 min [128]. Direct regulation of NO synthase can be beneficial for therapeutic purposes by producing NO [116]. iNOS and eNOS by upregulating the stress of tissue and constitutively expression, play crucial roles in wound healing. It has been reported that iNOS gene delivery using viral vectors in iNOS deficient mice accelerated wound closure time from 25 days to 15 days by generating [129]. Moreover, local delivery of eNOS to diabetic wounds using a fibrin scaffold was able to fasten the healing process as well [130].

### 3.1.4 N-diazeniumdiolates (NONOates)

N-diazeniumdiolates (NONOates) represent the most frequently employed NO donors capable of generating NO spontaneously through a dissociation reaction [131]. NONOates have the potential to be modified into protected forms that can be selectively activated to release NO in a controlled manner. The dissociation reaction of NONOates generates two moles of NO in the presence of protons through the pseudo-first-order rate law [4]. The rate of the dissociation reaction is dependent on the pH of the reaction media and the structure of the donor [5]. NONOates have a great potential for modification and can be easily derived into protected forms that can deliver NO to the targeted organ. For controlled delivery of NO using NONOates functional groups, several enzyme-responsive prodrugs have been developed. Various enzymes such as Glutathione S-transferase $\pi$ (GST$\pi$) [132], Galactosidase [133], nitroreductase [134], and β-glucuronidase [5] have been utilized to remove the protecting groups and activate NO prodrugs to produce NO. Among these enzymes, galactose-protected NONOates are the most well-known glycosylated NO prodrugs which release NO via breaking glycosidic bonds in the presence of galactosidase [135].

To engineer the enzyme-prodrug therapy, protected NONOates have been embedded in various polymers such as chitosan [136] and PCL [137], or implanted on the surface of a wide range and metal substrates [5]. However, the unintended disassociation of NONOates by β-galactosidase can decrease the stability of the prodrugs [138]. The bump and hole strategy, initially designed for targeting individual protein kinases, has been adapted to hinder the decomposition of NONOates in circulation. This strategy leads to precisely controlled NO release [5]. In addition to natural enzymes, mimic enzymes have been widely used to release NO [139]. The catalytic activity of some metals, metal oxidase, and nonmetallic particles to generate NO from exogenous (β-gal-NONOate) and endogenous (S-nitrosoglutathione) NO donors was investigated. Zinc oxide particles with a releasing rate of 28 × $10^{-6}$ M had the highest activity to produce NO from 100 × $10^{-6}$ M of β-gal-NONOate [140]. The release of NO could be adjusted by controlling the zinc oxide concentration since the release rate depended on the zinc oxide concentration.

Furthermore, NO prodrugs can dissociate and release NO in response to microenvironment conditions such as ROS concentration and pH. ROS-activated NO donors have shown better potential for cancer therapy than enzyme or light-response donors [5]. Arylboronate and α-ketoamide have been introduced as an $H_2O_2$-response switch to design NO donors [141]. Additionally, an $O_2^{\bullet-}$-responsive mitochondria-targeted NO donor has been designed to release NO and consume cytotoxic $O_2^{\bullet-}$ to alleviate ischemia reperfusion injuries in the heart [142]. The concentration of the physiological proton leads to unwanted NO release from NONOates during circulation. The proton-response release mechanism can be useful to deliver NO to organs with inflammation, infection, and malignant tumors [5]. A combination of NONOates pH response and an anticancer drug was loaded into a hollow microsphere based on poly lactic-co-glycolic acid (PLGA) for tumor treatment [131]. NONOates released NO by penetrating protons of the acidic microenvironment of the tumor [143]. Core/shell NPs pH-response containing NONOates were used to destroy bacteria. Accepting the protons of the infected environment by imidazole groups of the shell induced the proton-promoting NO release from incorporated NONOates [144].

Similar to SNOs, NONOates can release NO in a controlled manner by applying light, UV-vis, and X-ray radiation. NONOates release NO by decomposition of the zwitterionic structure via induction [5]. The concentration of protons and the temperature of the reaction media affect NO release. Hence the rate of NO release from NONOates may be adjusted by controlling the concentration of proton and the temperature by introducing the light-sensitive materials to the NO donors [145]. However, the main drawback of the light-triggered strategy is the poor stability of NO donors and the decomposition of most NO donors during normal physiological circumstances before

reaching the organ. To regulate NO release and minimize of rapid decomposition of NONOates in the early stage, the NONOates are physically and chemically bonded to other components [146].

### 3.1.5 N-nitrosoamines

N-Nitrosoamines are frequently utilized as NO donors, releasing NO through the triggering of light-induced heterolysis or homolysis of N-NO bonds [147]. The mechanism of NO release via N-Nitrosamines is similar to SNOs. However, the activation of N-nitrosoamines with short-wavelength light like UV or visible light restricts their biomedical applications due to inherent phototoxicity [148]. To overcome this limitation, chromophores with NIR or red absorbing capacity and upconversion NPs have been proposed to develop N-nitrosoamines with longer-wavelength activation [5]. NO donors based on coumarin, along with the use of palladium (II) tetraphenyltetrabenzoporphyrin, and a near-infrared (NIR) light-switchable NO release system employing magnesium silica and yolk-shell upconverting nanoparticles, have been documented in the literature [149]. The system could release around 30 μM of NO in 20 min with a 980 nm laser [149]. Additionally, photothermal materials can activate N-Nitrosoamines to release NO via absorbing photons and converting them into electrons. Folic acid-polyethylene glycol-modified polydopamine NPs containing an NO donor (N-Nitrosoamines ) have been synthesized for triple-combination therapy [150]. These NPs could convert absorbed NIR light into active electrons, leading to NO release from the NO donor.

An alternative approach to activating N-Nitrosoamines that aims to avoid undesired phototoxicity is the utilization of light energy in combination with glutathione (GSH). This method involves using light to initiate chemical reactions that produce N-Nitrosoamines while simultaneously utilizing GSH to decrease the potential toxicity associated with this process [16]. Sun et al. used a combination of GSH and a co-activatable photosensitizer to demonstrate this approach [151]. The emergence of a novel photosensitizing system, specifically at 800 nm with a value of 166 ± 22 GM, in addition to its fluorogenic properties, presents a promising opportunity for various biomedical applications. This system, particularly in the context of low-light dose PDT, demonstrates the potential for utilization in both normoxic and hypoxic conditions.

### 3.1.6 Silicon nitride ($Si_3N_4$)

Silicon nitride ($Si_3N_4$) is recognized as a new synthetic non-oxide ceramic composed of amorphous and crystalline grain-boundary phases [152]. Initially employed in industrial applications due to its high thermal and mechanical properties, $Si_3N_4$ has recently demonstrated excellent capabilities in enhancing osteoblast proliferation, differentiation, bone formation, and bactericidal activity through its nitrogen chemistry [152-153]. The aqueous protonation/dissociation reactions of basic secondary amines (Si-NH) and amphoteric silanols (Si-OH) on the surface of $Si_3N_4$ describe its nitrogen

chemistry [153b]. The amine surface sites of $Si_3N_4$ can dissociate from the silanol surface sites via a reaction between $Si_3N_4$ and nucleophilic agents, known as the $S_N2$ mechanism [153b]. This amine dissociation reaction results in the release of ammonia ($NH_3$) or ammonium ions ($NH_4^+$) at high and low pH values, respectively [153b, 154]. Acidic conditions lead to higher ammonia production than ammonium ions [153b]. The ammonium ions are vital nutrients employed in the synthesis of foundational proteins for genetic compounds and enzymes, leading to cell proliferation and differentiation [154]. Moreover, ammonium ions can enhance osteoblast-driven bone tissue synthesis, support the proliferation of skin fibroblasts, and encourage the synthesis of collagen type 1 in human osteoblasts in conjunction with the leaching of orthosilicic acid [153b, 154]. Furthermore, ammonium ions serve as nutrients for both prokaryotic and eukaryotic cells. In contrast to ammonium ions, ammonia can penetrate the external membrane of DNA and RNA structures in both bacteria and mammalian cells, reducing their stability and resulting in cellular toxicity. [153b]

The liberation of unpaired electrons caused by the nitrogen release reaction converts ammonia into hydroxylamine ($NH_2OH$). The hydroxylamine further reduces into nitrite ($NO_2^-$) via the hydroxylamine oxidoreductase process, contributing to nitric oxide (NO) formation. The nitric oxide formation reaction is related to the generation of four additional electrons, which contribute to ammonia oxidation and the generation of proton gradients [153b, 154]. The $Si_3N_4$ surface plays a role similar to catalyzing enzymes such as iNOS and eNOS. In an oxidative environment, $Si_3N_4$ can release NO in an aqueous solution. Further reactions of the generated NO with superoxides lead to the production of peroxynitrite with high antibacterial activity [153b].

### 3.1.7 A comparison between the major classes of NO donors

Organic nitrates represent the earliest category of NO donor compounds and are presently the most widely utilized among NO donor drugs. This class includes substances like isosorbide mononitrate (ISMN), glyceryl trinitrate (GTN), nicorandil, and pentaerythritol tetranitrate (PETN). These drugs have high bioavailability through the oral cavity and have been shown to have anti-angina pectoris effects (Table 4). Organic nitrates release NO through metabolic or redox reactions and have a very short half-life (Table 4). They have limitations in clinical use due to their short shelf-life, and lack of stability [155]. Nevertheless, they are primarily employed for acute conditions that demand rapid vasodilation, such as angina. Their use may accompany several side effects including headache, hypotension, fainting, and the development of tolerance (Table 4) [155]. SNOs are an important class of NO donors which were found as intermediate components in various biological processes involving organic nitrates, nitrites, and nitroprusside. They are recognized as the body's inherent reservoir of NO, serving to store some of the generated NO through enzymatic reactions (Table 4). Due to these discoveries, there has been significant interest in their potential utility as NO donors in medicinal

applications. SNOs, with a few exceptions, are highly unstable in aqueous solutions, especially primary and secondary variants (Table 4).

While SNOs have not yet been employed clinically, several benefits have been reported for SNOs, particularly for biomedical applications in comparison with other NO donors, including 1) the presence of certain SNOs like S-nitroso glutathione (GSNO) within biological systems suggests that pharmacologically relevant levels of SNOs might not lead to significant toxicity. 2) Certain SNOs have displayed selectivity in their pharmacological effects. For instance, there are several reports that GSNO exhibits greater efficacy as an antithrombotic agent than as a vasodilator. This makes it suitable for anti-platelet aggregation at doses that don't impact blood pressure. 3) The capability of NO exchange between SNOs and thiols in biological systems (trans-nitrosation) facilitates the transfer of biological activity along a chain of other thiols without releasing free NO. This helps reduce potential oxidative stress caused by SNOs. 4) NO release from SNOs can be modulated through different triggers, including light.

NONOates release NO through hydrolysis [63]. They can release NO in a normal physiological environment, making them a suitable choice for biomedical research (Table 4) [156]. The release rate of NO from NONOates can be managed and directed by incorporating an enzyme or metabolite response group into the molecule [16]. NONOates have a longer half-life than organic nitrates, depending on the structure. They have shown promise in preclinical studies for various therapeutic applications, including pulmonary hypertension, cancer, and stroke [16].

Another photosensitive NO donor is metal nitrosyl compounds that release NO when exposed to light (Table 4). They have a strong ability to coordinate with metal ions. Altering the structure of the metal center or metal nitrosyl compound can adjust the range of light wavelength [111, 157]. The stability of metal nitrosyl compounds in that the metal center is Ru or Fe is higher than other metal nitrosyl compounds [111, 158]. They have been investigated for their potential use in cancer therapy and as imaging agents [111].

Table 4. A comparison between various NO donors with their advantages and disadvantages.

| NO donor | Mechanism | Advantages | Disadvantages | Refs |
|---|---|---|---|---|
| **NONOates** | Enzyme-response NO release, microenvironment-response NO release, light-triggered NO release | Controllable NO release kinetics, ability to bind with enzyme, generate two NO molecules with one molecule of NONOates, convenient use in biomedical applications | | [5, 63, 159] |
| **SNO** | Light-triggered NO release, X Ray-triggered NO release, ultrasound-triggered NO release, copper Ion-response | No unwanted NO release, suitable for targeted NO delivery | Need certain conditions to release NO | [5, 63, 159] |

| | | | | |
|---|---|---|---|---|
| | NO release, Enzyme-mimics-response NO release | | | |
| **Metal nitrosyl compounds** | Light-triggered NO release, | Suitable to use under physiological conditions, adjustable wavelength range | No NO release naturally, need induced photoelectron transition | [5, 63, 159] |
| **L-arginine** | Enzyme-response NO release, ROS-response NO release | Easy to use, biocompatible | Can react with NO synthases, need to protect against unwanted degradation | [5, 63] |
| **N-Nitrosoamines** | Light-triggered response NO release, ultrasound-triggered response NO release | No unwanted NO release, suitable for targeted NO delivery | Imitated biomedical application due to the need for short wavelength, need to upconversion NPs | [5, 63, 111, 159] |

## 3.2 NO therapy

Figure 11 represents the direct therapeutic effect of the generated NO either from endogenous or exogenous NO sources in various diseases. Given the importance of NO in human physiology, effective NO donors could have a wide range of biomedical applications, including in cardiovascular diseases, stroke, wound healing, cancer therapy, inflammation, and autoimmune diseases (Table 5). The overwhelming majority of currently available NO donors are unstable, and such donors have very limited biomedical applications, as random NO release would result in significant side effects such as severely low blood pressure and hypovolemic shock. Nevertheless, NO donor with a controlled NO release profile has significant therapeutic potential.

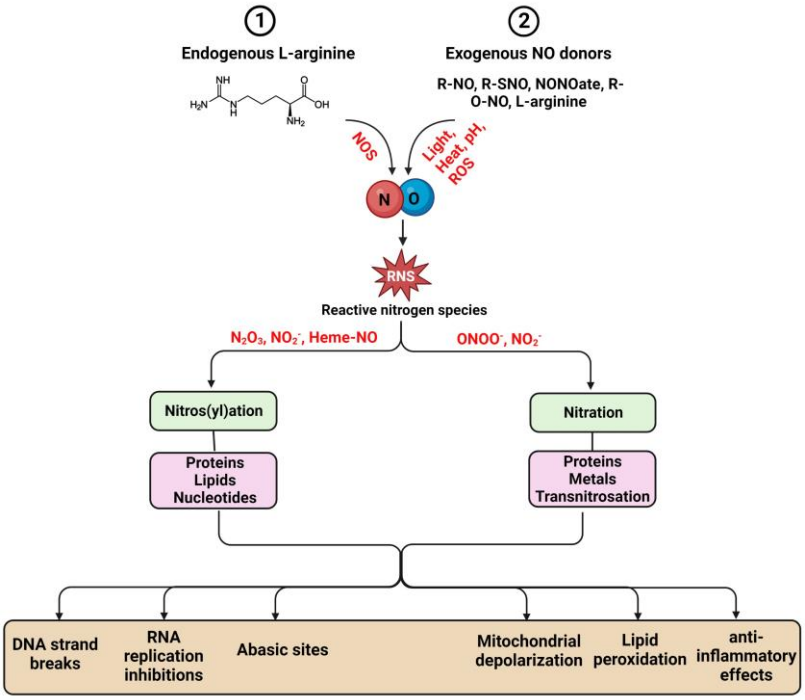


Figure 11. The direct effects of generated NO from endogenous L-arginine and exogenous NO donors on biomolecules. In addition, treatment mechanisms of the produced NO for various diseases [160]. Beyond the direct impact of NO on biomolecules, its interaction with $O_2$ or other ROS leads to the

formation of reactive nitrogen species (RNS). These RNS then exert effects on proteins, lipids, nucleosides, and metals. This interaction also induces transnitration, contributing to DNA strand breaks, abasic sites, enzyme activity inhibitions, mitochondrial depolarization, mitochondrial dysfunction, and DNA/RNA replication inhibitions.

### 3.2.1 Vasodilation and wound healing

NO plays a critical role in regulating various cellular processes. It coordinates with ferrous iron ($Fe^{2+}$) within the heme group of soluble guanylyl cyclase (sGC), prompting a conformational shift that triggers the enzyme's activation. This activation leads to the catalysis of guanosine triphosphate (GTP) into cyclic guanosine monophosphate (cGMP), resulting in a subsequent reduction in intracellular calcium ($Ca^{2+}$) [161]. $Ca^{2+}$ is a vital mediator in the relaxation of smooth muscle cells, which is necessary for maintaining normal cardiovascular function and blood flow (Figure 12 (Vasodilation)) [162]. NO also plays a crucial role in mediating angiogenesis and cell proliferation. It stabilizes hypoxia-inducible factor-1 (HIF-1) through the process of S-nitrosylation, which can induce the secretion of vascular endothelial and basic fibroblast growth factors [4].

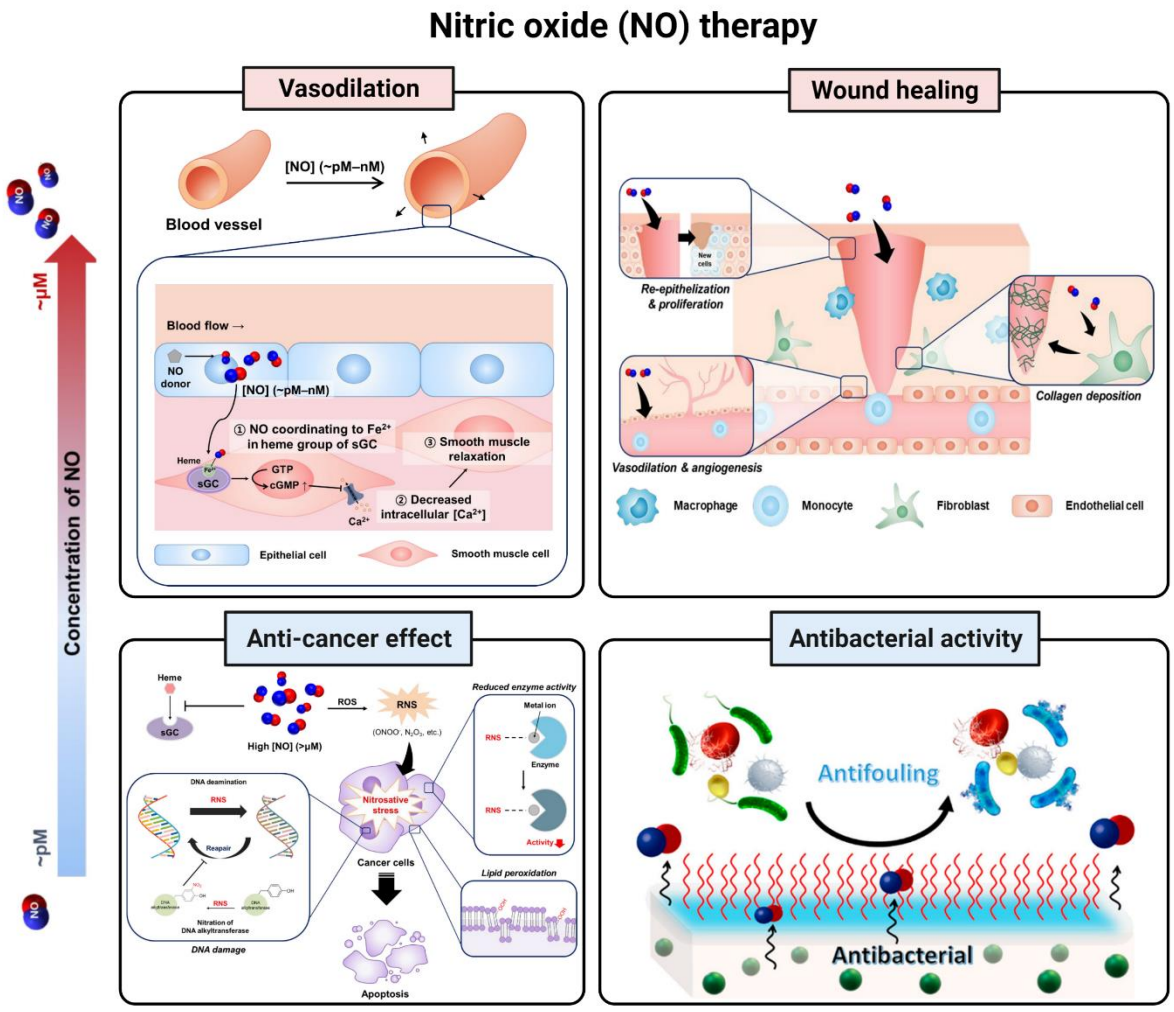

Figure 12. Concentration-dependent biomedical applications of NO, (Vasodilation) NO at nanomolar or picmolar coordinate to $Fe^{2+}$ in heme groups of sGC results in smooth muscle relaxation (Reproduced with copyright © 2022, American Chemical Society [4]), (Wound healing) Re-epithelization and proliferation, collagen deposition, vasodilation, and angiogenesis are some of the wound healing effects by NO (Reproduced with copyright © 2022, American Chemical Society [4]), (Anti-cancer effect) NO at a high concentration reacts with ROS and generates nitrosative stress to cancer cell and leads to cell apoptosis (Reproduced with copyright © 2022, American Chemical Society [4]), and (Antibacterial activity) the schematic represents the antibacterial activity of NO at a high concentration (Reproduced with copyright © 2022, Manjyot Kaur Chug and Elizabeth J. Brisbois, American Chemical Society [163]).

Healing of a normal wound is a complex process that involves four interconnected stages including hemostasis, inflammation, proliferation, and remodeling [164]. NO plays a beneficial role in promoting vascular homeostasis through vasodilation and inhibiting platelet aggregation, as well as promoting re-epithelization, angiogenesis, and collagen deposition (Figure 12 (wound healing)) [4]. The controlled delivery of NO is vital for wound healing since NO can have concentration-dependent behavior [4]. Chen et al. found that dinitrosyl iron complexes (DNICs) $[Fe_2(\mu\text{-}SCH_2CH_2OH)_2(NO)_4]$ (DNIC-1) had a controllable release of NO via activation of NO-sGC-cGMP pathway, which showed superior pro-angiogenesis activity compared to the vascular endothelial growth factor and accelerates the wound closure rate in diabetic mice [165].

NO delivery is an efficient approach to treating an acute myocardial infarction [166]. The cardioprotective impact and angiogenesis induced by NO help to maintain homeostasis in the cardiovascular system [166]. While a burst release of generated ROS by blood flow reperfusion can induce oxidative stress and consequently cardiovascular disorders [166]. To address this, Hao et al. developed an injectable dual-function hydrogel system that combines ROS scavenging with NO donation to regulate the proportion between NO/ROS and control myocardial ischemia [167].

### 3.2.2 Anticancer and antibacterial therapy

At high concentrations (~μM), NO can react with other free radicals and $O_2$ to generate RNS (indirect effects of NO), including dinitrogen trioxide ($N_2O_3$) and peroxynitrite ($ONOO^-$) [168]. This continuous accumulation of RNS can result in DNA damage through nitrosation of DNA alkyltransferase and deamination of DNA, resulting in blocking DNA repair (Figures 11 and 12 (Anti-cancer activity)).

In NO-mediated anticancer therapy, it's typical to administer elevated NO concentrations within a brief timeframe to target cancer cells. In this context, there are a few important points to

consider: 1) The delivery of μM level of NO to tumor tissue through systemic administration is very challenging. Particularly when NO at a much lower concentration (nM) relaxes vessels and drops blood pressure. It is possible that the administration of such a large concentration of NO (or an NO donor with a random NO release profile) will kill the patients before killing a single cancer cell. Therefore, it is vital to deliver the source of NO locally in the tumor site or apply a stable but stimuli-responsive NO donor. 2) Controlled delivery of NO at lower concentrations can also help tumor therapy by changing the pharmacokinetics of anticancer agents or sensitizing the tumor cells to radio-chemo-therapy. For example, NO donors have been shown to increase enhanced permeability and retention (EPR) effects of macromolecules in both preclinical and clinical studies. Further, NO donors have been shown effective in suppressing multi-drug resistance tumor chemotherapy. 3) Controlled NO delivery can overcome some of the biological barriers that hinder effective cancer therapy. For instance, the delivery of anticancer drugs to the hypoxic core of tumors or brain tumors still remains a major challenge, and controlled NO release has been shown a promising approach to address these issues.

Wang et al. developed an injectable hydrogel system with a NO-releasing capacity (NO-Gel), which was based on α-(nitrate ester) acetic acid-modified amphiphilic copolymers [169]. β-lapachone (Lapa)and glutathione (GSH)-sensitive CuCys NPs were loaded into the NO-Gel to enhance the effectiveness of the hydrogel in cancer therapy (Figure 13a). The controlled release of Lapa in cancer cells raises $H_2O_2$ levels, facilitating the rapid release of NO through CuCys NPs reduction by intracellular GSH. The sustained release of Lapa increases the concentration of $H_2O_2$ in cancer cells, and the reduction of CuCys NPs by intracellular GSH leads to the rapid release of NO (Figure 13a). The elevated levels of $H_2O_2$ in combination with the Cu(I)-catalyzed Fenton-like reaction results in hydroxyl radicals (·OH) generation. Subsequently, reactions among NO, $H_2O_2$, and ·OH lead to a more lethal pool of RNS. A single peritumoral injection of this hydrogel system was found to significantly suppress tumor growth by causing a cascade generation of ROS and RNS and by depleting intracellular GSH [169].

The utilization of nitrosative stress mediated by NO has gained significant attention as a potential strategy for combating antibiotic-resistant bacteria. This is due to the bactericidal activity of NO radicals and their derivatives, including peroxynitrite ($ONOO^-$) and dinitrogen trioxide ($N_2O_3$) (Figure 11 and 12 (Antibacterial activity)) [170]. S-nitroso-N-acetyl-penicillamine (SNAP) was loaded into commercial latex catheters (SNAP-UCs) by a solvent-swelling method [170]. The SNAP-UCs exhibited remarkable *in vitro* antimicrobial efficacy against 3 pathogens commonly corresponded with catheter-associated urinary tract infections (CAUTI) including *Escherichia coli*, *Proteus mirabilis*, and *Staphylococcus aureus* [170]. Figure 13b shows the antimicrobial reactions of NO [170]. Time-lapse fluorescent imaging with the membrane-permeable indicator diaminofluorescein-2 diacetate (DAF-2(NO)) revealed distinct NO production patterns in $Si_3N_4$-exposed bacteria (*S. epidermidis*). Bacteria

showed a dispersed NO distribution peaking at approximately 24 h, coinciding with the cessation of bacterial proliferation and the initiation of bacteriolysis. This discrepancy underscores $Si_3N_4$'s varied impact on bacteria [153b].

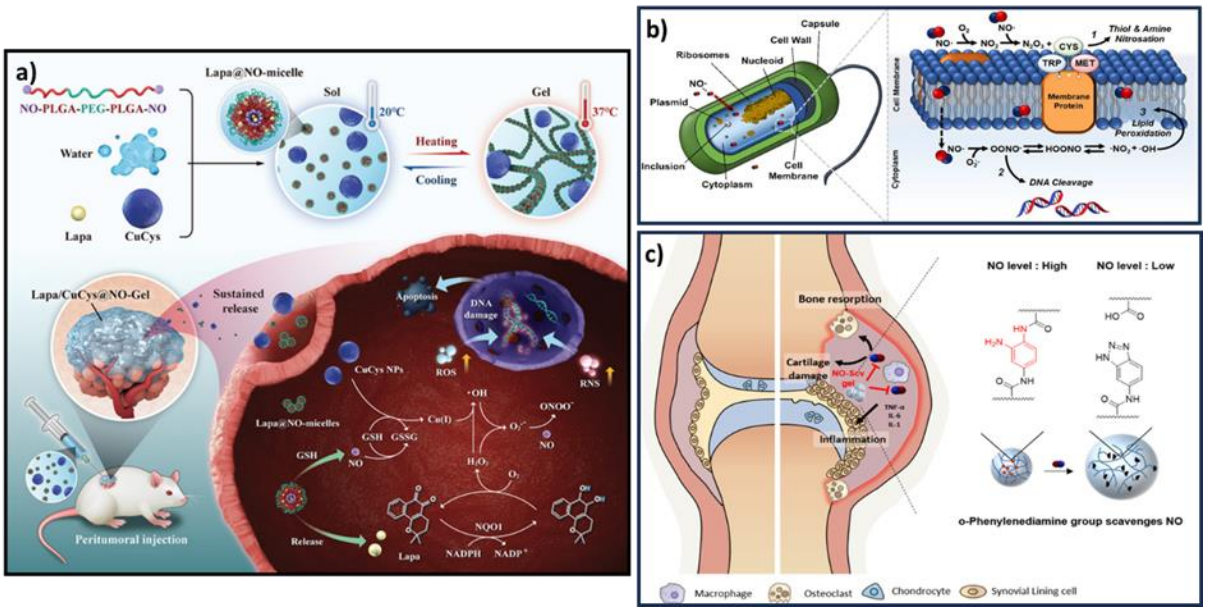


Figure 13. (a) A schematic of preparation of Lapa/CuCys@NO-Gel with the synergistic effect for cancer therapy. β-lapachone (Lapa) and glutathione (GSH)-sensitive CuCys NPs were incorporated into the self-assembly of amphiphilic NO-PLGA-PEG-PLGA-NO in water to develop the Lapa/CuCys@NO-Gel. The Lapa release increased the concentration of $H_2O_2$ in cancer cells, and the reduction of CuCys NPs by intracellular GSH leads to the rapid release of NO. The elevated levels of $H_2O_2$ in combination with the Cu(I)-catalyzed Fenton-like reaction results in hydroxyl radicals (·OH) generation. Subsequently, reactions among NO, $H_2O_2$, and ·OH lead to a more lethal pool of RNS (Copyright © 2022, Wiley) [169], (b) the schematic represents the different antimicrobial reactions of NO: 1) amine nitrosation and thiol, 2) DNA cleavage, and 3) lipid peroxidation (Copyright © 2022, American Chemical Society) [170], and (c) Schematic illustration of inflammatory effect of NO, which results in alleviation of RA: NO can directly upregulate osteoclasts, damaged cartilage, and aggravate the inflammation (Copyright © 2019, American Chemical Society) [171].

### 3.2.3 Anti-inflammation

NO is a pivotal inflammatory mediator that holds a crucial function in defending the body against pathogens. [170]. Immune cells, particularly macrophages, express iNOS to generate a high concentration of NO as a defense mechanism against pathogens. However, in pathological conditions, the expression of iNOS in the tissue or macrophages may lead to impaired cellular response, overexpression of proinflammatory cytokines, and triggering apoptosis [4]. Chronic inflammatory disorders or tissue destruction, such as diabetes, RA, and inflammatory bowel disease, can be caused

by NO overproduction. Therefore, regulation of NO concentration to normal physiological level is crucial in treating inflammatory diseases and needs further investigation [4].

RA is the most common autoimmune and inflammatory disease characterized by swollen and sore joints, which negatively impact the patient's quality of life. The RA mechanism has not been completely discovered, however, it is known that the overproduction of NO is closely related to the development of RA [171]. Furthermore, the overproduction of NO leads to recruit immune cells, nitrosative stress, and increases the number of osteoclasts, which destroy cartilage tissue [171]. Hence, normalizing NO concentration alleviates the symptoms of RA (Figure 13c) [171-172]. The moiety o-phenylenediamine (o-PD) has been studied for its highly selective reactivity towards NO in the presence of $O_2$ [173]. This property has led to the expansion of fluorescence sensors for NO detection *in vitro* and *in vivo* [173]. o-PD has been utilized to develop NO-responsive hydrogel to suppress RA symptoms in mice [174]. However, the practical applications of the hydrogel were limited by its small size, which can lead to diffusion into other organs and potential off-target NO depletion. Additionally, combining anti-inflammatory agents with NO scavengers has been evident to be more effective than each treatment alone [175].

### 3.2.4 Regulate the insulin secretion

NO plays a multifaceted role in the progression of hyperglycemia. NO generated in the endocrine pancreas contributes to the synthesis and secretion of insulin. During the advanced phases of diabetes, NO donors have been shown effective in the normalization of vascular function [176]. Dysfunction of eNOS can decrease the flow of microcirculation blood and delivery of insulin in hormone-sensitive organs [63]. In a study by Dr. Gu et al., a glucose oxidase-magnetic NPs hybrid (GOx-MMVs) was developed as a novel glucose stimulation system to decline the level of blood sugar [177]. The reaction of L-arginine and $H_2O_2$ was started through an alternating magnetic field to reach a controllable NO delivery [177]. However, excessive NO levels can interfere with insulin signal transduction pathways affect pancreatic β cell dysfunction, and develop type 2 diabetes. To counteract the cytotoxic effects of excessive production of NO under hyperglycemic conditions, specific iNOS inhibitors were administered [176].

Table 5. The typical paradigms of NO-releasing biomaterials for versatile biomedical applications. Listed 2022 and 2023.

| Gas | Source | Mechanism | Control method | Ultimate gas release | Release duration | Application | Remarks | Refs |
|---|---|---|---|---|---|---|---|---|
| **NO** | L-arginine | Light-responsive | Incorporating arginine into epigallocatechin gallate and ferric ions particles | ~40μM | 12 h | Synergistic photodynamic/gas/photothermal therapy | The particles did not show any NO production without light. The synergistic effect of the NO release particles was demonstrated with in vitro and in vivo studies. | [178] |
| | | | Encapsulating arginine into photosensitizer PEGylated indocyanine green integrated to polyphosphazene nano-vesicle | From ~20 to 40 μM with 0.5 to 1.5 $W/cm^2$ | 6 h | Cancer therapy | Arginine produced NO via reaction with generated ROS at 808 nm | [179] |
| | | | Loading arginine and doxorubicin hydrochloride into a nanovesicle system | ~20-30 μM | 4 h | Cancer treatment | the generated NO enhanced the therapeutic efficacy of multimodal therapy. | [180] |
| | | - | Self-assembly of arginine protein complex | - | - | Tumor hypoxia (cancer therapy) | pH-sensitive NO complex. Produce NO at a pH of 5.5 and 10 mM of $H_2O_2$. | [181] |
| | | $H_2O_2$-responsive | Encapsulating cisplatin into amphiphilic triblock copolymer based on polyethylene glycol, PCL, and polyarginine | ~6 μM | 50 h | Imaging guided therapeutic | Cisplatin accelerated NO production by elevating intracellular $H_2O_2$ levels. | [182] |
| | | | Encapsulating arginine and $H_2O_2$ into a hydrogel | ~4 μM | 30 h | Bacterial ablation and wound healing | The synergistic antibacterial effect of $H_2O_2$ and NO was observed. The hydrogel improved collagen and blood vessel formation. | [183] |
| | | | Loading arginine into cerium oxide | ~1-1.8 (value was not reported) | 12 h | Cancer therapy | The amount of NO generated was related to the concentration of cerium oxide and reaction time | [184] |
| | | Endogenous NOS | Using mesoporous silica NPs as arginine carrier | - | - | Preventing myocardial dysfunction | NO at a low level in the heart showed benefits in myocardial recovery. | [185] |
| | | Ultrasound | Mesoporous Mo-doped $Cu_9S_5$ loaded with arginine | ~20 μM | After 1 min with ultrasound | Chemodynamic therapy | NO gas was generated continuously during ultrasound excitation. | [186] |

| | | | | | | | | |
|---|---|---|---|---|---|---|---|---|
| | | Glutathione-responsive | Encapsulating L-arginine into PEG-modified mesoporous organosilicon NPs | - | - | Cancer therapy | The generated NO regulated vasodilation for alleviating tumor hypoxia | [187] |
| | NONOates | - | Conjugating NONOate to polyethyleneimine with a different molecular weight | 0.4 to 0.6 µmol | 45 h | Acute ischemic stroke | The NONOates significantly reduced the necrotic ratio compared to the control. | [188] |
| | | Heat-responsive | NONOates were conjugated on polydopamine-functionalized magnetic iron oxide nanoclusters | From ~12 to 125 µmol with different laser irradiation conditions | 20 min | Antibacterial and wound healing | Utilizing polydopamine and NONOates simultaneously inhibits the growth and biofilm formation significantly | [189] |
| | SNO | Heat-responsive | Blended by polymer zein and silk firoin to develop nanofiber | From $0.09\pm0.01\times10^{-10}$ to $1.39\pm0.26\times10^{-10}$ mol/min | From 1 to 24h | Antibacterial nanofibers | The combination of zein, silk fibroin, and NO showed a synergistically high antibacterial efficiency | [190] |
| | | Light-responsive | Incorporating s-nitrosothiols into mesoporous silica-coated gold nanorods | From ~2.5 to 5.5 µmol with different concentrations of the nanorods (25-100 µg/ mL) | 60 min | Inflammation immunotherapy against periodontal diseases | The NO-releasing nanorods could be effective for deep tissue treatment along with anti-inflammatory and antibacterial capabilities | [191] |
| | | | - | From 0 to ~ 600 nM | 750 s | Breast cancer therapy | NO was generated under the green light. NO represented remarkable toxicity under the green light irradiation | [192] |
| | | | Integrating PVA with S-nitrosoglutathione | From ~15 to 35 nmol/mg | 25 h | Wound healing | Targeted delivery of NO with microneedle structure disturbed the biofilm and inhibited bacterial growth | [193] |
| | GSNO | Physiological and heat-responsive | Covalently immobilized on titanium dioxide NPs | $240.05 \pm 74.94 \times 10^{-10}$ mol/ min. mg | 20 h | Antibacterial NPs | 5 mg/mL of the synthesized particles could inhibit 99.99% of gram-positive (*S. aureus*) and 99.70% of gram-negative (*E. coli*) bacteria | [194] |
| | Metal nitrosyl | Glutathione and immunogenic cell | Nanoassembly of polynitrosated polyesters | From ~ 50 to 180 µM | ~390 min | Cancer therapy | NO could expand the range of immunogenic cell death inducers | [195] |

| | | | | | | | | |
|---|---|---|---|---|---|---|---|---|
| | comp ound | death-responsive | | | | | | |
| | | Magnetic and heat-responsive | Conjugating [Fe(μ-S-thioglycerol)$(NO)_2]_2$ with a metal-organic framework-derived porous $Fe_3O_4$@C | From 0 to ~1.75 nmol/mg by changing temperature and from 0 to ~45 nmol/mg by altering the magnetic field | Within 60 min by temperature and 3000 s by altering the magnetic field | Treatment of bacteria-infected cutaneous wound | The Burst release of NO by altering the magnetic field showed an efficient antibacterial activity against *S. aureus* and *E. coli*. | [196] |
| | | Light-responsive | Loading Ru nitrosyl compound into lipid bilayers liposomes via hydrophobic interaction | From 3.39 to 7.71 μM with various amounts of NO donor (14.7- 50 μM) | 120 min | - | Water-insoluble Ru nitrosyl compound was loaded into liposomes with a hydrophilic surface to improve biocompatibility | [197] |
| | | | Newly designed bidentate ligands | From 1.56 to 5.63 μM | - | Antibacterial activity and wound healing | 50 μg/mL of the NO donor showed significant wound healing and inhibited more than 99% of bacteria after 1.5 h | [198] |
| | | | Synthesizing an amphiphilic terpyridine ligand containing RU nitrosyl complex | Quantum yield between $3.19\times10^{-3}$ – 0.12 | $t_{1/2}$= 0.4 – 5.5 min | Antibacterial activity | The synthesized complex could release NO at acidic and basic media and different temperature | [199] |

914

# 4 Carbon monoxide (CO)

## 4.1 CO delivery

In recognition of the potential of CO in the treatment of cardiovascular diseases, inflammation, bacterial infections, etc., when introduced in low concentrations, the controlled release of CO at target sites, using CO-releasing molecules (CORMs), was initially proposed by Motterlini et al. [200]. In their study, transition metal carbonyls of $[Mn_2(CO)_{10}]$ and $[RuCl_2(CO)_3]_2$ were produced and CO-release was subsequently achieved through ligand exchange and at physiological conditions. Notably, the need to enhance the functionality of these CORMs via the synthesis of molecules with a regulated CO release *in vivo* translated to several studies in the field. Several CORMs, which could be compounds of aldehydes, oxalates, boroncarboxylates, and silacarboxylates, were subsequently developed [201] and classified as CORM A to E based on the functional groups of the compounds as shown in Figure 14 [202].

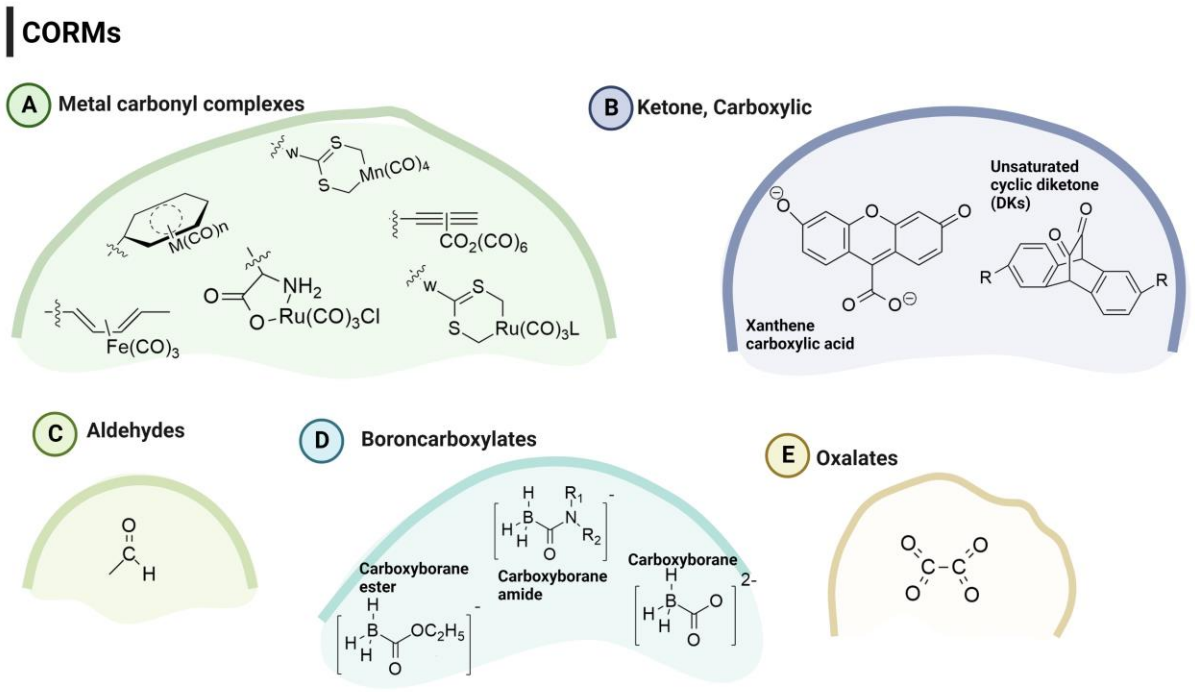


Figure 14. Schematic representation delineating diverse classifications of CO-releasing sources known as CORMs. This categorization is predicated on their functional groups, encompassing metal carbonyl complexes, ketones and carboxylic acids, aldehydes, boron carboxylates, and oxalates.

These CORMs can also be classified as endogenous, exogenous, and multiple stimuli-sensitive CORMs, depending on specific triggers imposed to stimulate CO release. For instance, in the study by Sitnikov, Li, Zhang, Yard, and Schmalz [203], protease-triggered CORMs of acyloxydiene-$Fe(CO)_3$ complexes were prepared. These complexes were composed of a penicillin G amidase (PGA)-cleavable

side chain capable of releasing CO under the endogenous stimuli of PGA. In another study, endogenous pH stimuli were employed to trigger the release of CO from rhenium(II)-based complexes of cis-trans-$[Re^{II}(CO)_2Br_2L]^n$ (i.e. L= monodentate) [204]. The study demonstrated that complexes with monodentate ligands could liberate CO in a pH-dependent manner, such that lower pH values led to an increase in CO release time. Similarly, exogenous and multiple stimuli-sensitive CORMs such as BODIPY chromophores [205] and $Mn_2(CO)_{10}$ [206] were also developed and shown to facilitate controlled CO release in the presence of external stimuli of near infrared (NIR) light and visible light, NIR light, $H_2O_2$ respectively.

Crucially, however, established issues of random diffusion, metal ions induced toxicity, and reduced cellular uptake efficiency have so far hindered the direct applicability of the CORMs in biological applications [207]. In this regard, the integration of CORMs with several scaffolds and conjugated formulations has been explored as a viable strategy to enhance CORM applicability, since such scenarios have the potential to promote CORM stability, enhanced CO release modulation, and localization of CO to target sites [207-208]. These platforms include metal-organic frameworks (MOFs) and NPs, peptides, proteins, vitamins, metallodendrimers, micelles, and nanofibers as summarized in Figure 15 [209]. For instance in the study by Dördelmann, Pfeiffer, Birkner, and Schatzschneider [208] a copper-catalyzed azide–alkyne 1,3-dipolar cycloaddition click reaction was employed in covalently linking the photoactivatable CORM of $[Mn(CO)_3(tris(pyrazolyl)methane)]^+$ containing an alkyne-functionalized tris(pyrazolyl)methane ligand with silicium dioxide nanoparticles. The study was able to show that the CORM-functionalized NPs could be employed to induce the release of CO to specific solid tumors. Similarly, targeted CO release was also shown to be achievable using mesoporous silica Al-MCM-41 NPs (MSP) to encapsulate the CORM of $[Mn(1,4,7\text{-triazacyclononane})(CO)_3]^+$ and the cisplatin drug. The study was able to demonstrate that the use of the MSP enabled controlled CO delivery as illustrated by the lower rate constant of CO release kinetics of encapsulated CORM of 0.017 $min^{-1}$ relative to the rate constant of 0.031 $min^{-1}$ [210].

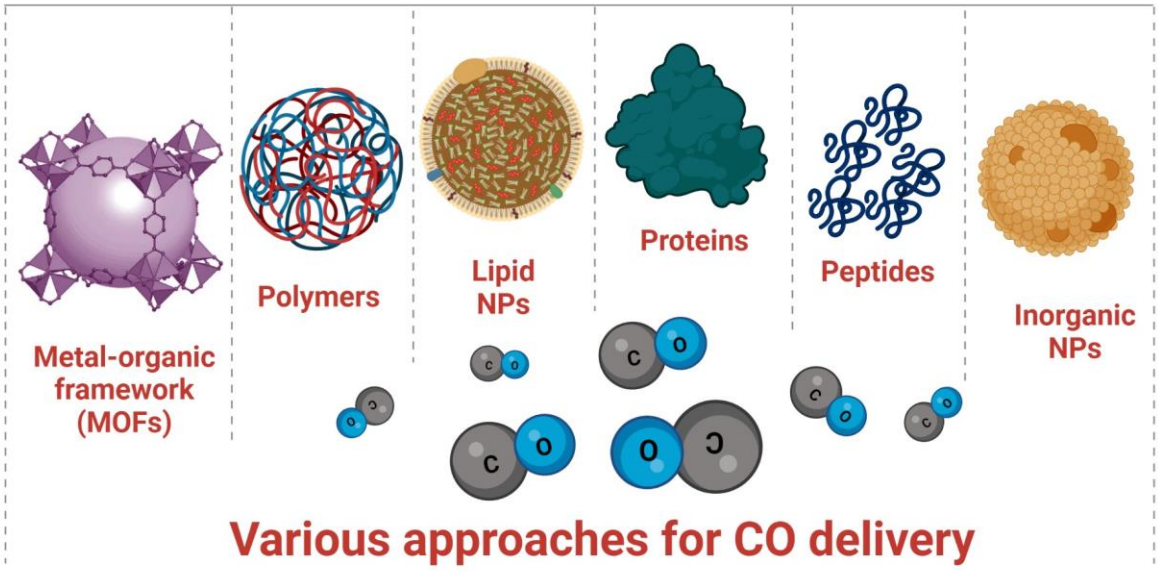


Figure 15. Schematic depiction showcasing diverse CO delivery methods for therapeutic applications, including metal-organic frameworks (MOFs) and nanoparticles (NPs), peptides, proteins, vitamins, metallodendrimers, micelles, and nanofibers. The controlled release of CO is influenced by the structural design, physico-chemical properties, shape, and size of the carriers.

MOFs of $NH_2$-MIL-88B-Fe and MIL-88B-Fe were also employed in facilitating CO delivery, with CO binding achieved using unsaturated coordination sites. CO release from the MOFs was examined under physiological conditions through a myoglobin assay with the study showing that the CO release rate was dependent on the MIL degradation with t ½ values of 38 min and 76 min, determined for MIL-88B-Fe and $NH_2$-MIL-88B-Fe respectively [211]. The use of micelles is based on the combination of triblock copolymers, namely a hydrophilic fragment (i.e. poly(ethylene glycol), the CO release filament, and a hydrophobic fragment (poly(n-butylacrylamide) [209]. In such micelles platforms, CO release is induced via exposure to compounds such as cysteine, glutathione, and protein that contain the thiol functional group [209]. The use of micelles in CO delivery was demonstrated in the study by Hasegawa, van der Vlies, Simeoni, Wandrey, and Hubbell [212]. In the study, micelles were prepared by combining hydrophilic poly(ornithine acrylamide) blocks and poly(ethylene glycol), a hydrophobic poly(n-butylacrylamide) block, and a CO-releasing moiety of $Ru(CO)_3Cl$(ornithinate) [212]. It was reported that the micelles formed were spherical, with hydrodynamic diameters ranging from 30-40 nm, and also exhibited high-level stability when in physiological conditions. It was determined that the micelles were capable of releasing CO when exposed to cysteine [212].

Furthermore, biomolecules of proteins and peptides have also been explored as preferred platforms for targeted CO release due to their favorable biocompatibility properties and the abundance of binding sites (i.e. via amino acid-based coordination) for CORMs. For instance, CO

releases through conjugation of Thr-Phe-Ser-Asp-Leu peptide to the CORM of $[Mn(CO)_3(tris(pyrazolyl)methane)]^+$ via by Pd-mediated Sonogashira cross-coupling, was shown to facilitate the controlled release of 1.7 CO equivalents per unit Mn when exposed to a light irradiation of 365 nm [213]. Another study also explored the conjugation of monomeric proteins of bovine serum albumin and CORMs containing moieties of $Ru(CO)_2$ and demonstrated that the spontaneous release of CO could be used to down-regulate expression levels of tumors while simultaneously circumventing secondary cytotoxicity issues [214].

## 4.2 CO therapy

In living organisms, it is possible to endogenously produce CO via the metabolism of heme for CO, iron, and biliverdin generation [215]. Heme metabolism is enabled via the action of the enzyme of heme O2ase (OH), which is determined to exist as three isoforms of, HO-1 (32 kDa), HO-2 (36 kDa), and HO-3 (33 kDa), although HO-2 and HO-3 are characterized by low activity[216]. The catabolism of heme CO is responsible for endogenous CO production with diffusion employed in the removal of CO from the cell to the blood with the CO subsequently bound to hemoglobin (Hb) to form COHb [217]. Although the literature shows that endogenously produced CO can enable signaling processes in the brain, liver, and endothelium, provided that the CO concentration is maintained at physiological levels, higher concentrations of CO are recognized as being toxic [218].

Indeed, for higher concentrations of CO, cases of tissue hypoxia, manifested as a range of symptoms ranging from headache and dizziness (i.e. for COHb 10-20%) to brain damage and death (i.e. for COHb > 70%) have been reported [218b]. At properly regulated and physiological levels, CO may however enable the regulation of vascular tone, neurotransmission, vasodilation, inflammatory mediators, and apoptosis mechanisms [217a, 218a]. The regulation of vascular tone, neurotransmission, and vasodilation is achieved via promoting cyclic guanosine monophosphate (cGMP) signaling pathway activation, which is an intracellular nucleotide cascade that also influences neuroplasticity [217a, 218a, 219]. Although not well understood, the promotion of the cGMP signaling pathway also facilitates the inhibition of proliferation and tumor angiogenesis. This inhibition is achieved via limiting β-catenin/ transcription factor 7 and SRY-box transcription factor 9 signaling [220]. The mediation of inflammatory mediators in the presence of CO is due to the associated modulatory effects on pro and anti-inflammatory cytokines[212].

The presence of CO has also been reported to be useful in the treatment of issues such as sepsis and chronic graft rejection [212]. These beneficial benefits of CO may however be antagonized by inhibition of the catabolism of heme, negatively impacting a vast range of biological processes, implying that in such scenarios, there is a need to introduce therapeutic volumes of CO using suitable

CORMs, discussed earlier above [215]. Additionally, CO is useful in cancer treatment due to its capacity to induce the so-called 'anti-Warburg' effect in cancerous cells by promoting cancer cell bioenergetics (i.e. for increased respiration) leading to terminal metabolic exhaustion [221]. For instance, Li, Dang, Liang, and Yin [222] investigated the use of a NIR-light-triggered CORM that was based on Pentacarbonyl iron and mesoporous Prussian blue (PB) NPs for the treatment of cancer via the promotion of metabolic exhaustion (Figure 17a). In the study, tumor-site-specific NIR light irradiation of 808 nm facilitated the release of CO from the Pentacarbonyl iron with the released CO demonstrated to expedite mitochondrial metabolic exhaustion. The CO-induced metabolic exhaustion was also shown to block ATP synthesis, and thus lead to a reversal of multidrug resistance, via the inhibition of ATP-dependent drug efflux (Figure 16a). This multidrug resistance is recognized as the main cause of chemotherapy failure [222]. Crucially, as stated earlier above, these benefits of CO require that its concentration is properly controlled to avoid toxic outcomes.

Although CO could demonstrate a high efficacy in cancer therapy by increasing the damage of mitochondria, the efficiency can be compromised by protective mitophagy (autophagy) [223]. To address this issue, Xiao et al. integrated cannabidiol into CO nanocomplexes (HMPOC@M) to induce excessive autophagy (Figure 16b) [223]. The $H_2O_2$ in the tumor environment stimulated the CO donor and generated CO and $Mn^{2+}$. Producing CO and $Mn^{2+}$ along with the release of cannabidiol results in cell apoptosis (Figure 16b) [223].

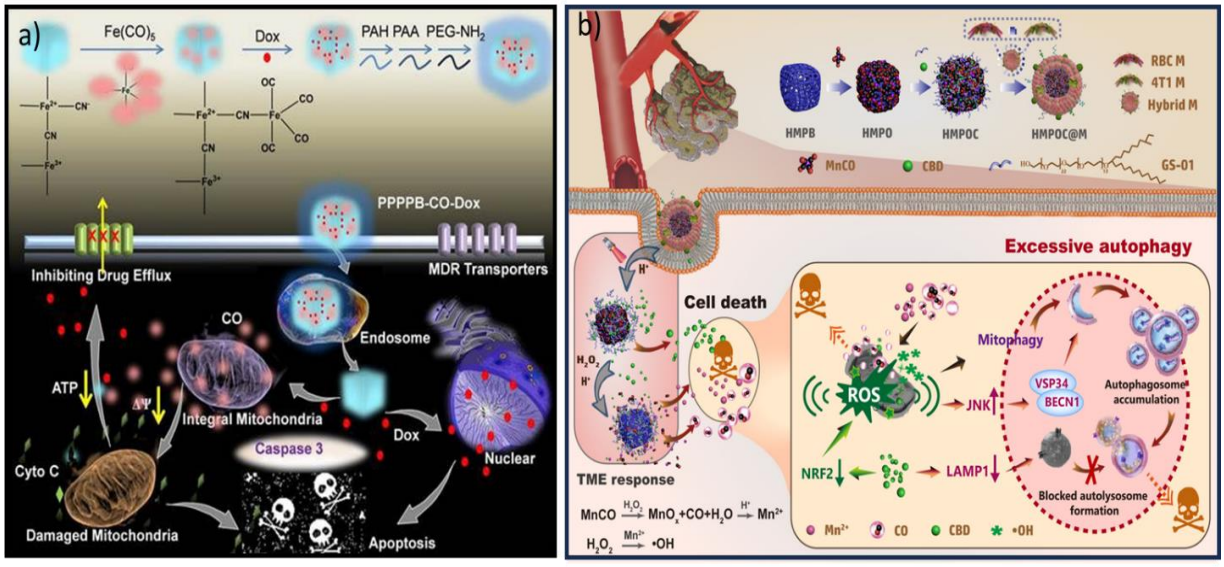


Figure 16. (a) A schematic of NIR-light-triggered CO release based on Pentacarbonyl iron and mesoporous Prussian blue (PB) NPs for the treatment of cancer via the promotion of metabolic exhaustion (Copyright © 2019, American Chemical Society, Open access) [222], and (b) Schematic illustration of the preparation of cannabidiol integration on CO nano complex (HMPOC@M) to

generate CO via $H_2O_2$ of tumor environment to enhance cancer therapy via excessive autophagy (Copyright © 2023, ScienceDirect, Open access) [223].

# 5 Hydrogen sulfide ($H_2S$)

In addition to CO and NO, $H_2S$ is considered 3rd gaseous signaling molecule. Although $H_2S$ was recognized as an environmental hazard for many decades, it gas has recently been regarded as a gas transmitter due to its unique functions such as cell membrane permeability, cellular signaling functions, and its role in tissue regenerations [224]. $H_2S$ is flammable and colorless, with high water solubility and a lower electronegativity than $O_2$ [225].

## 5.1 $H_2S$ delivery

$H_2S$ is present in the human body and can be produced via nonenzymatic and enzymatic methods. $H_2S$ endogenously can be produced mainly by four enzymes such as cystathionine $\beta$-synthase (CBS), cystathione $\gamma$-lyase (CSE), and 3- mercaptopyruvate sulfurtransferase (3-MST), and cysteine aminotransferase (CAT) in the enzymatic pathway (Figure 18) [226]. CBS and CSE-catalyzed enzymatic process results in $H_2S$ production, or a 3-MST-catalyzed desulfhydration process results in $H_2S$ production (Figure 17) [227].

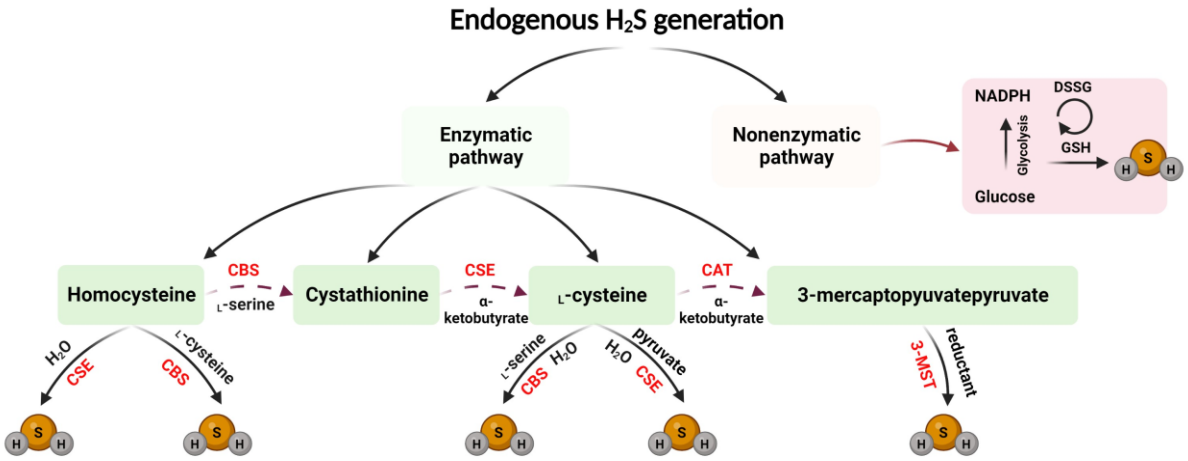


Figure 17. Nonenzymatic and enzymatic pathways for endogenous $H_2S$ generation. Four enzymes such as cystathionine $\beta$-synthase (CBS), cystathione $\gamma$-lyase (CSE), and 3- mercaptopyruvate sulfurtransferase (3-MST), and cysteine aminotransferase (CAT) can produce $H_2S$ in the enzymatic pathway. Besides the enzymatic pathway, nicotinamide adenine dinucleotide phosphate (NADPH), persulfides, and polysulfides can be utilized for $H_2S$ production via a reduction reaction.

In CBS, the CSE enzymatic pathway of $H_2S$ production -ketoglutarate and pyruvate are produced from L-homocysteine and L-cysteine as substrates for $H_2S$ production (Figure 17). Moreover,

different factors can affect enzyme activity and $H_2S$ production. For example, intracellular $Ca^{2+}$ concentration can adversely affect CSE activity, and a high concentration of $Ca^{2+}$ can suppress the production of $H_2S$, [228]. These enzymes are mainly present in mammalian tissues such as the kidney, liver, uterus, and pancreatic, as well as cardiac cells, which can contribute to cellular signaling [229]. Moreover, in addition to the enzymatic pathways, nonenzymatic chemicals can be employed for the endogenous production of $H_2S$. Chemicals such as nicotinamide adenine dinucleotide phosphate (NADPH), persulfides, and polysulfides can be utilized for $H_2S$ production via reduction reaction (Figure 17) [230].

Regarding the delivery of $H_2S$, the most straightforward approach is the inhalation of $H_2S$ which is not practical due to its toxic nature and reduced bioactivity caused by oxidation. To address the direct delivery of $H_2S$, "slow release" small molecule $H_2S$ donors have been suggested to mimic the endogenous production of $H_2S$ [231]. However, using small molecules for $H_2S$ has some limitations such as low water solubility, toxicity, and high clearance rates [232]. However, some of the issues associated with inorganic donors and small molecules can be overcome by macromolecular $H_2S$ donors. For example, the low water solubility of small molecule $H_2S$ donors can be improved by conjugation with a hydrophilic polymer.

Alternatively, small molecule donors can be encapsulated in polymeric matrices such as micelles, hydrogels, and nanofibers for local delivery of $H_2S$. Different macromolecular $H_2S$ donors can be classified as hydrolysis trigger [233], thiols trigger, and light trigger [234] macromolecular $H_2S$ donors (Figure 18). Hydrolysis triggers macromolecular $H_2S$ donor can release $H_2S$ in an aqueous solution; thiols hydrolysis trigger macromolecular $H_2S$ donor can generate $H_2S$ via reduction reacting with thiol-containing bioactive compounds, such as cysteine (Cys) and glutathione (GSH), which is more favorable for the pathological redox microenvironments [235]. Moreover, using exogenous stimuli such as light-triggered macromolecular $H_2S$ donors can pave the way for tissue-specific delivery without disrupting native biochemical processes [232]. However, due to the short wavelength of UV or visible light for activating the light-triggered macromolecular $H_2S$ donors, this approach results in poor tissue penetration, which needs to be improved.

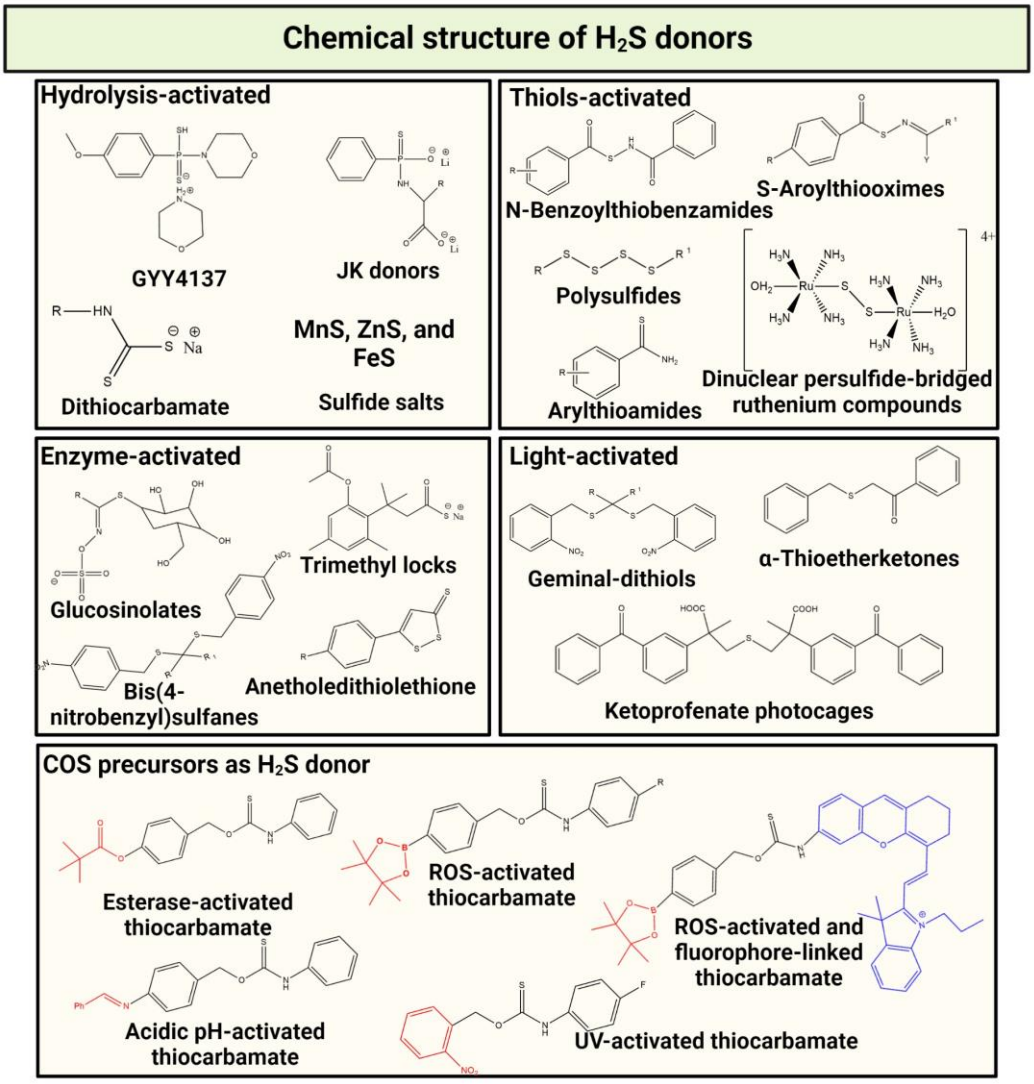


Figure 18. Various macromolecular $H_2S$ donors can be classified as hydrolysis-trigger, thiol-trigger, enzyme-trigger, and light-trigger macromolecular $H_2S$ donors. Incorporating the $H_2S$ donors into a hydrophilic matrix or modifying them with hydrophilic groups can improve their biocompatibility.

## 5.2 $H_2S$ therapy

Similar to NO and CO, $H_2S$ has been reported to exhibit therapeutic effects on numerous organs such as Anti-inflammatory, tissue regenerative, and antioxidant defense responses [236]. Recent studies revealed that $H_2S$ can reduce the expression of proinflammatory chemokines, cytokines, and enzymes leading to the inhibition of NF-κB pathways, macrophage differentiation, and apoptosis induction in neutrophils leading to modulating inflammatory responses [237]. Moreover, $H_2S$ can mitigate inflammation pain by diminishing edema formation [238]. Yu et al. investigated the $H_2S$ therapy using a PLA-based microsphere as a carrier for endogenous $H_2S$ modulators to release in vivo $H_2S$ for alleviating RA [239]. A prolonged in vivo release of $H_2S$ and a better Anti-Inflammatory therapeutical effect on RA rats were observed compared to the control groups (no intervention).

Moreover, Zhang et al. studied an $H_2S$-releasing hydrogel system for alleviating cardiac inflammation [240]. In vivo, investigation of myocardial ischemia-reperfusion on rat models showed that the $H_2S$-releasing hydrogel groups exhibited attenuated cardiac inflammation, prevented microvascular obstruction, and reduced myocardial fibrosis. However, unlike CO, which has definite anti-inflammatory effects [241], $H_2S$'s Anti-inflammatory effect is complicated, and even the proinflammatory effect of $H_2S$ has been reported [242]. Moreover, although several studies have examined how $H_2S$ contributes to reducing inflammation, the mechanisms remain obscure because their effects vary depending on the phase of inflammation.

Moreover, studies reported the role of $H_2S$ in tissue regeneration, such as bone tissue regeneration and wound healing [243]. Exogenous $H_2S$ can stimulate the proliferation and differentiation of human keratinocytes in a dose-dependent manner by regulating autophagy which is crucial in the wound healing process [244]. Moreover, endogenous $H_2S$ has shown wound healing properties. A recent study investigated the wound healing potential of sodium alginate sponges containing $H_2S$-releasing (SA/JK-1) as a pH-dependent $H_2S$ donor [245]. The sponge exhibited a sustainable release of $H_2S$ by absorbing exudate with acidic pH at the wound interface, resulting in fibroblast proliferation and migration, angiogenesis, and granulation tissue formation in a full-thickness rat model, indicating the influential wound healing potential of $H_2S$ therapy. Furthermore, ischaemic diabetic wound healing has been reported by $H_2S$ treatment via induction of different growth factors productions, such as epidermal growth factor (EGF), vascular endothelial growth factor (VEGF), and Platelet-derived growth factor (PDGF), as well as increasing the production of endothelial NO synthase (eNOS) in type 2 diabetic db/db mice [246].

$H_2S$ can regulate bone homeostasis, and recent studies showed that $H_2S$-releasing scaffolds promote bone tissue regeneration [247]. Indeed, the role of $H_2S$ in bone regeneration includes several mechanisms, such as bone cell activity regulation, decreasing oxidative stress, improving angiogenesis, and regulating the bone cells' calcium intake [248]. More specifically, the expression of CBS and CSE as $H_2S$-producing enzymes in mesenchymal stem cells (MSCs), and osteoblasts (OBs) can protect the OBs from homocysteine-induced mitochondrial toxicity and cell death by $H_2O_2$ as well as apoptosis [249]. A polycaprolactone (PCL)/gelatin (Gel) electrospun loaded JK-2 ($H_2S$ donor) exhibited a significant *in vivo* bone regeneration compared to the control group [247b]. PCL/Gel-JK-2 not only increased the MC3T3-E1 cells cell proliferation and attachment but also could improve the skull defects after 1 and 2 months of treatment in the rat model.

Moreover, $H_2S$ may act as an antioxidant and antibacterial agent in living organisms [250]. $H_2S$ works as an intracellular mediator that protects against oxidative stress in multicellular organisms by

acting as endogenous ROS scavengers [251]. Although the direct antibacterial activity of $H_2S$ is limited, $H_2S$ can be used to alleviate bacterial infection by regulating inflammation. Moreover, a high concentration of $H_2S$ (1 mM) could inhibit the growth of E. coli by inducing severe oxidative damage [250b]. However, a high concentration of $H_2S$ can also cause inflammation and tissue damage [252]. Similarly, a controversial effect of $H_2S$ as an antioxidant has been reported by Hamar *et al*. demonstrated a poor antioxidant activity of $H_2S$ in isolated arteries and veins without any impact on superoxide [251a]. Hence, it can be concluded that the direct antioxidant and antibacterial effect of $H_2S$ is not as definite as NO, and this function of $H_2S$ is debatable and needs further investigation.

# 6 Hydrogen ($H_2$)

In the past, it was commonly believed that $H_2$ had no significant role in the human body. However, recent research has demonstrated that $H_2$ is capable of selectively reducing harmful free radicals, such as $^{\bullet}OH$ and $ONOO^-$ [253]. These free radicals can induce harm to proteins and nucleic acids, leading to inflammation and cell toxicity. One of the most reactive free radicals, $^{\bullet}OH$, is produced by mitochondria and has a major impact on oxidation and inflammation in the body. Fortunately, $H_2$ has been found to reduce oxidative stress and inflammation by scavenging $^{\bullet}OH$ with the underlying mechanism presently unclear [253-254]. It is hypothesized that an exothermic reaction between $H_2$ and $O^{2-}$ radicals is responsible for this phenomenon, according to equations 1 to 3, which would contradict the idea of $H_2$'s selectivity. Regardless of the mechanism, the discovery of $H_2$'s ability to reduce free radicals marks a significant breakthrough in our understanding of its role in the body [255].

$$H_2 + \bullet OH \longrightarrow H_2O + \bullet H \qquad (\Delta E \sim 12 \text{ kcal/mol}) \qquad (1)$$

$$\bullet H + O_2^- \longrightarrow HO_2^- \qquad (2)$$

$$\bullet OH + \bullet H \longrightarrow H_2O \qquad (3)$$

## 6.1 $H_2$ delivery

The inhalation of $H_2$ is the primary method of delivering $H_2$ to the body. However, it is essential to monitor the desired concentration of $H_2$ during inhalation as high concentrations of $H_2$ can be flammable and explosive (>4.1% in $O_2$ and >4.6% in the air) [256]. While inhalation is a rapid method, it has some drawbacks, including being time and cost-consuming, non-targeted, and requiring extensive equipment. To overcome these limitations, $H_2$-rich water has been introduced as a simple, rapid, and cheap alternative. $H_2$-rich water is prepared by dissolving $H_2$ under high pressure, electrolysis of water, or a reaction of water with magnesium [257]. Although it is an untargeted method, it is an effective way of delivering $H_2$.

For more targeted $H_2$ delivery, the injection of $H_2$-rich fluids has been utilized, although it is not effective for deeper tissues. Nonetheless, this approach increases controllability and reduces the

amount of $H_2$ lost before reaching the targeted tissue or organ. Overall, the various delivery methods provide options for delivering $H_2$ to the body, each with its advantages and limitations. To maximize the efficacy of $H_2$ therapy, the amount of released $H_2$ per unit volume and the timing of $H_2$ release are crucial factors. To address these concerns, researchers have explored using 2D and 3D materials to dope $H_2$ and release it at a specific time and place [254b]. These materials include graphene, boron nitride, mesoporous silica, metal-organic and covalent-organic frameworks, microbubbles, and fullerene [254b]. By decreasing the size of $H_2$ carriers from micro to nano, their loading capacity and solubility can increase, which can lead to more effective $H_2$ therapy. However, the process of trapping gas into materials is complex, and there is a risk of losing some of the loaded $H_2$ during the delivery process [254b, 258]. To address this, in situ $H_2$-generating materials have shown better performance.

$H_2$ can be generated by chemical reactions, photocatalysis, and enzymatic catalysis in the tissue microenvironment, which has a rapid production rate [254b]. Incorporating $H_2$ generators into 2D and 3D materials extends $H_2$ release time and prevents burst release's side effects. Kong et al. developed NPs with a core-shell structure called Mg@p-$SiO_2$, which generated $H_2$ through a reaction between magnesium and water [259]. By adjusting the thickness of the layer of mesoporous silicon dioxide, the rate of generated $H_2$ could be controlled. The resulting $H_2$ was effective in protecting cells from oxidative stress by selectively scavenging harmful $^{\bullet}OH$. External stimuli such as ultrasounds [260], light [261], and magnetic fields generate $H_2$ [262], increase releasing efficacy, and help deeper penetration [254b]. To achieve sufficient penetration depth for in vivo therapy, an X-ray can be helpful [254b].

## 6.2 $H_2$ therapy

$H_2$ activates endogenous antioxidant enzymes such as catalase and superoxide dismutase, reduces the concentration of oxidative stress markers, and regulates the transcription of genes by activating proteins like ERK ½, nuclear factor kappa B, and extracellular signal-regulated kinase [263]. By controlling oxidative stress, $H_2$ can regulate inflammation mediators, thereby reducing inflammation [264]. However, a high concentration of $H_2$ may not be effective due to its low solubility in biological environments. Nonetheless, it has been shown to induce toxicity in cancer cells through the p-AMPK and caspase-independent pathway and reduce lipid oxidation [265]. Yang et al. decorated the surface of magnesium with platinum to generate $H_2$ continuously in aqueous media for cancer therapy (Figure 19a) [266]. The generated $H_2$ could induce mitochondrial dysfunction and destroy the intracellular redox homeostasis (Figure 19a) [266]. Furthermore, the synergistic effects of $H_2$ with common cancer treatments have been observed, although the exact mechanism remains unknown. Overall, $H_2$ exhibits promising potential as an antioxidant and anti-inflammatory agent with potential therapeutic applications. [266]

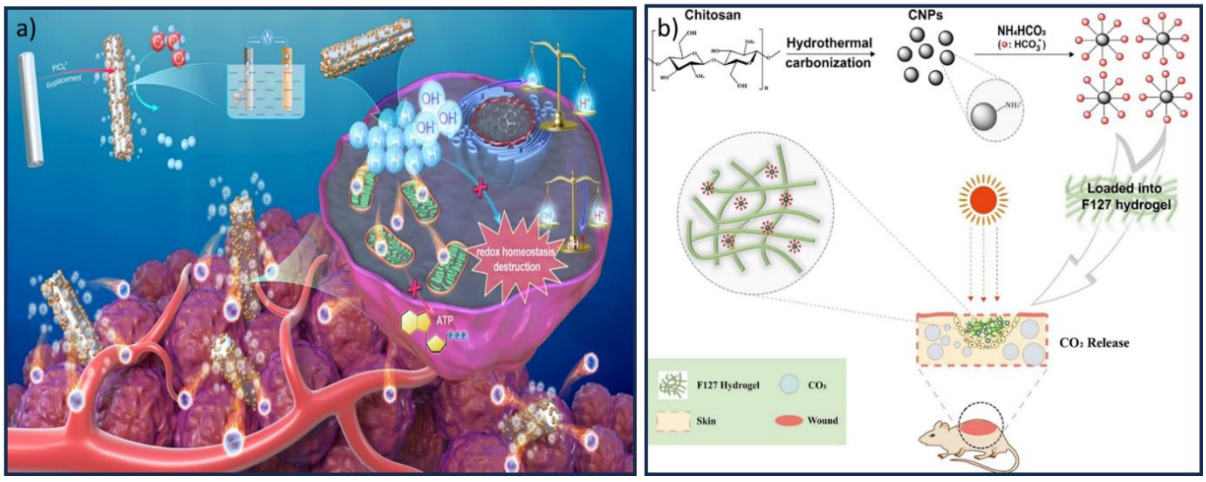


Figure 19. (a) The decorated magnesium with platinum generates $H_2$ in an aqueous media. The developed magnesium could generate $H_2$ continuously in a tumor media which resulted in the dysfunction of mitochondrial and destruction of intracellular redox homeostasis (Copyright © 2022, nature, Open access) [266], and (b) Illustration of the preparation of the photothermal hydrogel composed of the thermoresponsive block copolymer of carbon NPs and Pluronic F127 with amino groups to release CO for wound healing (Copyright © 2021, Elsevier) [267].

# 7 Carbon dioxide ($CO_2$)

Carbon dioxide ($CO_2$) is typically produced in nature as a byproduct of oxidative metabolism, which occurs during the citric cycle [268]. $CO_2$ is also produced in the environment as a result of anthropomorphic activities, involving the use of fossil resources, and is recognized as largely responsible for prevailing climate change and global warming issues [269]. This $CO_2$ emission influences marine organisms by leading to acidic aquatic environments, which negatively influence the biochemistry of organisms, such as reducing the ability of organisms to synthesize $CaCO_3$ for external skeleton production [270].

## 7.1 $CO_2$ delivery

Crucially, in spite of these highlighted negative impacts, $CO_2$, has been identified as constituting an important molecule in the biomedical industry, due to its potential as an antibacterial and wound healing aid, provided of course that its delivery is controlled. To achieve such controlled $CO_2$ release, biomaterials such as hydrogels containing carbonates are employed [267]. For instance, the use of a photothermal hydrogel composed of the thermoresponsive block copolymer of carbon NPs and Pluronic F127 with amino groups (Figure 19b), was employed for controlled $CO_2$ release and based on bicarbonate as a precursor, in the presence of light [267]. Another study reported the viability of employing photothermal hollow CuS NPs for $CO_2$ release after coordination with $Fe^{3+}$ ions to enable the incorporation of bicarbonate [271]. This composite is based on the ion-ligand coordination

nanoarchitecture and was demonstrated to have the capability to release $CO_2$ when exposed to near-infrared light [271].

## 7.2 $CO_2$ therapy

It is well-known that $CO_2$ is employed by plants in the synthesis of carbohydrates via the photosynthesis process. Additionally, $CO_2$ can influence several physiological processes via sugar sensing and signaling pathways [272]. $CO_2$ can therefore regulate gene expression, seed germination, hormonal crosstalk, etc., although the mechanism of this regulation, remains unclear [272]. It also plays an important role in oxidation phases during aerobic metabolism in microbial and human cells [273]. When retained in cells, $CO_2$ can lead to elevations of its concentration in the blood resulting in respiratory acidosis, leading to symptoms ranging from anxiety and dyspnea to hallucinations and coma, depending on if it is acute or chronic [274]. The respiratory acidosis may be acute or chronic depending on whether the compensatory elevation of the concentration of $HCO^{3-}$ in the blood is 1 mEq/L or 4 mEq/L for every 10 mm Hg increase in $Pa_{CO2}$ respectively [274b]. In regulated quantities, however, the literature reports that $CO_2$ can be employed in therapeutic applications, due to its unique properties of $CO_2$ as summarized in Figure 6.

For instance, it was shown that $CO_2$ has inflammatory, anti-cytokine effects, and can stimulate the immune system of humans [275]. $CO_2$ has also been reported to be capable of being used in cancer treatment due to its ability to induce mitochondrial apoptosis in cancer cells [276]. It is also possible for $CO_2$ to be employed in the deactivation of viruses via $CO_2$-protein binding, which leads to capsid damage [277]. Indeed, the administration of $CO_2$ was shown to facilitate the amelioration of COVID-19 symptoms via facilitating improvements in respiratory physiology and cardiovascular health as well as human nervous systems [275]. Additionally, $CO_2$ was reported to present therapeutic effects to enhance microcirculation and tissue oxygenation and thus can be employed in the treatment of chronic wounds [278]. This effect of $CO_2$ is known as the Bohr effect [279]. It has also been reported that $CO_2$ can increase the effects of other antibacterial agents, thus further improving the protection imparted.

Table 6. The typical paradigms of gas-releasing biomaterials for versatile biomedical applications. Listed 2022 and 2023.

| Gas | Source | Mechanism | Control method | Ultimate gas release | Release duration | Application | Remarks | Refs |
|---|---|---|---|---|---|---|---|---|
| **$H_2$** | Mg-based biomaterials | $H_2O$-responsive | Mg sheets and wires | From ~100 to 250 μM under different concentrations and pHs | 700 min | Cancer therapy | Topical delivery of $H_2$ improved the expression level of the P53 tumor suppressor protein. The minimum $H_2$ concentration for tumor apoptosis with magnesium-based biomaterials was recorded at 91.2 μL/mm$^3$ | [280] |
| | Mg and Mg-based galvanic cell | $H_2O$-responsive | Decorating platinum on the surface of Mg | ~40 μmol by Mg and ~160 by Mg-based galvanic cell | 160 h | Cancer therapy | The in situ generated $H_2$-induced mitochondria dysfunction. | [266] |
| | Mg | pH-responsive | - | 82.33 ± 3.21 μM at a pH of 5.6 | >700 min | colon carcinoma treatment | The study showed that the localized release of $H_2$ could increase the expression level of P53 tumor suppressor proteins | [281] |
| | $CaH_2$ | $H_2O$-responsive | Dispersion of $CaH_2$ in low molecular weight PEG | From 0 to ~1500 ppm with different concentrations of $CaH_2$ | - | Cancer therapy | The synthesized $CaH_2$ could generate $H_2$, calcium ions, and hydroxyl ions in the presence of $H_2O$ | [282] |
| **CO** | $Fe_3CO_{12}$ | $H_2O_2$-responsive | $Fe_3CO_{12}$ was conjugated on mPEG2000-SH | - | - | Photothermal therapy | $Fe_3CO_{12}$ generated CO in the presence of endogenous H2O2 via a Fenton-like reaction. The release of CO improved the efficiency of the PTT. | [283] |
| | Manganese carbonyl (MnCO) | pH/light/$H_2O_2$-responsive | PDA was functionalized with MnCO and folic acid. | From 0 to ~ 60% | In 25 min by NIR light | Antitumor therapy | The modified PDA could generate CO from the CO donor (MnCO) upon NIR light at 808 nm. | [284] |
| | | pH/glutathione (GSH)-Responsive | MNCO has incorporated coated silicon dioxide with $CaCO_3$. | From 0 to more than 1. (unit was not reported) | - | Gas therapy (cancer therapy) | The $CaCO_3$ was degraded in acidic media and resulted in CO release. | [285] |
| | Gaseous CO | Ultrasound-responsive | Loading gashouse CO into microbubbles. | - | - | Antitumor therapy | The synthesized microbubbles could encapsulate up to 337.1±8.0 (×10$^3$) ppm of CO. | [286] |

| | | | | | | | | |
|---|---|---|---|---|---|---|---|---|
| **$H_2S$** | $(NH_4)_2S$ | Light-responsive | $(NH_4)_2S$ was coated with self-assembled gold nanovesicles (GVs) | From 0 to ~ 80 µM in different pH (5-7.4) | In 40 min | Photothermal augmented gas therapy | Remarkable mitochondria damage was induced by the generated $H_2S$, which results in a reduction in the level of energy of adenosine triphosphate (ATP). | [287] |
| | Devo synthesized $H_2S$ donor (thiol-activated)(CL 2/3) | | Co-assembly with an amphiphilic pentapeptide. | Up to ~ 200 µM | In 6 hours | Cancer therapy | The co-assembly nanocarriers improved the sensitivity of tumors to radiotherapy. | [288] |
| | HSD-R (novel synthesized $H_2S$ donor) | ROS-responsive | - | From 0 to ~ 100 µM with and without $H_2O_2$ | 150 min | Myocardial infarction | The synthesized HSD-R could generate $H_2S$ and emit ROS-responsive fluorescence in the diseased sites. | [289] |
| **$CO_2$** | $CaCO_3$ | pH-responsive | Synthesizing $CaCO_3$ NPs by gas diffusion method. | From ~ 50 to ~ 800 ppm with different concentrations of the synthesized particles in different pHs from 5.5 to 7.4 | - | Enhance antitumor activity | The synthesized $CaCO_3$ NPs could decompose to $Ca^{2+}$ and $CO_2$ in acidic media. The produced $CO_2$ improved HIFUT so that its tumor ablation efficiency was about 61.04%. | [290] |

1254

# 8 Therapeutic biosafety of gas-releasing biomaterials

Gas therapy using gas-releasing biomaterials represents a novel and highly effective therapeutic approach for the treatment of various diseases in biomedicine. Unlike traditional therapies such as chemotherapy, surgeries, and RT, gas therapy has high therapeutic efficacy and biosafety, as well as supplementary functionality to enhance the effectiveness of other therapeutic approaches. The unique feature of gas therapy is its ability to achieve therapeutic outcomes with small amounts of introduced gases.

To achieve efficient delivery and release of therapeutic gases, diverse carriers, and generators are used in gas therapy. However, the biocompatibility and toxicity of these carriers and generators are crucial factors in determining the further clinical translation potential of gas-releasing biomaterials. While organic carriers such as liposomes and polymeric particles are highly biocompatible and easily degraded, their low stability in physiological conditions makes the control of gas delivery and release difficult. On the other hand, inorganic carriers have high stability and multifunctionality, allowing for specific on-demand gas release through endogenous and exogenous triggers. However, their low biodegradation rate may cause critical biosafety risks. Therefore, the rational design of organic-inorganic carriers is expected to solve the critical biosafety issue.

Although preliminary biosafety investigations have shown the promising therapeutic biosafety of gas-releasing biomaterials, detailed in vivo assessments on the biodistribution, biodegradation, excretion, histocompatibility, hemocompatibility, and specific toxicity to different tissues are necessary to guarantee their potential clinical translation. The concentration of delivered gases should also be controlled accurately to avoid inducing toxicity to normal cells or organs. After a full illustration of biocompatibility and high biosafety can gas releasing biomaterials enter the crucial step of clinical trials. However, it is important to note that gas therapies are still in their infancy and require further research and development to achieve their full therapeutic potential.

# 9 Conclusion and outlook

In recent years, gaseous molecules such as $O_2$, NO, CO, $H_2$, $H_2S$, and $CO_2$ have emerged as therapeutic agents with processing efficiency in various therapeutic applications. Moreover, gas-releasing biomaterials by supplying the gases at the site of diseases have enhanced the efficiency of PDT, radiotherapy, PTT, and ultrasound-responsive therapy. Figure 20 shows a representation of the research map of gas-releasing biomaterials timeline developments.

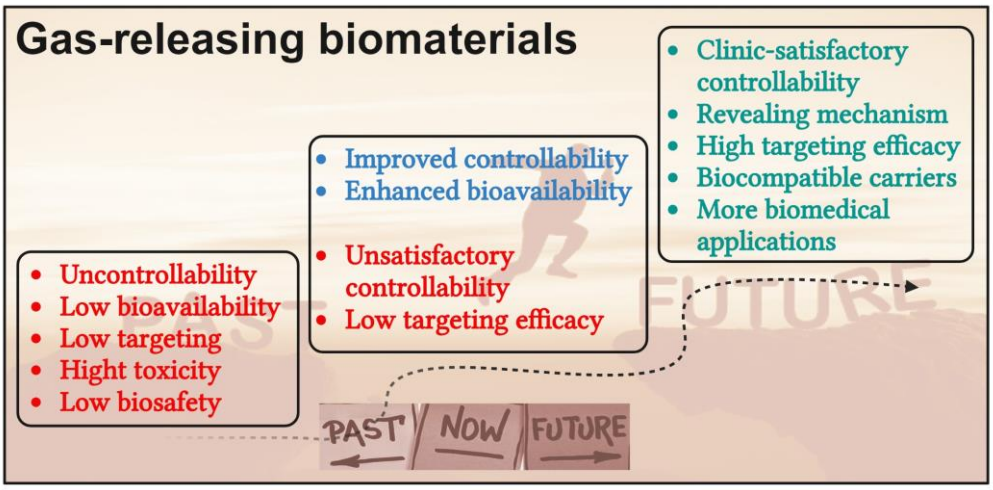


Figure 20. Schematic represents a research map of gas-releasing biomaterials timeline developments. (Adapted, 2018, Wily) [1b].

However, the therapeutic application of gas-releasing biomaterials is faced with critical challenges that should be addressed in the future. For example, delivering the gases with nano and micro platforms might differ in the therapeutic mechanism of the gases. Furthermore, the therapeutic potential of the delivered gases should be distinguished from their carrier therapeutic potential. Therefore, all the challenges should be carefully evaluated and responded to before clinical applications.

One way to address these challenges can be to focus on their biological, molecular, and physical mechanisms rather than the overall outcomes of gas-releasing biomaterials. While gas-releasing biomaterials have made progress in achieving controllable gas loading, delivery, and therapy, the results are not yet satisfactory. One challenge is the lack of controllability of the microenvironment-responsive diseases in gas therapy because of the significant variations among different diseases during distinct stages. Additionally, selecting the right carriers and generators for gas-releasing materials is critical, with a priority on high biocompatibility and biosafety. Therefore, another way can be to design and develop new smart gas carriers with expectable gas loading, controllable gas delivery, and clear gas therapy mechanisms, which are essential to reach favorable results.

The article highlighted the need for more research on the biocompatibility and biosafety of gas carriers and generators. The versatility and simplicity of gas-releasing biomaterials-enabled gas therapy are anticipated to demonstrate its therapeutic capabilities in diverse biomedical domains, including tissue engineering and cell therapy. Therefore, the article calls for extensive and close collaboration between experts in chemistry, material science, pharmacy, biology, and medicine for further clinical translation of gas-releasing biomaterials.

## 10 List of abbreviations

Calcium carbonate: $CaCO_3$

Calcium peroxide: CPO

Carbon dioxide: $CO_2$

Carbon monoxide: CO

CO-releasing molecules: CORMs

Glutathione: GSH

Hemoglobin: Hb

High-intensity focused ultrasound: HIFU

Hydrogen: $H_2$

Hydrogen peroxide: $H_2O_2$

Hydrogen sulfide: $H_2S$

Magnesium peroxide: MPO

Manganese dioxide: $MnO_2$

Metal-organic frameworks: MOFs

Myoglobin: Mb

Nanoparticles: NP

Nitric oxide: NO

Oxygen: $O_2$

Perfluorocarbons: PFCs

Photodynamic therapy: PDT

Photothermal therapy: PTT

Poly(lactic acid): PLA

Polycaprolactone-sodium percarbonate: PCL-SPC

Red blood cells: RBCs

Rheumatoid arthritis: RA

Sodium percarbonate: SPO

Sonodynamic therapy: SDT

## 11 Conflict of interest

The authors declare no financial interests/personal relationships that may be considered potential competing interests.

# 12 Acknowledgment

This research work was supported by an Aspirant fellowship from the Fund for Scientific Research Le Fonds de la Recherche Scientific de Belgique (FNRS) (grant number 38351, 2021 awarded to Pejman Ghaffari-Bohlouli). Figures are created with BioRender.com.

# 13 Biographies

**Pejman Ghaffari Bohlouli** obtained his master's degree in Polymer Engineering at Tehran University. His master's thesis focused on the synthesizing of polymeric scaffolds for applications in bone tissue engineering. Currently, he is pursuing a Ph.D., in Université libre de Bruxelles, where his research project centers on the development of a smart oxygen wound dressing. This innovative dressing aims to optimize the oxygen release profile within the wound area, ultimately facilitating the wound-healing process.

**Hafez Jafari** received his bachelor's in Polymer Engineering from Tehran University, Iran, and moved on to pursue a master's in Bioengineering (Tissue Engineering) from Tehran University. During his master's, he worked in the fields of bone tissue engineering. Hafez did his Ph.D. at BioMatter from 2019-2023 on developing 3-dimensional anti-infectious hydrogels with adhesive properties for skin wound healing application. He was granted a BOF postdoctoral fellowship in 2023 to join the Polymer Chemistry and Biomaterials Research Group at Ghent University.

**Oseweuba Okoro** is a Senior Researcher at the BioMatter research unit, at the Université Libre de Bruxelles. Previously, he was a Postdoctoral Researcher at the Department of Process/Chemical Engineering, Stellenbosch University, South Africa where he explored the modeling of biorefinery systems. He has also previously worked as a Research Fellow in the Energy Technology Unit at, the University of Otago, New Zealand. His previous academic qualifications include a Bachelor of Science degree in Chemical Engineering with First class (Nigeria), a Master of Science degree in Energy and environmental management with Distinction (UK), and a Ph.D. degree with an emphasis on Biorefineries (New Zealand). His main research interests include circular economy, biomaterial development, process design, chemical Engineering, and biorefinery design.

**Lei Nie** completed his Ph.D. (2013) from Huazhong University of Science and Technology, and after that received three years of postdoctoral training at Ningbo Institute of Materials Technology and Engineering (CAS, China) and Free University of Berlin (Germany). He began his research as an independent PI at Xinyang Normal University (China) in 2017. He started 3D bioprinting work at KU Leuven (Belgium) in 2019. His main research interests include biopolymers, drug delivery, nanoparticles, and tissue engineering.

**Amin Shavandi** studied Food Engineering in Iran and then obtained a Master of chemical engineering at the University of Putra Malaysia. He accomplished his Ph.D. at the University of Otago, New Zealand in 2017 for research on the bone scaffolds generated from waste marine shells. He then joined the Centre for Material Science and Technology at the University of Otago as a postdoctoral fellow in collaboration with Lincoln University (NZ) and Deakin University Australia. In 2018, Amin moved to the Université libre de Bruxelles (ULB) as an Assistant professor, where he is heading the BioMatter unit dedicated to research on biomaterials for tissue engineering and regenerative medicines with a focus on the valorization of biomass materials toward biomedical applications.

# 14 References


[1] a)Q. Jin, Y. Deng, F. Jia, Z. Tang, J. Ji, *Advanced Therapeutics* **2018**, 1, 1800084; b)L. Yu, P. Hu, Y. Chen, *Advanced Materials* **2018**, 30, 1801964.

[2] W. Gong, C. Xia, Q. He, *Wiley Interdisciplinary Reviews: Nanomedicine and Nanobiotechnology* **2022**, 14, e1744.

[3] R. Ahmed, R. Augustine, M. Chaudhry, U. A. Akhtar, A. A. Zahid, M. Tariq, M. Falahati, I. S. Ahmad, A. Hasan, *Biomedicine & Pharmacotherapy* **2022**, 149, 112707.

[4] T. Kim, Y. Nah, J. Kim, S. Lee, W. J. Kim, *Accounts of Chemical Research* **2022**, 55, 2384.

[5] S. Liu, G. Li, D. Ma, *Advanced Therapeutics* **2022**, 5, 2100227.

[6] N. Yang, F. Gong, L. Cheng, *Chemical Science* **2022**, 13, 1883.

[7] Y. Wang, T. Yang, Q. He, *National Science Review* **2020**, 7, 1485.

[8] a)N. G. Willemen, S. Hassan, M. Gurian, J. Li, I. E. Allijn, S. R. Shin, J. Leijten, *Trends in biotechnology* **2021**, 39, 1144; b)B. Alberts, D. Bray, K. Hopkin, A. D. Johnson, J. Lewis, M. Raff, K. Roberts, P. Walter, *Essential cell biology*, Garland Science, **2015**.

[9] a)E. Ortiz-Prado, J. F. Dunn, J. Vasconez, D. Castillo, G. Viscor, *American journal of blood research* **2019**, 9, 1; b)P. J. Diaz-Payno, D. Browe, F. E. Freeman, J. Nulty, R. Burdis, D. J. Kelly, *Tissue Engineering* **2022**.

[10] H. Zhang, J. E. Barralet, *Advanced Drug Delivery Reviews* **2017**, 122, 84.

[11] P. Lee, N. S. Chandel, M. C. Simon, *Nature reviews Molecular cell biology* **2020**, 21, 268.

[12] a)Y. B. Kang, J. Eo, B. Bulutoglu, M. L. Yarmush, O. B. Usta, *Biotechnology and bioengineering* **2020**, 117, 763; b)C. J. Siegfried, Y.-B. Shui, *American journal of ophthalmology* **2019**, 203, 12.

[13] a)S.-B. Catrina, X. Zheng, *Diabetologia* **2021**, 64, 709; b)A. Emami Nejad, S. Najafgholian, A. Rostami, A. Sistani, S. Shojaeifar, M. Esparvarinha, R. Nedaeinia, S. Haghjooy Javanmard, M.

Taherian, M. Ahmadlou, *Cancer Cell International* **2021**, 21, 1; c)Y. Yang, E. H. Lee, Z. Yang, *Tissue Engineering Part B: Reviews* **2022**.
[14] B. Ortmann, J. Druker, S. Rocha, *Cellular and molecular life sciences* **2014**, 71, 3569.
[15] a)N. Ashammakhi, A. Hasan, O. Kaarela, B. Byambaa, A. Sheikhi, A. K. Gaharwar, A. Khademhosseini, *Advanced healthcare materials* **2019**, 8, 1801048; b)S. Suvarnapathaki, X. Wu, D. Lantigua, M. A. Nguyen, G. Camci-Unal, *NPG Asia Materials* **2019**, 11, 1.
[16] N. Ashammakhi, M. A. Darabi, N. S. Kehr, A. Erdem, S.-k. Hu, M. R. Dokmeci, A. S. Nasr, A. Khademhosseini, *Biomacromolecules* **2019**, 21, 56.
[17] a)S. Suvarnapathaki, M. A. Nguyen, A. A. Goulopoulos, D. Lantigua, G. Camci-Unal, *Biomaterials Science* **2021**, 9, 2519; b)S. Sen, S. Sen, *Medical Gas Research* **2021**, 11, 30.
[18] S. Clement, A. Guller, S. B. Mahbub, E. M. Goldys, *Biomedicines* **2021**, 9, 322.
[19] J. L. Carson, S. J. Stanworth, J. A. Dennis, M. Trivella, N. Roubinian, D. A. Fergusson, D. Triulzi, C. Dorée, P. C. Hébert, *Cochrane Database of Systematic Reviews* **2021**.
[20] A. Villeneuve, V. Arsenault, J. Lacroix, M. Tucci, *Vox Sanguinis* **2021**, 116, 366.
[21] a)P. E. Marik, H. L. Corwin, *Critical care medicine* **2008**, 36, 2667; b)M. Rehn, A. Weaver, K. Brohi, S. Eshelby, L. Green, J. Røislien, D. J. Lockey, *Shock* **2019**, 51, 284.
[22] T. Matsuhira, H. Sakai, *Particuology* **2021**.
[23] S. Huo, X. Lei, D. He, H. Zhang, Z. Yang, W. Mu, K. Fang, D. Xue, H. Li, X. Li, *Artificial Organs* **2021**, 45, 1229.
[24] K. G. Flanders, L. R. Pessagno, J. F. Cerda, *Polyhedron* **2021**, 203, 115238.
[25] G. Zhou, W. Karlen, R. Brant, M. Wiens, N. Kissoon, J. M. Ansermino, *Pediatric Research* **2019**, 86, 732.
[26] X. Gu, A. F. Palmer, *ACS Applied Nano Materials* **2022**, 5, 5670.
[27] X. Shi, W. Yang, Q. Ma, Y. Lu, Y. Xu, K. Bian, F. Liu, C. Shi, H. Wang, Y. Shi, *Theranostics* **2020**, 10, 11607.
[28] L. Jiang, H. Bai, L. Liu, F. Lv, X. Ren, S. Wang, *Angewandte Chemie* **2019**, 131, 10770.
[29] T. Matsuhira, K. Yamamoto, H. Sakai, *Biomacromolecules* **2019**, 20, 1592.
[30] T. Matsuhira, K. Yamamoto, H. Sakai, *Nanobiotherapeutic Based Blood Substitutes* **2021**, 6, 433.
[31] M. M. T. Jansman, X. Liu, P. Kempen, G. Clergeaud, T. L. Andresen, P. W. Thulstrup, L. Hosta-Rigau, *ACS Applied Materials & Interfaces* **2020**, 12, 50275.
[32] G. Gregory, in *Liposome Technology*, CRC Press, 2018.
[33] Z. Tao, P. P. Ghoroghchian, *Trends in biotechnology* **2014**, 32, 466.
[34] A. Wijekoon, N. Fountas-Davis, N. D. Leipzig, *Acta biomaterialia* **2013**, 9, 5653.
[35] J. S. Ortega, R. Corrales-Orovio, P. Ralph, J. T. Egaña, C. Gentile, *Acta Biomaterialia* **2022**.
[36] J. G. Riess, *Chemical reviews* **2001**, 101, 2797.
[37] V. Jovicic, M. J. Khan, A. Zbogar-Rasic, N. Fedorova, A. Poser, P. Swoboda, A. Delgado, *Energies* **2018**, 11, 1290.
[38] N. B. Charbe, F. Castillo, M. M. Tambuwala, P. Prasher, D. K. Chellappan, A. Carreño, S. Satija, S. K. Singh, M. Gulati, K. Dua, *Blood Reviews* **2022**, 100927.
[39] M. P. Krafft, J. G. Riess, J. G. Weers, in *Submicron emulsions in drug targeting and delivery*, CRC Press, 2019.
[40] M. Wu, C. Chen, Z. Liu, J. Tian, W. Zhang, *Acta Biomaterialia* **2022**, 142, 242.
[41] A. P. Sherje, B. R. Dravyakar, D. Kadam, M. Jadhav, *Carbohydrate polymers* **2017**, 173, 37.
[42] J. Deng, Q. J. Chen, W. Li, Z. Zuberi, J. X. Feng, Q. L. Lin, J. L. Ren, F. J. Luo, Q. M. Ding, X. X. Zeng, *Journal of Materials Science* **2021**, 56, 5995.
[43] a)R. Cavalli, A. K. Akhter, A. Bisazza, P. Giustetto, F. Trotta, P. Vavia, *International journal of pharmaceutics* **2010**, 402, 254; b)C. Chu, Q. Li, W. Miao, H. Qin, X. Liu, D. Yao, S. Mao, *Applied Catalysis B: Environmental* **2022**, 121485.
[44] R. P. Seekell, A. T. Lock, Y. Peng, A. R. Cole, D. A. Perry, J. N. Kheir, B. D. Polizzotti, *Proceedings of the National Academy of Sciences* **2016**, 113, 12380.

[45] M. S. Khan, J. Hwang, K. Lee, Y. Choi, K. Kim, H.-J. Koo, J. W. Hong, J. Choi, *Molecules* **2018**, 23, 2210.
[46] a)R. Song, D. Hu, H. Y. Chung, Z. Sheng, S. Yao, *ACS applied materials & interfaces* **2018**, 10, 36805; b)P. Ganesan, P. Ramalingam, G. Karthivashan, Y. T. Ko, D.-K. Choi, *International journal of nanomedicine* **2018**, 13, 1569.
[47] Y. Xu, T. Fourniols, Y. Labrak, V. Préat, A. Beloqui, A. des Rieux, *ACS nano* **2022**, 16, 7168.
[48] P. Pędziwiatr, *Acta Innovations* **2018**, 45.
[49] X. Wang, Y. Mao, C. Sun, Q. Zhao, Y. Gao, S. Wang, *Biomaterials* **2021**, 276, 120985.
[50] a)R. R. Mallepally, C. C. Parrish, M. A. Mc Hugh, K. R. Ward, *International journal of pharmaceutics* **2014**, 475, 130; b)S. Suvarnapathaki, X. Wu, D. Lantigua, M. A. Nguyen, G. Camci-Unal, *NPG Asia Materials* **2019**, 11, 65.
[51] a)A. J. Waite, J. S. Bonner, R. Autenrieth, *Environmental engineering science* **1999**, 16, 187; b)W. M. Haynes, *CRC handbook of chemistry and physics*, CRC press, **2016**.
[52] A. McKillop, W. R. Sanderson, *Tetrahedron* **1995**, 51, 6145.
[53] P. Patnaik, *Handbook of inorganic chemicals*, Vol. 529, McGraw-Hill New York, **2003**.
[54] P. A. Shiekh, A. Singh, A. Kumar, *ACS applied materials & interfaces* **2018**, 10, 18458.
[55] C. Centeno-Cerdas, M. Jarquín-Cordero, M. N. Chávez, U. Hopfner, C. Holmes, D. Schmauss, H.-G. Machens, J. Nickelsen, J. T. Egaña, *Acta Biomaterialia* **2018**, 81, 184.
[56] M. N. Chávez, T. L. Schenck, U. Hopfner, C. Centeno-Cerdas, I. Somlai-Schweiger, C. Schwarz, H.-G. Machens, M. Heikenwalder, M. R. Bono, M. L. Allende, *Biomaterials* **2016**, 75, 25.
[57] W. Li, S. Wang, D. Zhong, Z. Du, M. Zhou, *Advanced Therapeutics* **2021**, 4, 2000107.
[58] D. Zhong, Z. Du, M. Zhou, *View* **2021**, 2, 20200189.
[59] P. Le Thi, Y. Lee, D. L. Tran, T. T. H. Thi, K. M. Park, K. D. Park, *Journal of Materials Chemistry B* **2020**, 8, 11033.
[60] a)R. Choudhury, *International journal of general medicine* **2018**, 431; b)E. M. M. Eltaky, *The Egyptian Journal of Hospital Medicine* **2022**, 86, 447; c)G. Lam, R. Fontaine, F. L. Ross, E. S. Chiu, *Advances in skin & wound care* **2017**, 30, 181.
[61] a)A. Mahmood, S. Neilson, V. Biswas, K. Muir, *Cerebrovascular Diseases* **2022**, 1; b)Z. Qi, W. Liu, Y. Luo, X. Ji, K. J. Liu, *Medical gas research* **2013**, 3, 1; c)M. H. Bennett, C. French, A. Schnabel, J. Wasiak, P. Kranke, S. Weibel, *Cochrane Database of Systematic Reviews* **2015**.
[62] C. G. Zilli, D. M. Santa-Cruz, K. B. Balestrasse, *Environmental and Experimental Botany* **2014**, 102, 11.
[63] Y. Yang, Z. Huang, L.-L. Li, *Nanoscale* **2021**, 13, 444.
[64] a)S. Suvarnapathaki, X. Wu, T. Zhang, M. A. Nguyen, A. A. Goulopoulos, B. Wu, G. Camci-Unal, *Bioactive Materials* **2022**, 13, 64; b)A. Rastinfard, B. Dalisson, J. Barralet, *Acta Biomaterialia* **2022**, 145, 390; c)S. Khorshidi, S. Younesi, A. Karkhaneh, *Colloids and Surfaces B: Biointerfaces* **2022**, 112832.
[65] Y. Wang, Y. Xue, T. Zhang, Q. Fang, M. Jin, X. Wang, Z. Wang, Y. Hu, W. Zhao, D. Lou, *Bio-Design and Manufacturing* **2021**, 4, 596.
[66] D. Rodriguez, D. Watts, D. Gaete, S. Sormendi, B. Wielockx, *International Journal of Molecular Sciences* **2021**, 22, 9191.
[67] A. Joshi, S. Choudhury, S. B. Gugulothu, S. S. Visweswariah, K. Chatterjee, *Biomacromolecules* **2022**, 23, 2730.
[68] H. Sun, J. Xu, Y. Wang, S. Shen, X. Xu, L. Zhang, Q. Jiang, *Bioactive Materials* **2023**, 24, 477.
[69] S. Mehrotra, R. D. Singh, A. Bandyopadhyay, G. Janani, S. Dey, B. B. Mandal, *ACS Applied Materials & Interfaces* **2021**, 13, 50744.
[70] D. C. Belisario, J. Kopecka, M. Pasino, M. Akman, E. De Smaele, M. Donadelli, C. Riganti, *Cells* **2020**, 9, 2598.
[71] J. Fu, T. Li, Y. Zhu, Y. Hao, *Advanced Functional Materials* **2019**, 29, 1906195.
[72] X. Dai, J. Ruan, Y. Guo, Z. Sun, J. Liu, X. Bao, H. Zhang, Q. Li, C. Ye, X. Wang, *Chemical Engineering Journal* **2021**, 422, 130109.

[73] H. Wang, Y. Guo, C. Wang, X. Jiang, H. Liu, A. Yuan, J. Yan, Y. Hu, J. Wu, *Biomaterials* **2021**, 269, 120621.
[74] C. Liu, Y. Cao, Y. Cheng, D. Wang, T. Xu, L. Su, X. Zhang, H. Dong, *Nature communications* **2020**, 11, 1735.
[75] C. Wang, H. Xu, C. Liu, Z. Peng, R. Min, Z. Zhang, J. Li, Y. Jin, Y. Wang, Z. Li, *Biomaterials Science* **2021**, 9, 3005.
[76] M. Zehra, W. Zubairi, A. Hasan, H. Butt, A. Ramzan, M. Azam, A. Mehmood, M. Falahati, A. A. Chaudhry, I. U. Rehman, *International journal of nanomedicine* **2020**, 15, 3511.
[77] J. Kim, H. Y. Kim, S. Y. Song, S.-h. Go, H. S. Sohn, S. Baik, M. Soh, K. Kim, D. Kim, H.-C. Kim, *ACS nano* **2019**, 13, 3206.
[78] X. Ren, H. Liu, X. Wu, W. Weng, X. Wang, J. Su, *Frontiers in Bioengineering and Biotechnology* **2021**, 9.
[79] S. Rodic, M. D. Vincent, *International journal of cancer* **2018**, 142, 440.
[80] C. Tapeinos, A. Larrañaga, J.-R. Sarasua, A. Pandit, *Nanomedicine: Nanotechnology, Biology and Medicine* **2018**, 14, 2397.
[81] A. O. Adeshakin, W. Liu, F. O. Adeshakin, L. O. Afolabi, M. Zhang, G. Zhang, L. Wang, Z. Li, L. Lin, Q. Cao, *Cellular immunology* **2021**, 362, 104286.
[82] S. Kumar, I. M. Adjei, S. B. Brown, O. Liseth, B. Sharma, *Biomaterials* **2019**, 224, 119467.
[83] S.-B. Yang, X.-L. Li, K. Li, X.-X. Zhang, M. Yuan, Y.-S. Guo, X. Bi, *Nanomedicine: Nanotechnology, Biology and Medicine* **2021**, 33, 102362.
[84] T. Yin, J. Yin, H. Ran, Y. Ren, C. Lu, L. Liu, Q. Shi, Y. Qiu, H. Pan, A. Ma, *Biomaterials Science* **2022**, 10, 294.
[85] M. M. T. Jansman, C. Coll-Satue, X. Liu, P. J. Kempen, T. L. Andresen, P. W. Thulstrup, L. Hosta-Rigau, *Biomaterials Advances* **2022**, 134, 112691.
[86] R. Tang, H. He, X. Lin, N. Wu, L. Wan, Q. Chen, Y. Hu, C. Cheng, Y. Cao, X. Guo, *Journal for ImmunoTherapy of Cancer* **2023**, 11, e006226.
[87] R. Kumar, N. S. Kehr, *Nanomaterials* **2022**, 12, 1304.
[88] X. Fu, S. Ohta, T. Kawakatsu, M. Kamihira, Y. Sakai, T. Ito, *Advanced Materials Technologies* **2022**, 7, 2100573.
[89] B. Huang, M. Chen, J. Tian, Y. Zhang, Z. Dai, J. Li, W. Zhang, *Advanced Healthcare Materials* **2022**, 11, 2102540.
[90] D. Huang, C. Zhao, B. Wen, X. Fu, L. Shang, W. Kong, Y. Zhao, *Chemical Engineering Journal* **2022**, 435, 134871.
[91] M. Mansouri, S. Beemer, C. R. Kothapalli, T. Rhoades, P. S. Fodor, D. Das, N. D. Leipzig, *ACS Applied Materials & Interfaces* **2022**, 14, 4899.
[92] M. Zhang, R. Zhang, Y. Dong, J. Liu, Z. Gao, X. Zhou, J. Cao, *Chemical Engineering Journal* **2023**, 141484.
[93] J. Wu, Y. Liu, M. Cao, N. Zheng, H. Ma, X. Ye, N. Yang, Z. Liu, W. Liao, L. Sun, *ACS Applied Materials & Interfaces* **2023**.
[94] Q. Chen, J. Li, F. Han, Q. Meng, H. Wang, Q. Wei, Z. Li, F. Li, E. Xie, X. Qin, *Advanced Functional Materials* **2022**, 32, 2201067.
[95] Z. Zhang, Z. Wang, Y. Xiong, C. Wang, Q. Deng, T. Yang, Q. Xu, Z. Yong, X. Yang, Z. Li, *Biomaterials Science* **2023**, 11, 108.
[96] P. Wei, S. Chen, J. Shi, J. Du, *Journal of Controlled Release* **2023**, 353, 975.
[97] Y. Xu, K. Wang, Z. Chen, R. Hu, Y. Zhao, X. Li, J. Qu, L. Liu, *Biomaterials Science* **2023**, 11, 119.
[98] J. Li, F. Han, J. Ma, H. Wang, J. Pan, G. Yang, H. Zhao, J. Zhao, J. Liu, Z. Liu, *Advanced Functional Materials* **2022**, 32, 2111208.
[99] S. Aghajanpour, M. Esfandyari-Manesh, T. Ghahri, M. H. Ghahremani, F. Atyabi, M. Heydari, H. Motasadizadeh, R. Dinarvand, *Colloids and Surfaces B: Biointerfaces* **2022**, 216, 112581.
[100] K. Mandal, S. Sangabathuni, R. Haghniaz, S. Kawakita, M. Mecwan, A. Nakayama, X. Zhang, M. Edalati, W. Huang, A. L. Hernandez, *Acta Biomaterialia* **2023**.

[101] J. Wu, P. Shen, X. Qin, Y. Yang, C. Lin, X. Li, W. Geng, P. Gao, L. Chen, L. Miao, *Chemical Engineering Journal* **2023**, 141507.
[102] J. I. Kang, K. M. Park, *Biomaterials* **2023**, 293, 121943.
[103] X. Zhang, C. He, Y. Chen, C. Chen, R. Yan, T. Fan, Y. Gai, T. Yang, Y. Lu, G. Xiang, *Biomaterials* **2021**, 275, 120987.
[104] Y. C. Chen, Y. J. Liu, C. L. Lee, K. Y. Pham, D. Manoharan, S. Thangudu, C. H. Su, C. S. Yeh, *Advanced Healthcare Materials* **2022**, 11, 2201613.
[105] T. Sun, Z. Yue, Y. Song, J. Ni, W. Wang, J. Zhao, J. Li, Y. Sun, B. Li, *Applied Organometallic Chemistry* **2022**, 36, e6888.
[106] R. Corrales-Orovio, F. Carvajal, C. Holmes, M. Miranda, S. González-Itier, C. Cárdenas, C. Vera, T. L. Schenck, J. T. Egaña, *Acta Biomaterialia* **2023**, 155, 154.
[107] X. Wang, C. Yang, Y. Yu, Y. Zhao, *Research* **2022**.
[108] M. Ou, C. Lin, Y. Wang, Y. Lu, W. Wang, Z. Li, W. Zeng, X. Zeng, X. Ji, L. Mei, *Journal of Controlled Release* **2022**, 345, 755.
[109] C. Gao, C. H. Kwong, Q. Wang, H. Kam, B. Xie, S. M.-Y. Lee, G. Chen, R. Wang, *ACS nano* **2023**, 17, 4034.
[110] M. M. Santana, J. M. Gonzalez, C. Cruz, *Frontiers in microbiology* **2017**, 8, 1947.
[111] H. Alimoradi, K. Greish, A. B. Gamble, G. I. Giles, *Pharmaceutical Nanotechnology* **2019**, 7, 279.
[112] a)D. Tousoulis, A.-M. Kampoli, C. Tentolouris Nikolaos Papageorgiou, C. Stefanadis, *Current vascular pharmacology* **2012**, 10, 4; b)C. Bogdan, *Nature immunology* **2001**, 2, 907.
[113] J. R. Kanwar, R. K. Kanwar, H. Burrow, S. Baratchi, *Current medicinal chemistry* **2009**, 16, 2373.
[114] J. O. Lundberg, E. Weitzberg, *Cell* **2022**, 185, 2853.
[115] A. M. Rezakhanlou, C. Miller, B. McMullin, A. Ghaffari, R. Garcia, A. Ghahary, *Cell Biology International* **2011**, 35, 407.
[116] M. J. Malone-Povolny, S. E. Maloney, M. H. Schoenfisch, *Advanced healthcare materials* **2019**, 8, 1801210.
[117] G. P. Zaloga, R. Siddiqui, C. Terry, P. E. Marik, *Nutrition in Clinical Practice* **2004**, 19, 201.
[118] X. Liu, Z. Yan, Y. Zhang, Z. Liu, Y. Sun, J. Ren, X. Qu, *ACS nano* **2019**, 13, 5222.
[119] Z. Ma, S. Liu, Y. Ke, H. Wang, R. Chen, Z. Xiang, Z. Xie, Q. Shi, J. Yin, *Biomaterials* **2020**, 255, 120141.
[120] M. Li, J. Li, J. Chen, Y. Liu, X. Cheng, F. Yang, N. Gu, *ACS nano* **2020**, 14, 2024.
[121] C. Zhang, T. D. Biggs, N. O. Devarie-Baez, S. Shuang, C. Dong, M. Xian, *Chemical Communications* **2017**, 53, 11266.
[122] W. Liu, X. Song, W. Liu, Q. Lin, R. Xu, H. Li, W. Xue, S. Yu, *Chemistry of Materials* **2022**.
[123] W. Fan, W. Bu, Z. Zhang, B. Shen, H. Zhang, Q. He, D. Ni, Z. Cui, K. Zhao, J. Bu, *Angewandte Chemie International Edition* **2015**, 54, 14191.
[124] J. Li, D. Zhu, W. Ma, Y. Yang, G. Wang, X. Wu, K. Wang, Y. Chen, F. Wang, W. Liu, *Nanoscale* **2020**, 12, 17064.
[125] Y. Zhou, T. Yang, R. Namivandi-Zangeneh, C. Boyer, K. Liang, R. Chandrawati, *Journal of Materials Chemistry B* **2021**, 9, 1059.
[126] P. Li, Y. Wang, X. Jin, J. Dou, X. Han, X. Wan, J. Yuan, J. Shen, *Langmuir* **2020**, 36, 4396.
[127] M. G. de Oliveira, S. M. Shishido, A. B. Seabra, N. H. Morgon, *The Journal of Physical Chemistry A* **2002**, 106, 8963.
[128] J. An, Y.-G. Hu, C. Li, X.-L. Hou, K. Cheng, B. Zhang, R.-Y. Zhang, D.-Y. Li, S.-J. Liu, B. Liu, *Biomaterials* **2020**, 230, 119636.
[129] K. Yamasaki, H. Edington, C. McClosky, E. Tzeng, A. Lizonova, I. Kovesdi, D. Steed, T. R. Billiar, *The Journal of clinical investigation* **1998**, 101, 967.
[130] S. P. Nichols, W. L. Storm, A. Koh, M. H. Schoenfisch, *Advanced drug delivery reviews* **2012**, 64, 1177.

[131] N. Shaikh, M. Valiev, S. V. Lymar, *Journal of Inorganic Biochemistry* **2014**, 141, 28.
[132] Z. Huang, J. Wu, Y. Zou, H. Yuan, Y. Zhang, Y. Fei, A. Bhardwaj, J. Kaur, E. E. Knaus, Y. Zhang, *Journal of Medicinal Chemistry* **2018**, 61, 1833.
[133] C. Chen, M. Vázquez-González, M. P. O'Hagan, Y. Ouyang, Z. Wang, I. Willner, *Small* **2022**, 18, 2104420.
[134] K. Sharma, K. Sengupta, H. Chakrapani, *Bioorganic & medicinal chemistry letters* **2013**, 23, 5964.
[135] C. Valdez, J. Saavedra, B. Showalter, K. Davies, T. Wilde, M. Citro, J. Barchi Jr, *J. Med. Chem* **2008**, 51, 3961.
[136] Q. Zhao, J. Zhang, L. Song, Q. Ji, Y. Yao, Y. Cui, J. Shen, P. G. Wang, D. Kong, *Biomaterials* **2013**, 34, 8450.
[137] X. Zhou, H. Wang, J. Zhang, X. Li, Y. Wu, Y. Wei, S. Ji, D. Kong, Q. Zhao, *Acta biomaterialia* **2017**, 54, 128.
[138] J. Hou, Y. Pan, D. Zhu, Y. Fan, G. Feng, Y. Wei, H. Wang, K. Qin, T. Zhao, Q. Yang, *Nature Chemical Biology* **2019**, 15, 151.
[139] M. Huang, H. Wang, D. He, P. Jiang, Y. Zhang, *Chemical Communications* **2019**, 55, 3634.
[140] T. Yang, A. S. Fruergaard, A. K. Winther, A. N. Zelikin, R. Chandrawati, *Small* **2020**, 16, 1906744.
[141] a)A. T. Dharmaraja, G. Ravikumar, H. Chakrapani, *Organic letters* **2014**, 16, 2610; b)J. Fu, J. Han, T. Meng, J. Hu, J. Yin, *Chemical Communications* **2019**, 55, 12904.
[142] J. Hou, H. He, S. Huang, M. Qian, J. Wang, X. Tan, G. Han, Y. Song, Z. Xu, Y. Liu, *Chemical Communications* **2019**, 55, 1205.
[143] M. F. Chung, H. Y. Liu, K. J. Lin, W. T. Chia, H. W. Sung, *Angewandte Chemie International Edition* **2015**, 54, 9890.
[144] T. Liu, J. Wei, G. Fu, P. Zhang, Z. Zhang, D.-S. Guo, X. Yang, *Polymer Chemistry* **2021**, 12, 1023.
[145] L. K. Keefer, *Current topics in medicinal chemistry* **2005**, 5, 625.
[146] V. S. Sharma, T. Traylor, R. Gardiner, H. Mizukami, *Biochemistry* **1987**, 26, 3837.
[147] N. Ieda, Y. Hotta, N. Miyata, K. Kimura, H. Nakagawa, *Journal of the American Chemical Society* **2014**, 136, 7085.
[148] a)D. Park, G. Saravanakumar, W. J. Kim, in *Therapeutic Application of Nitric Oxide in Cancer and Inflammatory Disorders*, Elsevier, 2019; b)L. Gao, J. Cheng, Z. Shen, G. Zhang, S. Liu, J. Hu, *Angewandte Chemie* **2022**, 134, e202112782.
[149] S. Li, X. Song, W. Zhu, Y. Chen, R. Zhu, L. Wang, X. Chen, J. Song, H. Yang, *ACS applied materials & interfaces* **2020**, 12, 30066.
[150] G. Wei, G. Yang, B. Wei, Y. Wang, S. Zhou, *Acta Biomaterialia* **2019**, 100, 365.
[151] J. Sun, X. Cai, C. Wang, K. Du, W. Chen, F. Feng, S. Wang, *Journal of the American Chemical Society* **2021**, 143, 868.
[152] R. B. Heimann, *Materials* **2023**, 16, 5142.
[153] a)X. Du, S. S. Lee, G. Blugan, S. J. Ferguson, *International Journal of Molecular Sciences* **2022**, 23, 6551; b)G. Pezzotti, *ACS applied materials & interfaces* **2019**, 11, 26619.
[154] G. Pezzotti, E. Marin, T. Adachi, A. Rondinella, F. Boschetto, W. Zhu, N. Sugano, R. M. Bock, B. McEntire, S. B. Bal, *Scientific reports* **2017**, 7, 44848.
[155] C. V. Rao, B. S. Reddy, V. E. Steele, C. Wang, X. Liu, N. Ouyang, J. M. Patlolla, B. Simi, L. Kopelovich, B. Rigas, *Molecular cancer therapeutics* **2006**, 5, 1530.
[156] Y. Li, B. Yoon, A. Dey, J. H. Park, *Journal of Controlled Release* **2022**, 352, 179.
[157] S. Kundu, P. N. Phu, P. Ghosh, S. A. Kozimor, J. A. Bertke, S. C. E. Stieber, T. H. Warren, *Journal of the American Chemical Society* **2019**, 141, 1415.
[158] N. Lehnert, E. Kim, H. T. Dong, J. B. Harland, A. P. Hunt, E. C. Manickas, K. M. Oakley, J. Pham, G. C. Reed, V. S. Alfaro, *Chemical Reviews* **2021**, 121, 14682.
[159] S. Huerta, S. Chilka, B. Bonavida, *International journal of oncology* **2008**, 33, 909.
[160] Z. Wang, A. Jin, Z. Yang, W. Huang, *ACS nano* **2023**, 17, 8935.

[161] B. Nossaman, E. Pankey, P. Kadowitz, *Critical care research and practice* **2012**, 2012.
[162] A. M. Martinelli, C. N. dos Santos Rodrigues, T. F. de Moraes, G. J. Rodrigues, *Journal of Pharmacy & Pharmaceutical Sciences* **2018**, 21, 38.
[163] M. K. Chug, E. J. Brisbois, *ACS Materials Au* **2022**, 2, 525.
[164] A. C. d. O. Gonzalez, T. F. Costa, Z. d. A. Andrade, A. R. A. P. Medrado, *Anais brasileiros de dermatologia* **2016**, 91, 614.
[165] Y.-J. Chen, S.-C. Wu, H.-C. Wang, T.-H. Wu, S.-S. F. Yuan, T.-T. Lu, W.-F. Liaw, Y.-M. Wang, *Molecular Pharmaceutics* **2019**, 16, 4241.
[166] J. M. Loughlin, L. Browne, J. Hinchion, *Perfusion* **2022**, 37, 656.
[167] T. Hao, M. Qian, Y. Zhang, Q. Liu, A. C. Midgley, Y. Liu, Y. Che, J. Hou, Q. Zhao, *Advanced Science* **2022**, 2105408.
[168] V. Somasundaram, D. Basudhar, G. Bharadwaj, J. H. No, L. A. Ridnour, R. Y. Cheng, M. Fujita, D. D. Thomas, S. K. Anderson, D. W. McVicar, *Antioxidants & Redox Signaling* **2019**, 30, 1124.
[169] Y. Wang, X. Yang, X. Chen, X. Wang, Y. Wang, H. Wang, Z. Chen, D. Cao, L. Yu, J. Ding, *Advanced Functional Materials* **2022**, 32, 2206554.
[170] M. Douglass, S. Ghalei, E. Brisbois, H. Handa, *ACS applied bio materials* **2022**, 5, 700.
[171] J. Yeo, Y. M. Lee, J. Lee, D. Park, K. Kim, J. Kim, J. Park, W. J. Kim, *Nano letters* **2019**, 19, 6716.
[172] a)T. Kim, J. Suh, W. J. Kim, *Advanced Materials* **2021**, 33, 2008793; b)A. Łuczak, M. Madej, A. Kasprzyk, A. Doroszko, *Oxidative Medicine and Cellular Longevity* **2020**, 2020.
[173] J. Hu, M. R. Whittaker, H. Duong, Y. Li, C. Boyer, T. P. Davis, *Journal of controlled release: official journal of the Controlled Release Society* **2015**, 213, e55.
[174] J. Park, S. Pramanick, D. Park, J. Yeo, J. Lee, H. Lee, W. J. Kim, *Advanced Materials* **2017**, 29, 1702859.
[175] S. Tao, J. Cheng, G. Su, D. Li, Z. Shen, F. Tao, T. You, J. Hu, *Angewandte Chemie International Edition* **2020**, 59, 21864.
[176] F. Paneni, S. Costantino, F. Cosentino, *World journal of diabetes* **2015**, 6, 326.
[177] F. Yang, M. Li, Y. Liu, T. Wang, Z. Feng, H. Cui, N. Gu, *Journal of Controlled Release* **2016**, 228, 87.
[178] H. Shi, C. F. Xiong, L. J. Zhang, H. C. Cao, R. Wang, P. Pan, H. Y. Guo, T. Liu, *Advanced Healthcare Materials* **2023**, 2300012.
[179] K. Wang, L. Jiang, L. Qiu, *Acta Biomaterialia* **2022**, 140, 506.
[180] L. Jiang, K. Wang, L. Qiu, *Asian Journal of Pharmaceutical Sciences* **2022**, 17, 924.
[181] Y. Hou, Y. Kuang, Q. Jiang, S. Zhou, J. Yu, Z. He, J. Sun, *Nano Research* **2022**, 15, 5183.
[182] L. Wen, H. Liu, C. Hu, Z. Wei, Y. Meng, C. Lu, Y. Su, L. Lu, H. Liang, Q. Xu, *ACS Applied Materials & Interfaces* **2023**, 15, 10477.
[183] J. Yu, R. Zhang, B. Chen, X. Liu, Q. Jia, X. Wang, Z. Yang, P. Ning, Z. Wang, Y. Yang, *Advanced Functional Materials* **2022**, 32, 2202857.
[184] M. Sun, Y. Sang, Q. Deng, Z. Liu, J. Ren, X. Qu, *Nano Research* **2022**, 15, 5273.
[185] M. Ouyang, X. Ouyang, Z. Peng, M. Liu, G. Xu, Z. Zou, M. Zhang, Q. Shang, *Journal of Nanobiotechnology* **2022**, 20, 1.
[186] Z. Zhou, Z. Gao, W. Chen, X. Wang, Z. Chen, Z. Zheng, Q. Chen, M. Tan, D. Liu, Y. Zhang, *Acta Biomaterialia* **2022**, 151, 600.
[187] Y. Feng, H. Zhang, X. Xie, Y. Chen, G. Yang, X. Wei, N. Li, M. Li, T. Li, X. Qin, *Materials Today Bio* **2022**, 14, 100288.
[188] W. Zhang, B. Chen, R. Lin, H. Dai, Y. Zhang, M. Qunlong, Y. Huang, *Nitric Oxide* **2023**.
[189] Z. Liang, W. Liu, Z. Wang, P. Zheng, W. Liu, J. Zhao, Y. Zhong, Y. Zhang, J. Lin, W. Xue, *Acta Biomaterialia* **2022**, 143, 428.
[190] S. Ghalei, M. Douglass, H. Handa, *ACS Biomaterials Science & Engineering* **2022**, 8, 3066.
[191] M. Qi, X. Ren, W. Li, Y. Sun, X. Sun, C. Li, S. Yu, L. Xu, Y. Zhou, S. Song, *Nano Today* **2022**, 43, 101447.

[192] C. Parisi, F. Moret, A. Fraix, L. Menilli, M. Failla, F. Sodano, C. Conte, F. Quaglia, E. Reddi, S. Sortino, *ACS omega* **2022**, 7, 7452.
[193] C. J. Ma, Y. He, X. Jin, Y. Zhang, X. Zhang, Y. Li, M. Xu, K. Liu, Y. Yao, F. Lu, *Biomaterials Advances* **2022**, 134, 112555.
[194] H. Massoumi, R. Kumar, M. K. Chug, Y. Qian, E. J. Brisbois, *ACS applied bio materials* **2022**, 5, 2285.
[195] W. Jiang, W. Dong, M. Li, Z. Guo, Q. Wang, Y. Liu, Y. Bi, H. Zhou, Y. Wang, *ACS nano* **2022**, 16, 3881.
[196] C.-W. Chung, B.-W. Liao, S.-W. Huang, S.-J. Chiou, C.-H. Chang, S.-J. Lin, B.-H. Chen, W.-L. Liu, S.-H. Hu, Y.-C. Chuang, *ACS Applied Materials & Interfaces* **2022**, 14, 6343.
[197] N. Sharma, P. Arjunan, S. Marepally, N. Jain, A. R. Naziruddin, A. Ghosh, C. Mariappan, D. A. Jose, *Journal of Photochemistry and Photobiology A: Chemistry* **2022**, 425, 113703.
[198] S. Singh, G. R. Navale, M. Mahale, V. K. Chaudhary, K. Kodam, K. Ghosh, *Nitric Oxide* **2022**, 129, 30.
[199] N. Sharma, D. A. Jose, N. Jain, S. Parmar, A. Srivastav, J. Chawla, A. R. Naziruddin, C. Mariappan, *Langmuir* **2022**, 38, 13602.
[200] R. Motterlini, J. E. Clark, R. Foresti, P. Sarathchandra, B. E. Mann, C. J. Green, **2002**, 90, e17.
[201] a)Y. Zhou, W. Yu, J. Cao, H. Gao, *Biomaterials* **2020**, 255, 120193; b)C. C. Romão, W. A. Blättler, J. D. Seixas, G. J. J. C. S. R. Bernardes, **2012**, 41, 3571.
[202] M. Faizan, N. Muhammad, K. U. K. Niazi, Y. Hu, Y. Wang, Y. Wu, H. Sun, R. Liu, W. Dong, W. Zhang, *Materials* **2019**, 12, 1643.
[203] N. S. Sitnikov, Y. Li, D. Zhang, B. Yard, H.-G. Schmalz, **2015**, 54, 12314.
[204] F. Zobi, A. Degonda, M. C. Schaub, A. Y. Bogdanova, *Inorganic Chemistry* **2010**, 49, 7313.
[205] E. Palao, T. Slanina, L. Muchová, T. Šolomek, L. Vítek, P. Klán, *Journal of the American Chemical Society* **2016**, 138, 126.
[206] S. H. C. Askes, G. U. Reddy, R. Wyrwa, S. Bonnet, A. Schiller, *Journal of the American Chemical Society* **2017**, 139, 15292.
[207] H. Inaba, K. Fujita, T. Ueno, *Biomaterials Science* **2015**, 3, 1423.
[208] G. Dördelmann, H. Pfeiffer, A. Birkner, U. Schatzschneider, *Inorganic Chemistry* **2011**, 50, 4362.
[209] M. Faizan, N. Muhammad, K. U. K. Niazi, Y. Hu, Y. Wang, Y. Wu, H. Sun, R. Liu, W. Dong, W. Zhang, Z. Gao, *Materials (Basel, Switzerland)* **2019**, 12.
[210] F. J. Carmona, I. Jiménez-Amezcua, S. Rojas, C. C. Romão, J. A. R. Navarro, C. R. Maldonado, E. Barea, *Inorganic Chemistry* **2017**, 56, 10474.
[211] M. Ma, H. Noei, B. Mienert, J. Niesel, E. Bill, M. Muhler, R. A. Fischer, Y. Wang, U. Schatzschneider, N. Metzler-Nolte, **2013**, 19, 6785.
[212] U. Hasegawa, A. J. van der Vlies, E. Simeoni, C. Wandrey, J. A. Hubbell, *Journal of the American Chemical Society* **2010**, 132, 18273.
[213] H. Pfeiffer, A. Rojas, J. Niesel, U. Schatzschneider, *Dalton Transactions* **2009**, 4292.
[214] M. Chaves-Ferreira, I. S. Albuquerque, D. Matak-Vinkovic, A. C. Coelho, S. M. Carvalho, L. M. Saraiva, C. C. Romão, G. J. L. Bernardes, **2015**, 54, 1172.
[215] J. A. Donald, in *Handbook of Hormones*, (Eds: Y. Takei, H. Ando, K. Tsutsui), Academic Press, San Diego 2016.
[216] M. Wang, W. Liao, *Front Plant Sci* **2016**, 7, 572.
[217] a)D. Morse, in *Encyclopedia of Respiratory Medicine*, (Eds: G. J. Laurent, S. D. Shapiro), Academic Press, Oxford 2006; b)D. G. Levitt, M. D. Levitt, *Clinical pharmacology : advances and applications* **2015**, 7, 37.
[218] a)R. Motterlini, R. Foresti, **2017**, 312, C302; b)W. Adach, M. Błaszczyk, B. Olas, *Chemico-Biological Interactions* **2020**, 318, 108973.
[219] G. W. Reierson, S. Guo, C. Mastronardi, J. Licinio, M. L. Wong, *Current neuropharmacology* **2011**, 9, 715.

[220] D. D. Browning, I. K. Kwon, R. Wang, *Future medicinal chemistry* **2010**, 2, 65.
[221] B. Wegiel, D. Gallo, E. Csizmadia, C. Harris, J. Belcher, G. M. Vercellotti, N. Penacho, P. Seth, V. Sukhatme, A. Ahmed, P. P. Pandolfi, L. Helczynski, A. Bjartell, J. L. Persson, L. E. Otterbein, *Cancer research* **2013**, 73, 7009.
[222] Y. Li, J. Dang, Q. Liang, L. Yin, *ACS Central Science* **2019**, 5, 1044.
[223] C. Xiao, Y. Sun, J. Fan, W. Nguyen, S. Chen, Y. Long, W. Chen, A. Zhu, B. Liu, *Acta Pharmaceutica Sinica B* **2023**.
[224] E. Cuevasanta, M. N. Möller, B. Alvarez, *Archives of biochemistry and biophysics* **2017**, 617, 9.
[225] X. Cao, L. Ding, Z.-z. Xie, Y. Yang, M. Whiteman, P. K. Moore, J.-S. Bian, *Antioxidants & redox signaling* **2019**, 31, 1.
[226] P. Kamoun, *Amino Acids* **2004**, 26, 243.
[227] O. Kabil, R. Banerjee, *Journal of Biological Chemistry* **2010**, 285, 21903.
[228] Y. Mikami, N. Shibuya, Y. Ogasawara, H. Kimura, *Biochemical and biophysical research communications* **2013**, 431, 131.
[229] W. Zhao, J. Zhang, Y. Lu, R. Wang, *The EMBO journal* **2001**, 20, 6008.
[230] K. R. Olson, E. R. DeLeon, Y. Gao, K. Hurley, V. Sadauskas, C. Batz, G. F. Stoy, *American Journal of Physiology-Regulatory, Integrative and Comparative Physiology* **2013**, 305, R592.
[231] M. C. Urquhart, F. Ercole, M. R. Whittaker, B. J. Boyd, T. P. Davis, J. F. Quinn, *Polymer Chemistry* **2018**, 9, 4431.
[232] C. R. Powell, K. M. Dillon, J. B. Matson, *Biochemical pharmacology* **2018**, 149, 110.
[233] A. K. Gilbert, Y. Zhao, C. E. Otteson, M. D. Pluth, *The Journal of organic chemistry* **2019**, 84, 14469.
[234] A. K. Sharma, M. Nair, P. Chauhan, K. Gupta, D. K. Saini, H. Chakrapani, *Organic letters* **2017**, 19, 4822.
[235] F. Rong, T. Wang, Q. Zhou, H. Peng, J. Yang, Q. Fan, P. Li, *Bioactive Materials* **2023**, 19, 198.
[236] a)J. L. Wallace, R. W. Blackler, M. V. Chan, G. J. Da Silva, W. Elsheikh, K. L. Flannigan, I. Gamaniek, A. Manko, L. Wang, J.-P. Motta, *Antioxidants & redox signaling* **2015**, 22, 398; b)D. J. Elsey, R. C. Fowkes, G. F. Baxter, *Cell Biochemistry and Function: Cellular biochemistry and its modulation by active agents or disease* **2010**, 28, 95; c)H. Ding, D. Ma, X. Huang, J. Hou, C. Wang, Y. Xie, Y. Wang, H. Qin, T. Guo, *Acta Physiologiae Plantarum* **2019**, 41, 1.
[237] a)N. Bazhanov, T. Ivanciuc, H. Wu, M. Garofalo, J. Kang, M. Xian, A. Casola, *Viruses* **2018**, 10, 249; b)K. K. Zimmermann, S. G. Spassov, K. M. Strosing, P. M. Ihle, H. Engelstaedter, A. Hoetzel, S. Faller, *Inflammation* **2018**, 41, 249.
[238] T. M. Cunha, D. Dal-Secco, W. A. Verri Jr, A. T. Guerrero, G. R. Souza, S. M. Vieira, C. M. Lotufo, A. F. Neto, S. H. Ferreira, F. Q. Cunha, *European journal of pharmacology* **2008**, 590, 127.
[239] Y. Yu, Z. Wang, Q. Ding, X. Yu, Q. Yang, R. Wang, Y. Fang, W. Qi, J. Liao, W. Hu, *Pharmaceutics* **2021**, 13, 742.
[240] Q. Zhang, L. Wang, Y. Yin, J. Shen, J. Xie, J. Yuan, *Journal of Materials Chemistry B* **2022**, 10, 5344.
[241] J. Cheng, B. Zheng, S. Cheng, G. Zhang, J. Hu, *Chemical science* **2020**, 11, 4499.
[242] L. Li, M. Bhatia, P. K. Moore, *Current opinion in pharmacology* **2006**, 6, 125.
[243] a)H. Zhao, S. Lu, J. Chai, Y. Zhang, X. Ma, J. Chen, Q. Guan, M. Wan, Y. Liu, *Journal of Diabetes and its Complications* **2017**, 31, 1363; b)F. Liu, D.-D. Chen, X. Sun, H.-H. Xie, H. Yuan, W. Jia, A. F. Chen, *Diabetes* **2014**, 63, 1763; c)R. V. Pinto, S. Carvalho, F. Antunes, J. Pires, M. L. Pinto, *ChemMedChem* **2022**, 17, e202100429; d)X. Han, L. Wang, Y. Shang, X. Liu, J. Yuan, J. Shen, *Journal of Materials Chemistry B* **2022**, 10, 8672; e)X. Shi, H. Li, F. Guo, D. Li, F. Xu, *Journal of Advanced Research* **2023**.
[244] I. Goren, Y. Köhler, A. Aglan, J. Pfeilschifter, K.-F. Beck, S. Frank, *Nitric Oxide* **2019**, 87, 31.
[245] X. Zhao, L. Liu, T. An, M. Xian, J. A. Luckanagul, Z. Su, Y. Lin, Q. Wang, *Acta Biomaterialia* **2020**, 104, 85.
[246] G.-G. Wang, W. Li, *Iranian journal of basic medical sciences* **2019**, 22, 1192.

[247] a)L. Gambari, E. Amore, R. Raggio, W. Bonani, M. Barone, G. Lisignoli, B. Grigolo, A. Motta, F. Grassi, *Materials Science and Engineering: C* **2019**, 102, 471; b)A. M. Al-Bishari, K. H. R. Yie, M. A. Al-Baadani, B. A. Al-Shaaobi, Z. Zhou, K. Fang, A. Sun, Y. Shen, L. Cai, L. Yao, *Materials Science and Engineering: C* **2021**, 130, 112471; c)A. K. Gilbert, T. D. Newton, M. H. Hettiaratchi, M. D. Pluth, *Free Radical Biology and Medicine* **2022**.
[248] L. Gambari, B. Grigolo, F. Grassi, *International Journal of Molecular Sciences* **2019**, 20, 5231.
[249] a)L. Gambari, G. Lisignoli, E. Gabusi, C. Manferdini, F. Paolella, A. Piacentini, F. Grassi, *Journal of cellular physiology* **2017**, 232, 3574; b)Y. Zhai, J. Behera, S. C. Tyagi, N. Tyagi, *Journal of cellular physiology* **2019**, 234, 18602; c)M. Lv, Y. Liu, T.-H. Xiao, W. Jiang, B.-W. Lin, X.-M. Zhang, Y.-M. Lin, Z.-S. Xu, *American Journal of Translational Research* **2017**, 9, 1183.
[250] a)A. A. H. Abdel Latef, M. F. Dawood, H. Hassanpour, M. Rezayian, N. A. Younes, *Biology* **2020**, 9, 172; b)L.-H. Fu, Z.-Z. Wei, K.-D. Hu, L.-Y. Hu, Y.-H. Li, X.-Y. Chen, Z. Han, G.-F. Yao, H. Zhang, *journal of microbiology* **2018**, 56, 238.
[251] a)J. Hamar, M. Solymar, E. Tanai, P. Cseplo, Z. Springo, G. Berta, B. Debreceni, A. Koller, *Acta Physiologica Hungarica* **2012**, 99, 411; b)A. Sivarajah, M. McDonald, C. Thiemermann, *Shock* **2006**, 26, 154.
[252] A. G. Buret, T. Allain, J.-P. Motta, J. L. Wallace, *Antioxidants & Redox Signaling* **2022**, 36, 211.
[253] S.-i. Hirano, Y. Ichikawa, B. Sato, F. Satoh, Y. Takefuji, *Clean Technologies* **2020**, 2, 529.
[254] a)X.-Q. Wang, M. Peng, C.-X. Li, Y. Zhang, M. Zhang, Y. Tang, M.-D. Liu, B.-R. Xie, X.-Z. Zhang, *Nano Letters* **2018**, 18, 6804; b)Y. Wu, M. Yuan, J. Song, X. Chen, H. Yang, *ACS nano* **2019**, 13, 8505.
[255] M. Dole, F. R. Wilson, W. P. Fife, *Science* **1975**, 190, 152.
[256] X. Zhai, X. Chen, S. Ohta, X. Sun, *Medical Gas Research* **2014**, 4, 1.
[257] C. Nie, X. Ding, A. Rong, M. Zheng, Z. Li, S. Pan, W. Yang, *Life Sciences* **2021**, 272, 119248.
[258] M. Sano, T. Tamura, *Current pharmaceutical design* **2021**, 27, 650.
[259] L. Kong, C. Chen, F. Mou, Y. Feng, M. You, Y. Yin, J. Guan, *Particle & Particle Systems Characterization* **2019**, 36, 1800424.
[260] N. Merabet, K. Kerboua, *International Journal of Hydrogen Energy* **2022**.
[261] P. Zhang, D. Luan, X. W. Lou, *Advanced Materials* **2020**, 32, 2004561.
[262] J. Yao, W. Huang, W. Fang, M. Kuang, N. Jia, H. Ren, D. Liu, C. Lv, C. Liu, J. Xu, *Small Methods* **2020**, 4, 2000494.
[263] B. Han, H. Zhou, G. Jia, Y. Wang, Z. Song, G. Wang, S. Pan, X. Bai, J. Lv, B. Sun, *The FEBS Journal* **2016**, 283, 738.
[264] H.-m. Li, L. Shen, J.-w. Ge, R.-f. Zhang, *Medical Gas Research* **2017**, 7, 265.
[265] J. Runtuwene, H. Amitani, M. Amitani, A. Asakawa, K.-C. Cheng, A. Inui, *PeerJ* **2015**, 3, e859.
[266] N. Yang, F. Gong, B. Liu, Y. Hao, Y. Chao, H. Lei, X. Yang, Y. Gong, X. Wang, Z. Liu, *Nature Communications* **2022**, 13, 2336.
[267] G. Xie, N. Zhou, Y. Gao, S. Du, H. Du, J. Tao, L. Zhang, J. Zhu, *Chemical Engineering Journal* **2021**, 403, 126353.
[268] E. P. Cummins, A. C. Selfridge, P. H. Sporn, J. I. Sznajder, C. T. Taylor, *Cellular and molecular life sciences : CMLS* **2014**, 71, 831.
[269] O. V. Okoro, Z. Sun, J. Birch, *Journal of Cleaner Production* **2017**, 142, 1583.
[270] P. Hunter, *EMBO reports* **2007**, 8, 1104.
[271] W. P. Li, C. H. Su, S. J. Wang, F. J. Tsai, C. T. Chang, M. C. Liao, C. C. Yu, T. T. Vi Tran, C. N. Lee, W. T. Chiu, T. W. Wong, C. S. Yeh, *ACS nano* **2017**, 11, 5826.
[272] M. Thompson, D. Gamage, N. Hirotsu, A. Martin, S. Seneweera, **2017**, 8.
[273] R. Maniarasu, M. Kumar, R., *Journal of Cell Science & Therapy* **2022**, 13.
[274] a)M. T. Wong-Riley, Q. Liu, X. P. Gao, *Respiratory physiology & neurobiology* **2013**, 185, 156; b)T. D. DuBose, L. L. Hamm, *Acid-base and electrolyte disorders: a companion to Brenner & Rector's the kidney*, WB Saunders Company, **2002**.
[275] A. M. M. El-Betany, E. M. Behiry, M. Gumbleton, K. G. Harding, **2020**, 7.

[276] T. Ueha, T. Kawamoto, Y. Onishi, R. Harada, M. Minoda, M. Toda, H. Hara, N. Fukase, M. Kurosaka, R. J. O. r. Kuroda, **2017**, 37, 3688.
[277] X. Cheng, T. Imai, J. Teeka, M. Hirose, T. Higuchi, M. Sekine, *Environmental technology* **2013**, 34, 539.
[278] C. Brandi, L. Grimaldi, G. Nisi, A. Brafa, A. Campa, M. Calabrò, M. Campana, C. D'Aniello, *In vivo (Athens, Greece)* **2010**, 24, 223.
[279] F. B. Jensen, **2004**, 182, 215.
[280] R. Zan, H. Wang, W. Cai, J. Ni, B. J. Luthringer-Feyerabend, W. Wang, H. Peng, W. Ji, J. Yan, J. Xia, *Bioactive Materials* **2022**, 9, 385.
[281] R. Zan, H. Wang, W. Cai, J. Ni, B. J. C. Luthringer-Feyerabend, W. Wang, H. Peng, W. Ji, J. Yan, J. Xia, Y. Song, X. Zhang, *Bioactive materials* **2022**, 9, 385.
[282] F. Gong, J. Xu, B. Liu, N. Yang, L. Cheng, P. Huang, C. Wang, Q. Chen, C. Ni, Z. Liu, *Chem* **2022**, 8, 268.
[283] G. Ma, Z. Liu, C. Zhu, H. Chen, R. T. Kwok, P. Zhang, B. Z. Tang, L. Cai, P. Gong, *Angewandte Chemie International Edition* **2022**, 61, e202207213.
[284] J. Liu, Q. Tang, Y. Wang, H.-L. Zhang, B. Ren, S.-P. Yang, J.-G. Liu, *New Journal of Chemistry* **2022**, 46, 8413.
[285] Y. Li, Y. Pan, C. Chen, Z. Li, S. Du, X. Luan, Y. Gao, X. Han, Y. Song, *Small* **2022**, 18, 2204244.
[286] W. Guo, S. Huang, J. An, J. Zhang, F. Dong, J. Dang, J. Zhang, *ACS Applied Materials & Interfaces* **2022**, 14, 50664.
[287] Y. He, M. R. Younis, C. Jiang, G. He, J. He, Y. Zhang, H. Liu, P. Huang, J. Lin, *Applied Materials Today* **2022**, 26, 101313.
[288] H. Chen, X. Guan, Q. Liu, L. Yang, J. Guo, F. Gao, Y. Qi, X. Wu, F. Zhang, X. Tian, *ACS Applied Materials & Interfaces* **2022**, 14, 53475.
[289] M. Yao, Y. Lu, L. Shi, Y. Huang, Q. Zhang, J. Tan, P. Hu, J. Zhang, G. Luo, N. Zhang, *Bioactive Materials* **2022**, 9, 168.
[290] H. Gao, Z. Wang, M. Tan, W. Liu, L. Zhang, J. Huang, Y. Cao, P. Li, Z. Wang, J. Wen, *International Journal of Nanomedicine* **2022**, 333.